https://doi.org/10.15388/vu.thesis.291
https://orcid.org/0000-0001-5791-7483

VILNIUS UNIVERSITY
NATURE RESEARCH CENTRE

Vytautas
SAMALAVIČIUS

THE GROUNDWATER ISOTOPE-GEOCHEMISTRY ANOMALIES FORMATION FEATURES IN THE BALTIC ARTESIAN BASIN

DOCTORAL DISSERTATION

Natural Sciences,
Geology (N 005)

VILNIUS 2022

This dissertation was written between 2017 and 2021 at Vilnius University.

Academic supervisor:
Prof. Habil. Dr. Robert Mokrik (Vilnius University, Natural Sciences, Geology - N 005).

Chairman – Assoc. Prof. Dr. Kęstutis, Jokšas (The Nature Research Centre, Natural Sciences, Geology – N 005).
Members:
Prof. Dr. Albertas, Bitinas (The Nature Research Centre, Natural Sciences, Geology – N 005),
Prof. Dr. Egidijus, Rimkus (Vilnius University, Natural Sciences, Physical Geography – N 006),
Dr. Tomas, Saks (University of Fribourg, Natural Sciences, Geology – N 005),
Dr. Žana, Skuratovič (The Nature Research Centre, Natural Sciences, Geology – N 005).

The dissertation shall be defended at a public meeting of the Dissertation Defence Panel at 12:00 on 25th March 2022 in meeting room 214 of the Institute of Geosciences (Vilnius University).

Address: M. K. Čiurlionio g. 21/27, LT-03101 Vilnius, Lithuania
Tel. 370 5 239 8202; e-mail: info@chgf.vu.lt.

The text of this dissertation can be accessed at the libraries of Nature Research Centre, Vilnius University, as well as on the website of Vilnius University: *www.vu.lt/lt/naujienos/ivykiu-kalendorius*

https://doi.org/10.15388/vu.thesis.291
https://orcid.org/0000-0001-5791-7483

VILNIAUS UNIVERSITETAS
GAMTOS TYRIMŲ CENTRAS

Vytautas
SAMALAVIČIUS

BALTIJOS ARTEZINIO BASEINO IZOTOPINIŲ-HIDROGEOCHEMINIŲ ANOMALIJŲ FORMAVIMOSI DĖSNINGUMAI

DAKTARO DISERTACIJA

Gamtos mokslai,
Geologija (N 005)

VILNIUS 2022

Disertacija rengta 2017– 2021 metais Vilniaus universitete.

Mokslinis vadovas:
Prof. habil. dr. Robert Mokrik (Vilniaus universitetas, gamtos mokslai, geologija – N 005).

Gynimo taryba:
Pirmininkas – **doc. dr. Kęstutis Jokšas** (Gamtos tyrimų centras, gamtos mokslai, geologija – N 005).
Nariai:
Prof. dr. Albertas Bitinas (Gamtos tyrimų centras, gamtos mokslai, geologija – N 005),
Prof. dr. Egidijus Rimkus (Vilniaus universitetas, gamtos mokslai, fizinė geografija – N 006),
Dr. Tomas Saks (Fribourgo universitetas, gamtos mokslai, geologija – N 005),
Dr. Žana Skuratovič (Gamtos tyrimų centras, gamtos mokslai, geologija – N 005).

Disertacija ginama viešame Gynimo tarybos posėdyje 2022 m. kovo mėn. 25 d. 12 val. Vilniaus universiteto Chemijos ir geomokslų fakulteto Geomokslų instituto 214 auditorijoje.

Adresas: M. K. Čiurlionio g. 21/27, LT-03101 Vilnius, Lietuva, tel. +370 5 239 8202; el. paštas info@chgf.vu.lt.

Disertaciją galima peržiūrėti Gamtos tyrimų centro ir Vilniaus universiteto bibliotekose ir VU interneto svetainėje adresu:
https://www.vu.lt/naujienos/ivykiu-kalendorius

CONTENTS

MAIN ABBREVIATIONS

AEW - Atmosphere Equilibrated Water
AR - Activity Ratio
ATTA - Atomic Trap Trace Analysis
BAB - Baltic Artesian Basin
BABHEGM - Hydrogeological Models of BAB developed in DHEG (Department of Hydrogeology and Engineering Geology, Vilnius University) in 2016-2019
BIL - Baltic Ice Lake
CB - Crystalline Basement
EH - Estonian Homocline
EM - End-Member
GMWL - Global Meteoric Water Line
GNIP - Global Network of Isotopes in Precipitation
IAEA - International Atomic Energy Agency
ICP-OES - Inductively Coupled Plasma Optical Emission Spectrometer
HEG - Department of Hydrogeology and Engineering Geology, Vilnius University
LGM - Last Glacial Maximum
NPP - Nuclear Power Plant
PDB - Pee Dee Belemnite Standard
QMS - Quadrupole Mass Spectrometer
TDS - Total Dissolved Solids
SDL - Seawater Dilution Line
SI - Saturation Index
SMA - Simple Moving Averages
STP - Standard Temperature and Pressure
TFZ - Telšiai Fault Zone
VSMOW - Vienna Standard Mean Ocean Water
WISER - Water Isotope System for Data Analysis, Visualization, and Electronic Retrieval (IAEA resources)

INTRODUCTION

The knowledge of the Baltic Artesian Basin (BAB) groundwater formation plays a significant role in hydrogeology. Apart from the significant interest in fundamental research of groundwater isotope-geochemistry, the applications of these investigations include social-economical projects, environmental assessments, an actual part of the prognosis of changes in natural environments, and their impact on urban areas, agricultural objects, industry, balneology, etc. Studies of groundwater composition in the BAB include many topics: regional research, classifications, paleohydrogeology, dating, origin, and formation scenarios. Groundwater isotope-geochemistry data is beneficial when evaluating resources, pollution, flow path velocity, and fresh, brackish, and brine groundwater formation in the BAB. Yet, the isotope or chemical composition of groundwater formation often cannot be easily explained separately. In such cases, groundwater should be analyzed using coupled research methods. Anomalous groundwater may have various definitions: 1. a significant deviation from surrounding sites' groundwater chemical or isotopic content; 2. unique geological-hydrogeological conditions, lithological settings, or physical factors leading to groundwater alterations; 3. a variety of hydraulic boundary conditions for flow paths.

This study aimed to investigate BAB groundwater background, the origin of isotope-geochemistry anomalies, and their formation scenarios.

The object of this study was shallow, intermediate, and deep groundwater flow systems and their interaction resulting in isotopic-chemistry anomalies of the BAB.

The main objectives of this study:

1. to describe anomalous sites for shallow (<300 m), intermediate (300-1000 m), and deep (>1000 m) aquifers groundwater by isotope-geochemistry data and reveal the main factors that influenced its formation, such as geological and hydrogeological settings, paleo-climate aspects during Pleistocene and Holocene;
2. to establish a distinction between the background groundwater composition and anomalies in the context of local, intermediate, and deep flow systems interaction for the formation of chemical and isotopic content;
3. to use a coupled calibrated steady-state basin-scale groundwater flow modeling with particle track schemes and noble gas data to identify groundwater formation pathways and residence times.

Scientific novelty

- The development of groundwater anomalies' spatial distribution structure is based on its isotopic-geochemistry characteristics and flow modeling.
- A new concept of the Estonian Homocline Cm-V and O-Cm aquifer systems groundwater isotope-geochemistry anomaly formation is proposed. The formation of isotopically fractionated residual groundwater is due to cryogenic processes and the influence of the talik system net.
- The comparison of coupled ^{81}Kr and conventional ^{4}He ages with numeric modeling of groundwater flow particle track times for intermediate-deep groundwater bodies in the BAB was executed for the first time.

Defended statements of this study:

1. According to isotope-geochemistry data and thermodynamic calculations, a major part of the northern BAB Cm-V and O-Cm aquifers groundwater formed in the periglacial environment before LGM. Depleted δ^{18}O values, hydrogeochemistry, and noble gas excess in Estonia O-Cm-V-B hydrogeological unit originate from the *in situ* freezing of paleogroundwater.
2. The interaction of the shallow and intermediate groundwater flows on the central-southern BAB occurs in the vicinity of coastal rivers valleys, and lowlands where anomalies form by winter time seasonal changes of depleted isotope-geochemistry in the local flow recharge-discharge balance. Toward the southern region, the δ^{18}O enrichment tendency predominates by upward discharge from intermediate-depth at the places of tectonic faults.
3. Deep and intermediate-depth flows are separated by regional-scale aquitards, which is proved by steady-state 3D groundwater flow model where particles trajectory times are compared to radioisotopic groundwater ages. The difference among radiokrypton, helium ages, and particle travel times are significant. The absence of fractured fault zone permeability characteristics at the numerical model may be corrected after more detailed field studies of hydraulic parameters within layers to reflect an actual hydrogeological internal boundary setting accurately.

Approbation of the research results. The dissertation results were published in four scientific articles, two of which have an impact factor in the Clarivate Analytics Web of Science (CA WoS) database, and four presentations at international conferences.

Content of the dissertation: introduction, four chapters, conclusions, reference list. Dissertation extent: 31 figures, 11 tables, and 199 reference list entries.

1. PREVIOUS RESEARCH OVERVIEW

1.1. Research of Groundwater Anomalies at the Estonian Homocline and Central-Southern BAB Sites

Two exclusive cases were studied in northern Estonia Cm-V (Cambrian-Vendian (Ediacaran)) and O-Cm (Ordovician-Cambrian) aquifer systems groundwater strongly depleted with stable isotopes ($\delta^{18}O$ down to -22 ‰) (Babre et al., 2016; Karro et al., 2009; Pärn et al., 2019; Raidla et al., 2016; Raidla, Pärn, Schloemer, et al., 2019; Vaikmäe et al., 2001). The depletion is considered in respect to average annual meteoric water, with $\delta^{18}O$ value -10.4 ‰ (Punning et al., 2008, 1987; Weißbach, 2014). The radiocarbon dating supports the theory that this groundwater formed during the Pleistocene (Banys et al., 1979; Pärn et al., 2019; Raidla et al., 2012). According to this theory, the variety of isotope-geochemistry parameters was caused by glacial meltwater, crystalline basement brackish water mixing, and modern groundwater recharge as well as the influence of seawater (Babre et al., 2016; Delina et al., 2012; Raidla, Pärn, Aeschbach, et al., 2019; Sterckx et al., 2017, 2018; Vaikmäe et al., 2001). Stable isotope depletion was also hypothesized to result from the gravitational sink of heavy stable isotopes (Babre et al., 2016). The influence of Baltic Ice Lake (BIL) water recharge into aquifers in the Gulf of Finland resulting in isotopically depleted groundwater was proposed by Bondarenko et al., 1981. Despite the dominant hypothesis that this groundwater originated from glacial meltwater recharge, *in situ* brackish and modern water mixing (Babre et al., 2016; Karro et al., 2009; Pärn et al., 2019; Raidla et al., 2009, 2016; Raidla, Pärn, Aeschbach, et al., 2019; Sterckx et al., 2017, 2018; Vaikmäe et al., 2001), a significant amount of samples have elevated TDS values, low bicarbonate content, high pH, and a wide range of chemical facies may contradict this theory. On the contrary, cryogenic brine rejection and isotopic Rayleigh distillation could explain the evolution of the northern Estonian Cm-V and O-Cm aquifer groundwater (Mokrik, 1996, 1997, 2003; Mokrik & Vaikmäe, 1988). Cryogenic influence on the northern Estonian isotopically depleted groundwater formation was suggested by Mokrik & Vaikmäe, 1988. Detailed analysis on this topic was done and proven by isotope-geochemistry evidence later on (Mokrik, 1996, 1997, 2003).

The exploitation of Cm-V aquifer groundwater began in 1842 when the first well was bored. Anomalous Ca-Cl-HCO_3 groundwater facies was observed (Gatalski, 1954). During the exploitation of the Cm-V aquifer, a recharge of modern groundwater occurred in buried valleys areas resulting in a stable isotope enrichment (Mokrik, 1996; Mokrik et al., 2005; Raidla, 2010; Raidla et al., 2009; Vaikmäe et al., 2001; Yezhova et al., 1996). Due to the significant intake in Tallinn, a 30 m drop of the hydraulic head resulted in seawater intrusion (Mokrik, 1996; Raidla, Pärn, Aeschbach, et al., 2019). After 1990, the exploitation was reduced drastically; therefore, the hydrodynamic regime had reversed to natural conditions. The observed Ca-Cl type groundwater in the aquifer was suggested to be sedimentogenic, but this theory is inconsistent with depleted isotopic values (Karro et al., 2004; Savitski & Belkina, 1985; Yezhova et al., 1996).

The case study of Cm-V aquifer groundwater isotope-geochemistry in the North Estonia and St. Petersburg area has lasted for 50 years. It was conducted by the Leningrad branch of the Russian Geological Survey, the Lithuanian Geological Scientific Research Institute (LGSRI), and the Estonian Geological Survey (EGS). Radiocarbon dating was implemented on demand for additional data resource evaluation previously modeled by utilizing electrical analog simulation (Banys et al., 1979; Gregorauskas et al., 1988; Mokrik, 1978). Glacier meltwater recharge 13 ka BP from Baltic Ice Lake (BIL) was suggested by Yezhova et al., 1996. However, it was not clear how this recharge occurred. An instant injection through Lontova aquitard was due to lower hydrostatic pressure in the Cm-V aquifer (Yezhova et al., 1996). Yet, Lontova is a clayey confining aquifer that is unlikely to be permeable enough for such recharge. *In situ* groundwater should be discharged somewhere in this case.

A case study of Tallinn groundwater was thoroughly explored, resulting in the theory that multiple factors (subglacial meltwater recharge, BIL influence, seawater intrusion, and modern meteoric injection) influenced the formation of Cm-V groundwater (Mokrik, 1996, 1997, 2003; Mokrik et al., 2005). Using transient flow and mass transport code, AQUA-01 models proved that sea intrusion and crystalline basement cryogenic groundwater altered isotope-geochemistry $\delta^{18}O$ background values and increased TDS up to 2.5 g/L at Kopli site (Gregorauskas et al., 1988). The model of Cm-V aquifer connection with the isotopically depleted surface waters through the thawed ground zone at the beginning of the Late Glacial Period takes into account the subsequent factors: the impact of subglacial meltwater recharge after glacier degradation, BIL influence, Baltic Seawater intrusion, and modern meteoric recharge in the terrestrial part of the Baltic Artesian Basin. Again, the formation of Cm-V aquifer groundwater was unclear and required more data and elaboration (Mokrik, Monkevicius, et al., 2000; Mokrik, Petkevičius, et al., 2000).

The origin of the brackish groundwater and its formation at the northern coast is not completely defined. The following two primary sources may be the reason explaining the phenomenon: seawater intrusion or basement saline groundwater recharge (Raidla, Pärn, Schloemer, et al., 2019). Due to groundwater exploitation on the Viimsi site, chloride content increases together with the changes in other hydrochemical parameters. The main source of salinity seems to be the bedrock brackish groundwater (Raidla, Pärn, Aeschbach, et al., 2019). Other authors suggest mixing relic saline groundwater with seawater (Suursoo et al., 2017). Yet, the results and discussion on this topic are inconclusive.

Depleted isotope anomalies in the northern BAB groundwater may be due to local glacial meltwater recharge in the talik zones and cryogenic processes. It may explain such anomalies in intermediate depth aquifers, where direct lateral vector recharge with meltwater had a crucial role. A vertical meltwater recharge of aquifers could occur near the taliks in subglacial conditions, where no permafrost could form. The talik system was reconstructed using lineaments on the seabed with the help of bathymetry data of the Gulfs of Riga and Finland, the Eastern Gotland Basin, the North Baltic Proper, and the bottom of Lake Peipus (Mokrik & Samalavičius, 2022). It is necessary to mention that permafrost persisted in most areas of the BAB during the glaciations; therefore, meltwater could only recharge near taliks. During the regression of the ice-sheet, higher glacial pressure was in the northern part of the BAB leading to intensified meltwater injection through the taliks into lower pressure areas, where the glacier was significantly thinner.

These circumstances make recharge possible at the late stage of glacier retreat, coinciding with the dating results of the groundwater in O-Cm and Cm-V aquifers (Late Pleistocene). The talik scheme does not contradict cryogenic groundwater theory as permafrost is a part of this paradigm. It accompanies the explanation of a wide variety of groundwater anomalies in the northern Estonia groundwater.

Radiocarbon dating of exclusive Pleistocene time groundwater in Cm-V and O-Cm aquifers in Estonia was executed to evaluate isotope-geochemistry formation scenarios, seawater intrusion, and meteoric water leakage (Banys et al., 1979; Pärn et al., 2018, 2019; Raidla et al., 2012). The groundwater of the O-Cm aquifer where the ^{14}C model obtained age, tritium activity, and ^{4}He content suggest a wide age amplitude mainly due to the mixing of multiple different water sources (Pärn et al., 2019). Isotope-geochemistry and noble gas content, along with established ages, suggest that groundwater originated before the Last Glacial Maximum (LGM) (Mokrik & Samalavičius, 2022).

According to radiocarbon dating, Cm-V aquifer groundwater ages vary from 7 to 33 ka BP (Banys et al., 1979; Pärn et al., 2018, 2019; Raidla et al., 2012). Modern meteoric water recharge significantly lowered the groundwater age (7-10 ka). The groundwater age of two Cm-V system aquifers, Voronka (V_2vr) and Gdov (V_2gd) aquifers, is 17-27 and 23-33 ka (Banys et al., 1979). Groundwater age 26–34 ka (radiocarbon content 1.7-3 pmC) could be related to a permafrost condition in Estonia, which most likely occurred before the glacial transgression of LGM (Mokrik, 1997, 2003).

Multiple isotope-geochemistry anomalies of shallow-intermediate-deep interaction levels were observed and studied in the central-southern BAB. Saline groundwater and brine discharge into shallow freshwater aquifers through vertical tectonic faults occur in the southeastern Lithuania (Gregorauskas et al., 2017). A vertical flow of salty groundwater forces binary mixing and creates dome-shaped and elevated salinity local groundwater anomalies. The dome of saline water can sometimes reach the ground surface, and mineralized water springs occur. Due to the variety of hydrochemical composition, it is often extracted and used as potable mineral water or for recreational activities in baths, pools, etc. (Juodkazis et al., 1997). The result of the binary mixing is a range of different groundwater chemical facies, stable isotope values, and increased salinity (Zuzevičius et al., 2007). Similar cases are observed in Latvia (Babre et al., 2016; Levins, 1990).

Sodium-bicarbonate facies groundwater is observed in the western-southern part of Lithuania, in the Cretaceous aquifer. Calcium-sodium and magnesium-sodium chloride facies are abundant in Kaliningrad aquifers of the same aquifer system (Juodkazis & Mikalauskas, 1994; Mokrik, 2003). Sodium bicarbonate facies coincide with glauconite mineral deposits in the aquifer matrix and may be due to the cation exchange (Na-Ca) processes with calcium-bicarbonate meteoric groundwater (Juodkazis & Mikalauskas, 1994). Binary mixing of meteoric Ca-HCO_3 and paleoseawater Na-Mg-Cl was proposed as a theory for sodium bicarbonate facies formation. During Pleistocene (Holstein and Eemian interglacial stages), Sea transgressions could have recharged the Cretaceous aquifers with seawater, which is presently replaced by meteoric water. Seawater-meteoric chemical type water reaction leads to dolomite precipitation and the formation of Na-

HCO_3, and chloride-bicarbonate dominant facies found in Cretaceous aquifer systems (Mokrik, 2003).

Deep Riga site brines in O-Cm aquifer are very alkaline, pH value is up to 8.7 (Babre et al., 2016; Delina et al., 2012; Gerber et al., 2017). Authors suggest that this may be due to unreliable readings from the pH meter. Yet, this pH anomaly was observed in a few measurements (Vaikmäe et al., 2020). In the deep aquifers of Lithuania, groundwater is usually acidic (down to pH-6,5 and less) as a result of clay mineral metamorphosis, during which the mineral adsorbs bicarbonate; therefore, shifting the carbonate equilibrium toward acidity (Appelo & Postma, 1993; Mokrik, 2003). However, thermodynamic conditions, especially thermal regime, are entirely different in Latvia, Riga (20 °C) area compared to the western Lithuanian deep groundwater (over 90 °C), which could influence the rate of rock-water interaction and pH, accordingly (Juodkazis et al., 1997; Mokrik, 2003; Šliaupa, 2009).

Calcium-dominant sulfate groundwater is found in the northern Lithuania and the Latvian Devonian aquifers. This groundwater originates from meteoric water precipitation recharging the gypsum-rich aquifer, where it dissolves. Due to geohazards importance in this region (gypsum dissolution associated karst), geochemistry of groundwater is well studied and monitored (Juodkazis, 1994, 2003; Mokrik et al., 2009; Paukštys et al., 1999; Paukštys & Narbutas, 1996; Rudzianskaitė, 2017; Taminskas & Marcinkevičius, 2002). Groundwater in the Lithuanian Devonian aquifer is slightly depleted with oxygen-18, dated with radiocarbon to the corrected age from modern up to 23 ka (Mokrik et al., 2009).

1.2. Groundwater Anomalies Dating in the BAB during the Last Decades

Groundwater age studies in the BAB involved many isotopic and other techniques. In this study, the term *age* is equivalent to the definition of *mean residence time*. A study of numeric modeling particle track, radiocarbon, and tritium age comparison was conducted by Mokrik et al., 2014 and Štuopis et al., 2012. The latest results helped develop the gradient method to solve the initial tritium activity absence (Samalavičius & Mokrik, 2016).

A complex study of the Lithuanian mineral groundwater in Birštonas involved isotope-geochemistry analysis and radiocarbon dating (Zuzevičius et al., 2007).

A thorough analysis of the Lithuanian Devonian aquifer systems groundwater was conducted by Mokrik et al., 2009. The obtained results include radiocarbon age corrected by Fontes-Garnier matrix exchange model considering dolomitization effect and dilution influence with the support of tritium and carbon-13 data (Mokrik et al., 2009).

A valuable dataset of intermediate and deep groundwater radiokrypton data was developed in 7 wells of the BAB (Gerber et al., 2017; Vaikmäe et al., 2020). Radiokrypton ages in 5 samples vary from 319 to 1157 ka. Residence time estimation in Genčiai and Riga brines could not be calculated as the samples appear to be older than 1300 ka, which is above the detection limit of the krypton-81 technique. However, the data were corrected using a three-member groundwater mixing model (brine-glacial-modern), dating Riga site sample >1279 ka. A case study of Klaipėda site (Well No. 25872) was conducted by applying the results for groundwater geothermal energy extraction evaluation at the Klaipėda Geothermal Demonstration Plant (KGDP), Lithuania (Brehme et al., 2019). The origin of this groundwater was suggested to be evapoconcentrated seawater altered by water-rock interaction and glacial meltwater or interglacial recharge. The brine component of this groundwater is estimated to be 3-5 Ma old (supported by ^{40}Ar and ^{4}He data), while the meteoric and glacial parts vary 0.3-1.3 Ma (Brehme et al., 2019; Gerber et al., 2017).

For 40 years, helium distribution in the BAB was studied using the INGEM-1 device (Juodkazis & Tibar, 1989; Mokrik et al., 2002). Helium data was used for conventional dating (Mokrik et al., 2021; Mokrik, et al., 2022).

A significant part of the research, including groundwater dating, focused on the Ignalina Nuclear Power Plant (NNP) surroundings (Mažeika, 1999; Petrošius, 1990). Radiocarbon data and estimated age were measured for the planned Visaginas Nuclear Power Plant construction area to characterize the groundwater circulation (Mažeika et al., 2013). Groundwater sampling, analysis, and dating where executed by the Department of Hydrogeology and Engineering Geology of Vilnius University as a part of the international research program F33022 within the International Atomic Energy Agency (IAEA): Integrated studies of crustal permeability based on environmental isotopes, noble gas data, and shallow-deep groundwater flow and particle track modeling in the surrounding area of Ignalina NPP (Mokrik et al., 2022). A set of geochemical, isotopic, noble gas, hydraulic data, and flow modeling was used to evaluate sedimentary cover permeability. Groundwater age obtained with ^{4}He were compared to particle track time and ^{81}Kr methods on the investigated sites (Mokrik, et al., 2021). This analysis reveals groundwater circulation rates in the Ignalina NPP. The developed numeric model was verified with the hydraulic head and other parameters of the boreholes in the BAB to obtain a more accurate MODPATH particle tracking (Mokrik et al., 2022). Environmental factors which could be significant for the Ignalina NPP safety had been studied before, including monitoring programs: meteorological, seismic conditions in the region; geotechnical factors; flood risk assessments, isotope, and chemical content monitoring in the surrounding area. Two main programs that required attention to the Ignalina NPP's environmental issues were the decommissioning plan and Radioactive Waste Management. Strategies, principles, policies, and laws within the Republic of Lithuania were established to ensure a proper NPP Decommissioning and Radioactive Waste Management (Mokrik et al., 2022).

Each noble gas (NG) isotope may originate from a few sources such as crust, mantle, atmosphere, or result in anthropogenic contamination (Aeschbach-Hertig & Solomon, 2013; Ballentine & Burnard, 2002; Ozima & Podosek, 2002; Porcelli & Turekian, 2014; Sano et al., 2013; Steiger & Jager, 1977). It is a valuable tool to determine a groundwater formation processes, origin, and age. Noble gas content in groundwater results is usually being corrected for the atmosphere equilibrated water (AEW). It shows either oversaturation or undersaturation of each noble gas (neon, argon, krypton, xenon, and sometimes helium) compared to AEW under specific thermodynamic conditions (usually STP, Standard Temperature and Pressure) (Aeschbach-Hertig et al., 1999; Aeschbach-Hertig & Solomon, 2013; Burnard, 2012; Jähne et al., 1987). Deviation from AEW could be due to water formation conditions, geochemical environment, groundwater flow, exchange ratio, recharge, discharge, open or closed system, aquitard confining properties, etc. (Aeschbach-Hertig et al., 1999; Aeschbach-Hertig & Solomon, 2013; Burnard, 2012; Jähne et al., 1987).

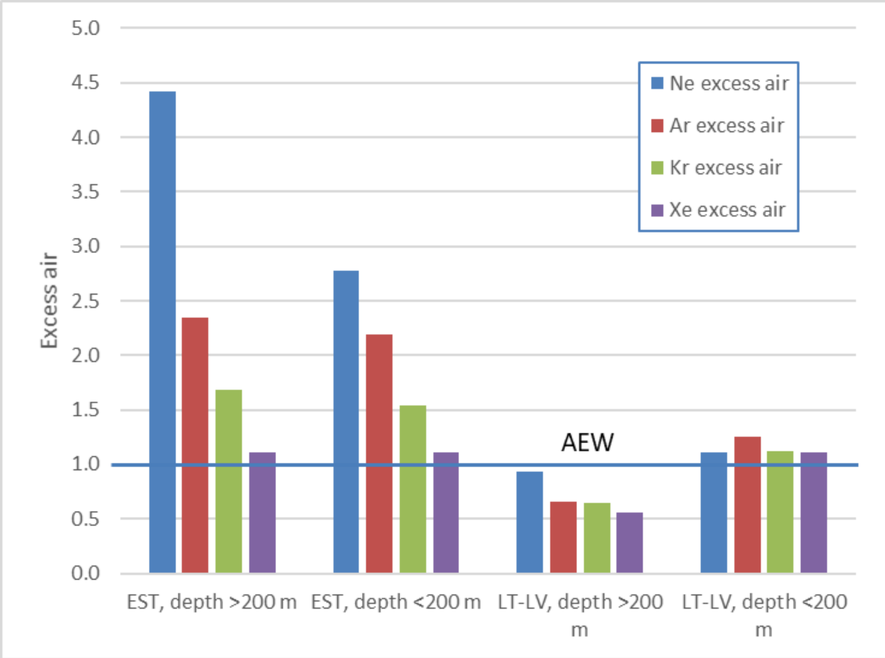

Figure 1.1. Average values of noble gas excess air in the Estonian (EST) and Lithuanian-Latvian (LT-LV) deep-intermediate and shallow groundwater. The blue line represents air-equilibrated water (AEW) at Standard Temperature and Pressure (STP).

Figure 1.1. represents the average excess air calculated from the noble gas dataset. A total of 48 data entries are present in this dataset. All data were divided into four groups: the Estonian groundwater aquifer depth above and below 200 m, and an identical depth subdivision of Lithuania-Latvia. Average values are calculated from EST>200 m: 10 samples, EST<200 m:18 samples, LT-LV>200 m: 13 samples, LT-LV<200 m: 7 samples. Noble gases analysis for groundwater dating is relatively new in the Baltic states; therefore, a volume of data is minor, but the current dataset is sufficient to make some insights into NG setting of the BAB. The Lithuanian and Latvian deep and intermediate aquifers groundwater lack noble gas excess air for Ne, Ar, Kr, and Xe. Smaller amounts of noble gases could result from prolonged saline and brine groundwater stagnation leading to gradual degassing. An elevated temperature in deep aquifers could also significantly diminish noble gas solubility and force degassing. Deep groundwater may be undersaturated with respect to AEW in the aquifer, but become oversaturated while extracting due to a decrease of pressure (Gerber et al., 2017). Groundwater thermal anomalies in the Cambrian, the Lower-Middle Devonian, and the Upper-Middle Devonian aquifers of the western

part of the BAB (Juodkazis et al., 1997; Šliaupa, 2009; Šliaupa et al., 2010; Suveizdis, 2000) may be a significant factor for noble gas content.

Considering the noble gas anomalies in the BAB groundwater, it is necessary to establish possible average background values in various depths and origin groundwater. A partitioning between gas and water phase results in an equilibrated system (Aeschbach-Hertig et al., 1999, 2008). In the case of natural water, such a system could be a shallow groundwater-atmosphere, which is expressed as air-equilibrated water (under STP conditions). Such water is likely to be a modern meteoric origin fresh groundwater observed in shallow confined or unconfined aquifer systems. In this case, a slight air excess is tolerable because of air dissolution during the recharge and saturation aquifer with water (Aeschbach-Hertig et al., 2008; Weißbach, 2014). Shallow aquifer Lithuanian groundwater is almost in equilibrium with air.

In deeper aquifers, the noble gas content differs from modern aquifers. It could be due to a temperature variation during the Holocene and Pleistocene recharge. Yet, other conditions *in situ* may be more important, such as groundwater age - the factor determining groundwater's exposure to certain thermodynamic conditions resulting in NG content. Gas solubility dependence on temperature, pressure, and salinity are the factors that must be accounted for while analyzing deep and intermediate-depth groundwater.

2. GEOLOGICAL AND HYDROGEOLOGICAL SETTING OF THE BAB

2.1. Geology and Hydrogeology of the BAB

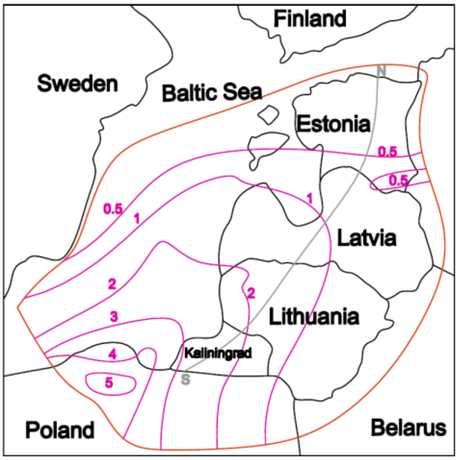

a)

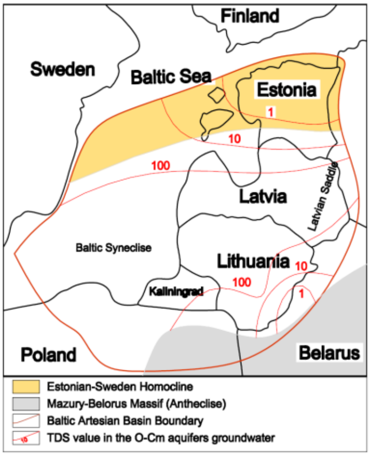

b)

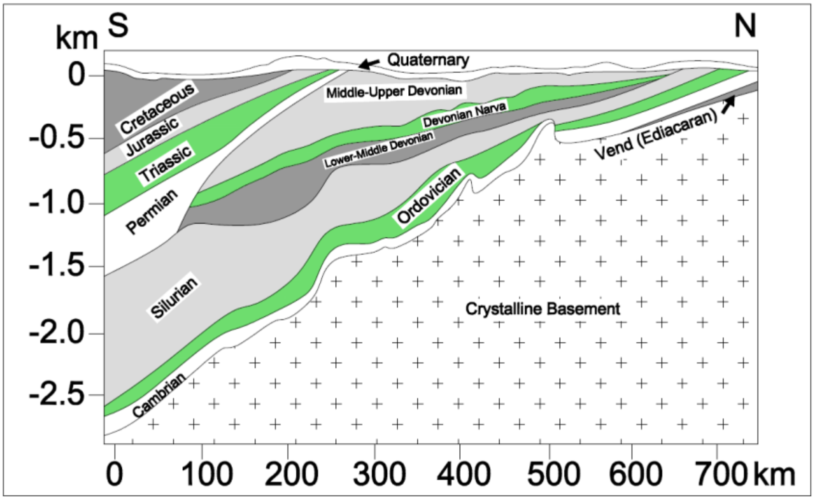

c)

Figure 2.1. a) Location of the Baltic Artesian Basin. N-S cross-section line. Brown line - the BAB boundary, purple lines and numbers - crystalline basement depth below sea level (km). b) Main structural elements of the BAB, and deep-intermediate-shallow groundwater lateral distribution in the O-Cm aquifer based on Total Dissolved Solids content, based on Mokrik, 2003. c) Longitudinal cross-section N-S of the BAB, After: Juodkazis, 1980a, 1980b; Mokrik et al., 2021; Pärn et al., 2016; Virbulis et al., 2013.

The Baltic Artesian Basin is a large sedimentary basin in the northern Europe, underlaid by a crystalline rock basement of the East European Craton. The Baltic Artesian Basin's total area is around 426 thousand square kilometers (Cheban, 1966; Delina et al., 2012; Juodkazis, 1980a, 1989; Juodkazis & Mokrik, 1981; Kondratas et al., 1969). It covers the whole territory of Lithuania, Latvia, Estonia, and Kaliningrad (Russia) as well as the territory of Poland up to the Teisseyre-Tornquist Lineament. A significant part of the BAB is under the Baltic Sea (Juodkazis & Mokrik, 1981).

Sedimentary basin depths reach more than 5 km in the southern part of the BAB (Kondratas et al., 1969; Mokrik, 2003; Suveizdis, 2003). All major aquifer system layers are found in the cross-section of the BAB starting from Ediacaran (Vend) to Quaternary (Figure 2.1.) (Juodkazis, 1980a, 1989, 2003; Kondratas et al., 1969; Mokrik, 2003; Mokrik et al., 2004). Crystalline basement consist of igneous and metamorphic rock (Kirs et al., 2009; Puura et al., 1997; Skridlaitė & Motuza, 2001; Wiszniewska & Krzemińska, 2005). The main geostructures of the Baltic Sedimentary Basin are the Baltic Syneclise (the Polish-Lithuanian Trough), the Latvian Saddle, the southern slope of the Baltic Shield, the northern slope of the Mazury-Belarus Anteclise, and the Estonian Homocline (Brangulis & Kaņevs, 2002; Paškevičius, 1994; Suveizdis, 1994, 2003).

Hydrostratigraphic division of the BAB includes the following aquifers or their systems: Cm-V (in the eastern part of Estonia subdivided into V_2gd, V_2vr and the Kotlin formation V_2kt (aquitard in between), O-Cm, D_{2-1}, D_2šv-ar, D_3dg-pl, D_3st, P_2-D_3fm, T_1, J_3-J_1, K_2cm-K_1, K_2, and the multilayered Quaternary aquifer system. It is essential to notice that the weathered upper part of the crystalline rock basement is supposed to act as an aquifer significantly changing the view on groundwater flow, mass transport, origin, composition, and other features on the regional scale. Regional-scale aquitards in the BAB generally separate groundwater into three main zones: shallow freshwater (active exchange, depth <360 m), mostly brackish and saline groundwater (delayed, depth 360-1850 m), and brine (stagnant, depth >1850 m) (Mokrik, 2003). The interaction among these zones was analyzed in this study as shallow-intermediate-deep levels.

During the last years, the BAB regional 3D mathematical flow model of BAB sedimentary basin groundwater body had been created at the Department of Hydrogeology and Engineering Geology of Vilnius University. Hydraulic parameters, piezometric heads, and the occurrence of the aquifer systems, aquifers, aquitards, and crystalline basement (CB) were obtained from the calibration procedure and verification for

MODFLOW2000 simulation of the BABHEGM (the latest update in 2016-2019) (Figure 2.2.).

In the BABHEGM there are two separate layers of CB representing this situation: CB aquitard (k=1E^{-5} m/d) and aquifer (k=0.1 m/d) (Table 2.1.). Cm-V aquifer systems include V_2gd, V_2vr aquifers with the hydraulic conductivity value range k=0.5-6 m/d, Kotlin formation, and overlaying Lontova aquitard k=1E^{-7}-1E^{-5} m/d. The Cm-V aquifer system is located mainly in the eastern part of the BAB and Estonia with the general flow direction northward, a discharge zone appearing in the bottom of the Gulf of Finland (Figure 2.2.).

Similarly, in the O-Cm aquifer system, groundwater flows from the deepest parts of the BAB in Poland towards the periphery (north-east direction) (Mokrik, 2003). However, tectonic faults divide the aquifer into separate blocks preventing groundwater's smooth flow. This phenomenon is critical in the stagnant flow conditions in depth, where hydraulic heads distribution is observed to be discontinuous along the flow path (Juodkazis & Mikalauskas, 1994). The Lithuanian and Latvian Cm, and the Estonian O-Cm aquifer system is k=0.2-5 m/d. The occurrence of the O-Cm aquifer system covers almost all of the BAB (Figure 2.2.). In southern and central parts, it is in the deep parts of sedimentary cover with a stagnant water regime. On the Estonian Homocline, it is in the intermediate-shallow level. O-Cm confined with regional S-O aquitard, through which vertical upward leakage occurs (k=1E^{-9}-1E^{-3} m/d). Yet, in the northern part of the BAB, an inversion of the hydraulic heads leads to downward percolation.

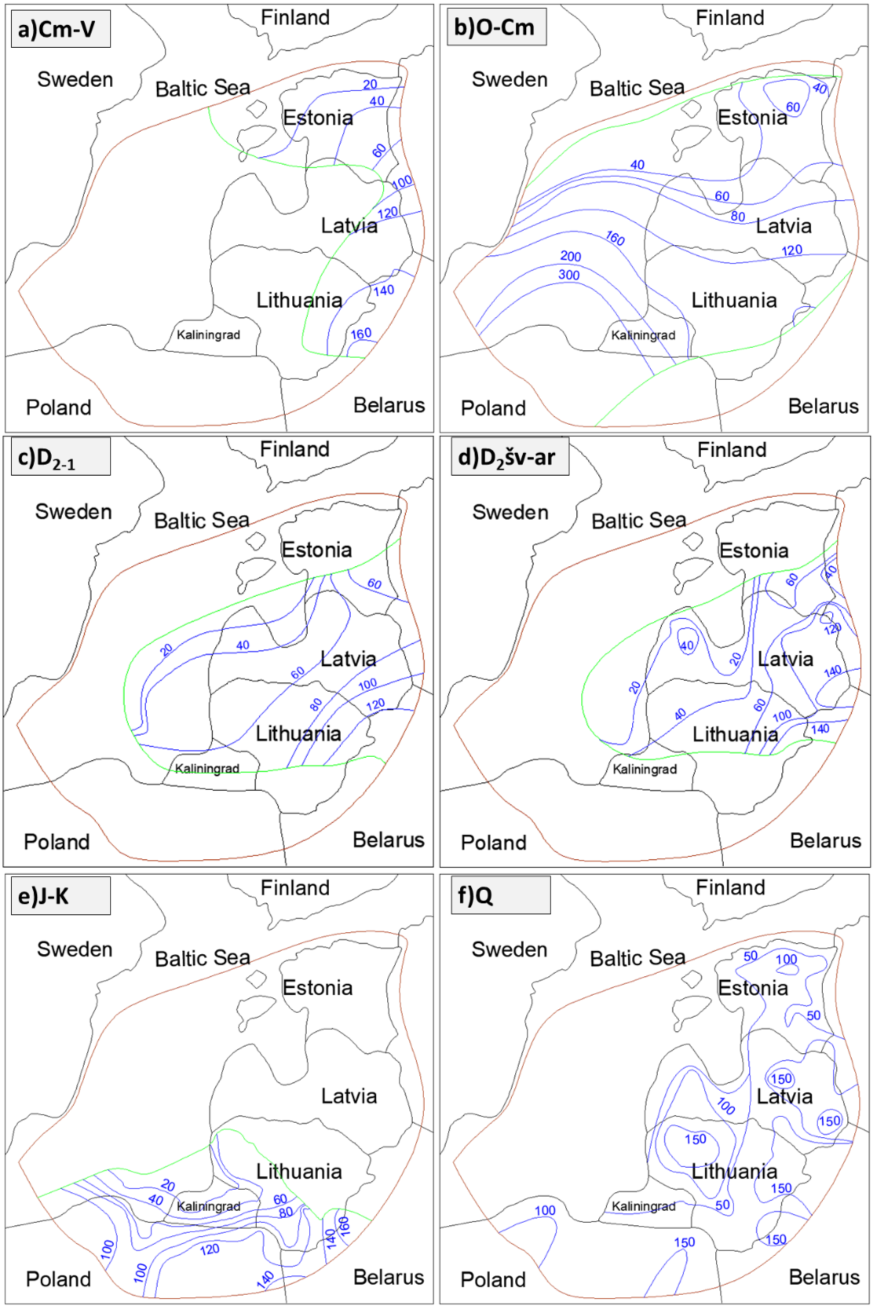

Figure 2.2. General hydraulic head of aquifers is represented with blue lines, abs. l. m. Hydrodynamic units planar location is marked with a green and red line (BAB outward boundary): a) Cm-V+Cmln; b) O-Cm; c) D_{2-1}pr-tl +D_2nr, d) D_2šv-ar, e) K and J formations; f) Q. Quaternary aquifer heads are plotted on the continental part of the BAB.

In Estonia, the S-O formation is subdivided into the aquifer (upper part) and the aquitard. The thickness of the layer increases from north towards the southwestern part (>300 m) (Cheban, 1966; Juodkazis, 1980a).

The Middle-Lower Devonian aquifer groundwater flows from the southeastern part of the BAB to discharge into the sea (Figure 2.2.). Due to this aquifer's inclination and varying thickness, flow transects shallow-intermediate-deep levels resulting in various isotope-geochemistry groundwater. The shallow part is in South Estonia-North Latvia, the deepest being in the western Lithuania and the Kaliningrad District (Figure 2.2.) (Mokrik, 2003). The range of hydraulic conductivity is 0.2-2.4 m/d. The overlying Devonian Narva regional aquitard (k=1E^{-8}-1.7E^{-5} m/d) occurrence is similar to D_{2-1} (Figure 2.2., Table 2.1.). The Middle Devonian aquifer D_2šv-ar planar occurrence is close to D_{2-1}; however, the profile mainly covers intermediate and shallow levels. The recharge and discharge places coincide with the elevated ground levels, general flow from highlands toward lowlands. Modeled hydraulic conductivity varies 0.5-5.6 m/d. The Upper Devonian hydrostratigraphic unit consists of the following formations: D_3am, D_3st, D_3pm, D_3dg-pl in this study is united into one. In this multilayered aquifer-aquitard unit, hydraulic conductivity varies from 5E^{-7} to 15 m/d (Table 2.1.). These aquifers were studied and modeled previously in more detail (Bujanauskas, 2018; Gregorauskas et al., 2008). The general flow in these aquifers is from the highlands in Latvia toward the Baltic Sea.

Mesozoic aquifers K_2cm-$K_{1,}$ K_2, $J_{3-1,}$ and P_2-D_3fm are located in the southwestern part of the BAB scaled to J-K unit (Figure 2.2.). Hydraulic conductivity in these layers varies 0.2-8 m/d. K_2, K_1, and T_1-P_2pr aquitards, which separate J-K unit aquifers k=1E^{-8}-1E^{-5} m/d (Table 2.1.). Due to relevance of injection anomalies in the southern Lithuania (Druskininkai, Birštonas, etc.), a local Triassic aquifer T_1 was modeled (k=0.2-4 m/d) to represent the layer from which the discharge into overlaying aquifers occur (Table 2.1.). Paleogene and Neogene formations occur sporadically throughout the BAB, and the Quaternary aquifer system is heterogeneous; therefore, these layers were modeled as a single unit, indexed as Q (Bujanauskas, 2018). Hydraulic conductivity was adjusted to represent the semi-permeable layer k=2E^{-7}-0.1 m/d. A similar approach was successfully applied in the previous modeling of the BAB (Bujanauskas, 2018; Gregorauskas et al., 2008, 2009, 2012; Kuzinas et al., 1981, 1982; Stravinskas et al., 1984). Hydraulic heads of the Quaternary aquifer system are plotted on the continental part of the BAB where it occurs; general flow goes from the highlands toward the Baltic Sea and major river valleys (Figure 2.2.).

Table 2.1. The hydraulic conductivity of the BABHEGM aquifer, aquifer systems, aquitards, and united hydrodynamic units.

Index	Description	Hydraulic conductivity (x-y for aquifers; z for aquitards) m/d (BABHEGM values)
Q	Unconfined aquifer	$2E^{-7}$-0.1
Q-Pg	Quaternary, Neogene, paleogene layers separating unconfined/underlaid confined aquifers	$2E^{-7}$-0.1
K_2	Aquifer	0.5-8
K_2	Part of the upper Cretacious layer separating K_2/K_2cm-K_1 aquifers	$8E^{-6}$-$1E^{-4}$
K_2cm-K_1	Aquifer	0.5-8
K_1	Part of the lower Cretacious layer separating K_2cm-K_1 /Jurassic aquifers	$1E^{-5}$-$1E^{-4}$
J_3-J_1	Aquifer system	0.2-1
T_1-P_2pr	Aquitard	$1E^{-8}$-$1E^{-5}$
T_1	Local Triassic aquifer	0.2-4
P_2-D_3fm	Aquifer system	0.2-4
D_3	Aquifer/aquitard multilayered unit of upper Devonian (D_3am, D_3st, D_3pm, D_3dg-pl, D_3jr)	$5E^{-7}$-15
D_2šv-ar	Aquifer system	0.5-5.6
D_2nr	Regional aquitard	$1E^{-8}$-$1.7E^{-5}$
D_{2-1}pr-tl	Aquifer system	0.2-2.4
S	Aquifer	0.2-2
S-O	Regional aquitard	$1E^{-9}$-0.001
O-Cm	Aquifer system	0.2-5
Cmln	Aquitard	$1E^{-7}$-$1E^{-5}$
V_2vr*	Aquifer	0.5-6
V_2kt	Aquitard	$1E^{-7}$-$1E^{-5}$
V_2gd*	Aquifer	0.5-6
Basement, PR	Aquitard	$1E^{-5}$
Basement, PR	Aquifer	0.1

2.2. Isotope-Geochemistry Setting

A chemical classification of the BAB groundwater is based on multiple parameters: hydrochemical facies, salinity, aquifer depth, and major ion ratios (Mokrik, 1996, 1997, 2003).

A **shallow active exchange** fresh groundwater zone covers the continental part of the BAB. Meteoric water recharge aquifers mainly in the highlands discharging in coastal submarine areas. Recharge and discharge areas are separated by a transitional zone, where the inversion of the groundwater heads occurs. A general flow in shallow and intermediate-depth aquifers is directed towards the Baltic Sea, discharging in the sea bottom and lowland river valleys (Juodkazis, 1980a, 1989, 2003; Kondratas et al., 1969; Mokrik, 2003).

The groundwater of Lithuania, Latvia, Kaliningrad shallow aquifers $\delta^{18}O$ vary from -7.7 to -13.9 ‰ (Mokrik, 2003; Rozanski & Zuber, 2000). However, past processes may have influenced the oxygen-18 content in shallow aquifers significantly. In Estonia, a strongly isotopically depleted groundwater is found $\delta^{18}O$ from -14 to -22.5 ‰. A wide range of $\delta^{18}O$ values signifies varying paleoclimatic conditions during the Pleistocene and Holocene (Mokrik, 2003). A completely different scenario was observed in Gotland Island, where isotopically enriched saline groundwater was found at the same depth with $\delta^{18}O$ values from -5.7 to -6.1 ‰ (Mokrik, 1997). Shallow BAB groundwater's Craig line equation is 7.9x+7.5, closely following GMWL (Figure 2.5.). The depletion of shallow groundwater stable isotopes in Lithuania (down to -12 per mil) and Latvia (-13.6 per mil) could result from seasonal variation in some cases or paleometeoric recharge. However, it could also be due to Pleistocene water recharge in well-confined aquifer groundwater.

Shallow freshwater is mainly bicarbonate type with Ca- and Mg-dominant cations with the rare exception of $Na\text{-}HCO_3$. Calcium-magnesium-bicarbonate facies are usually shallow modern groundwater (blue circle, Figure 2.3.) originating from the current meteoric water recharge. Modern groundwater TDS rarely exceeds 1 g/L and is found at the depth of 300 m (Juodkazis & Mikalauskas, 1994; Kondratas et al., 1969; Mokrik, 2003). Sodium-bicarbonate is exclusive groundwater detected in North Estonia O-Cm aquifer and associated with the processes of the Pleistocene glaciations (Cheban, 1966; Mokrik, 1996, 1997, 2003; Mokrik & Vaikmäe, 1988; Vaikmäe et al., 2001). Another case of $Na\text{-}HCO_3$ facies is found in the southwestern BAB Cretaceous aquifers - groundwater altered by cation exchange with glauconite mineral found in aquifer matrix, (Juodkazis &

Mikalauskas, 1994). Both cases are represented by a black dotted circle (Figure 2.3.). The northern Estonia Cm-V aquifer groundwater (Ca-Na)-(Cl-HCO_3) type was affected by carbonate mineral precipitation, cryogenic salt rejection, and other processes during the Pleistocene and Holocene periods (black dashed circle, Figure 2.3.) (Cheban, 1966; Gatalski, 1954; Mokrik, 1996, 1997, 2003; Mokrik & Vaikmäe, 1988; Vaikmäe et al., 2001). An elevated amount of sulfate is found in some intermediate and shallow aquifers regions: the Devonian, O-S layers in Latvia, and the northern Lithuania region (green circle, Figure 2.3.) (Babre et al., 2016; Delina et al., 2012; Juodkazis, 1980a, 1989, 1994; Kondratas et al., 1969; Levins et al., 1998; Mokrik, 1996, 2003; Paukštys et al., 1999). An exclusive shallow depth anomaly is found in the Kaliningrad District's Cretaceous and Jurassic aquifers groundwater where sodium-sulfate type groundwater exists and should be associated with seawater influence (blue star, Figure 2.4.) (Mokrik, 2003).

More **saline** groundwater is found in the **delayed zone** of the BAB, where TDS values vary from 5 to ~100 g/L. Due to hydrostatic and lithostatic pressure in intermediate and deep aquifers, groundwater flows towards the periphery (Mokrik, 2003). Stable isotope $\delta^{18}O$ values range from -13 to -6 ‰. According to isotope-geochemistry, this zone is intermediate, between stagnant fossil brines and shallow freshwater. Delayed groundwater mostly evolved during mixing and *in situ* alterations of groundwater (Mokrik, 2003).

The deep-intermediate groundwater Craig line equation is 7.2x-3.3 (Figure 2.6.). Two Craig lines could be plotted on this graph to represent the isotopically depleted and enriched groundwater deviation from GMWL. Modern groundwater is considered a separation point (oxygen-18 -10.5 ‰). The isotopically depleted water line equation is 8.2x+10.2, enriched groundwater equation is 6.8x-6.6 (Figure 2.6.). Depleted groundwater occurs in intermediate depth in Estonia, Latvia, and some sites of Lithuania, while enriched values are found in Lithuania, Latvia, and Kaliningrad's intermediate-deep groundwater. Insufficient or unevenly distributed data entries of the BAB groundwater isotope-geochemistry information in the databases may cause such differences.

Sodium-chloride type is saline (TDS up to 2->100 g/L); intermediate-depth groundwater is found in all Baltic states as well (red circle, Figure 2.3.). Based on stable isotope data, its origin may be different. A separate case of Na-Cl groundwater is the southern Lithuania anomaly, where brine groundwater discharges into shallow freshwater aquifers making it sodium and chloride dominant with a range of TDS from 2 to 50 g/L (Juodkazis, 1989, 1994, 2003; Juodkazis et al., 1997; Zuzevičius, 2010; Zuzevičius et al., 2007). Usually, these groundwater facies are located below at a depth of a few hundred meters, but in anomalous regions, Na-Cl groundwater occurs in the shallow level or may discharge to the surface in the form of springs (Juodkazis & Mikalauskas, 1994).

High salinity brines stagnate in the deep aquifers of the BAB at the depth of >1.5-1.8 km. Due to an elevated temperature gradient and pressure at this depth, TDS could reach 140-400 g/L. Mainly enriched isotopic content is observed at the stagnant zone ($\delta^{18}O$ from -6 to -3 ‰) (Mokrik, 2003; Mokrik et al., 2021).

Sodium-calcium-chloride (in extreme cases, calcium-sodium-chloride) type brines evolve due to a prolonged cation exchange of stagnant groundwater with minerals in deep aquifers (>1 km) of Lithuania, Latvia, and Kaliningrad (yellow circle, Figure 2.3.) (Kondratas et al., 1969; Mokrik, 1997, 2003). Alteration degree ((rNa+rCl)/$rHCO_3$) is used to distinguish groundwater in the BAB down to a depth of 1800 m. Deeper chloride groundwater is predominant with calcium ions; therefore, the rCa/rNa ratio (eq/L) is suited better (Mokrik, 1996, 1997, 2003). This ratio reveals Ca-Cl type groundwater anomaly in the stagnant zone of the O-Cm aquifer brines which occur on the Lithuanian-Kaliningrad coast and offshore zone (the area is about 5 thousand km^2). The local geothermal regime since the Cretaceous Period preconditioned the origin of this anomaly (Mokrik, 2003). Due to geothermal gradient inconsistency throughout the BAB, the temperature in the Cambrian-Ordovician aquifer varies from 98 °C to 21 °C in the western Lithuania and Riga (Latvia), accordingly (Mokrik, 2003; Mokrik, Samalavičius, Bujanauskas, et al., 2021). Higher temperatures catalyze groundwater isotope-geochemistry altering processes, for example, ion-exchange, membrane filtration, isotopic fractioning, gas dissolution, and dissolved solids diffusion through layers. The TDS value of the southern BAB groundwater on Poland territory is up to 300-400 g/L in the deepest parts of evaporitic rocks (Mokrik, 2003).

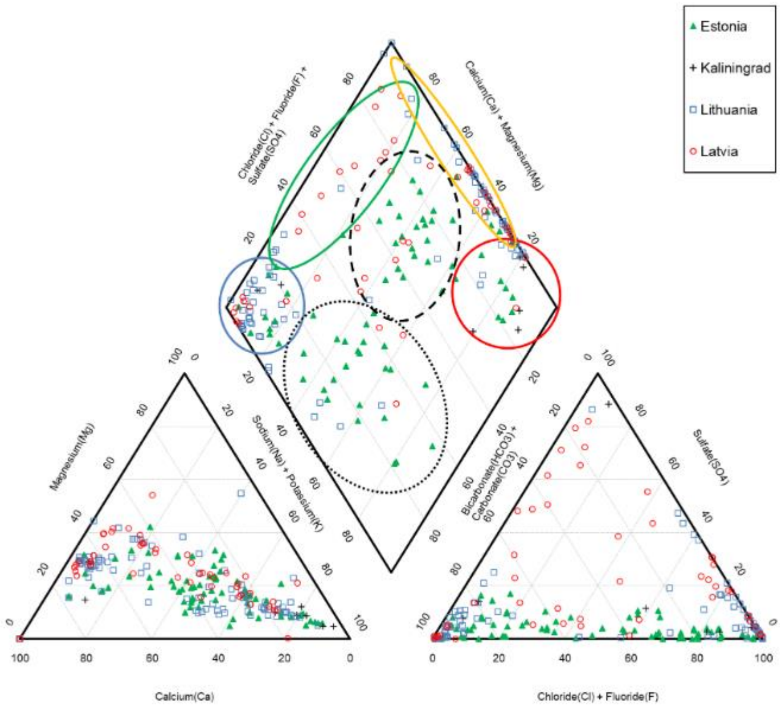

Figure 2.3. PIPER diagram of Estonia, Latvia, Lithuania, and Kaliningrad groundwater. Calcium-magnesium-bicarbonate facies are represented by a blue circle. Sodium-chloride type groundwater is represented by a red circle. Sodium-calcium-chloride type brines are represented by a yellow circle. Calcium-sulfate groundwater is represented by a green circle. Sodium-bicarbonate facies are represented by a black dotted circle. Varying (Ca-Na)-(Cl-HCO_3) type groundwater is represented by a black dashed circle. Exclusive sodium-sulfate type groundwater is represented by a blue star.

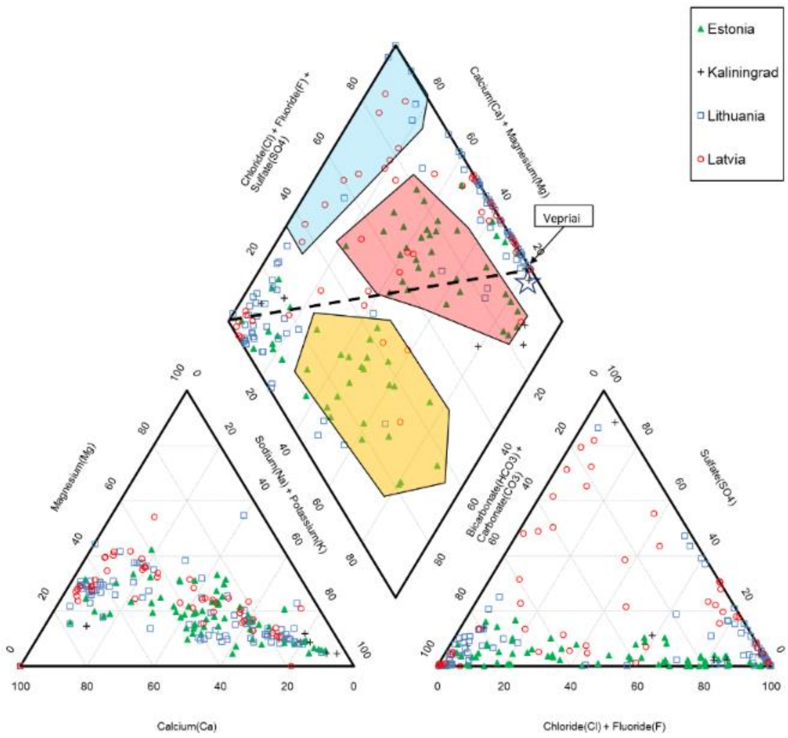

Figure 2.4. PIPER diagram of Estonia, Latvia, Lithuania, and Kaliningrad groundwater anomalies. Estonia Cm-V aquifer system anomaly represented by a red area, O-Cm by a yellow area. Sulfate-type groundwater in Latvia and Lithuania Devonian aquifers are in the blue area. Binary mixing in the southern Lithuanian interaction sites is represented with a black dashed line. A blue star represents exclusive sodium-sulfate type groundwater.

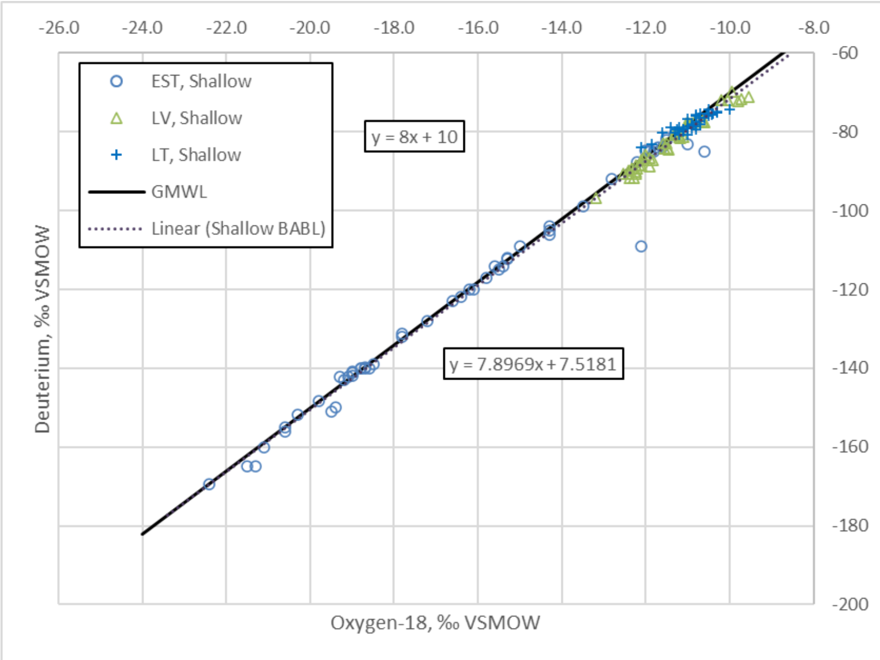

Figure 2.5. Craig diagram of the BAB in shallow groundwater.

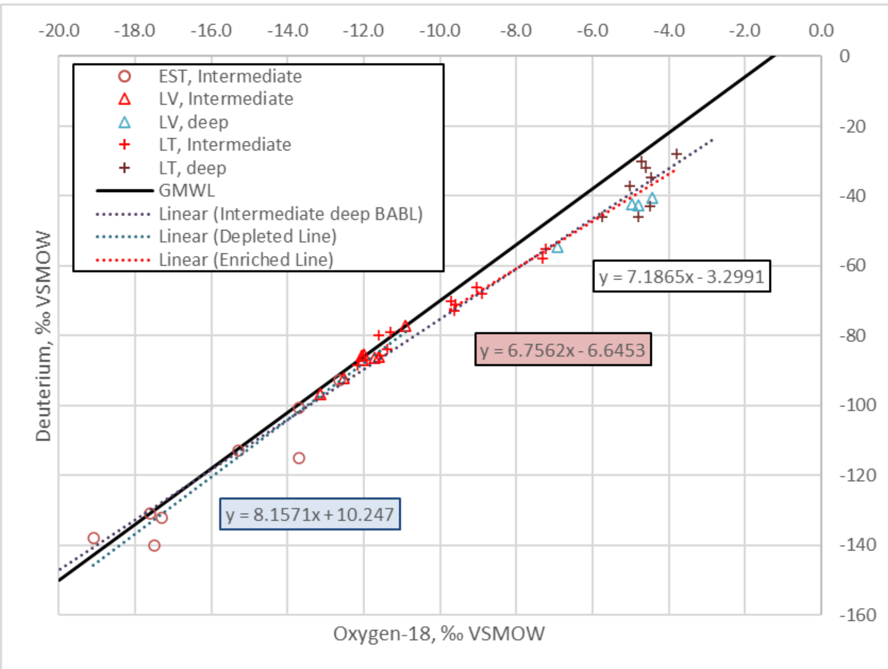

Figure 2.6. Craig diagram of the BAB in deep and intermediate groundwater. The blue dotted line represents depleted groundwater (oxygen-18 <-10.4 per mil). The red dotted line represents enriched groundwater (oxygen-18 >-10.4 per mil). Equations are colored accordingly.

2.3. Environmental Isotope Background Values and End-Member Reference Points

The background stable isotope content of modern groundwater in the BAB is average precipitation (or meteoric) water recharging shallow aquifers. Oxygen-18 and deuterium values of meteoric water depend on a couple of factors such as continental, latitude, altitude, and other effects (Mokrik & Mažeika, 2006; Raidla et al., 2016; Skuratovič, 2013). Mean weighted values of the BAB region precipitation are presented in Table 2.2. Data of $\delta^{18}O$ vary from -10.2 to -10.7 per mil. Marginal values in Belarus, Brest (-9.8 ‰), and Russia, St. Petersburg (-11.5 ‰), sites are not in the BAB region but are close to its southern and northern boundaries, accordingly. A clear latitude effect could be observed.

The value of $\delta^{18}O$ -10.5 per mil could be considered a starting point of isotope content evolution of modern groundwater towards depletion or enrichment. This value is almost identical to the average annual oxygen-18 value -10.4 ‰ used in previous research (Punning et al., 2008, 1987; Weißbach, 2014). Therefore, a depletion or enrichment in stable isotopes is considered in reference to modern groundwater. Yet, a study in which precipitation and shallow groundwater stable isotope content differences were analyzed showed isotopic depletion of groundwater compared to meteoric water of the BAB (Raidla et al., 2016). Modeling temperatures in 1981-2010 resulted in relatively depleted values, explained by more intense transpiration by plants in warm seasons; therefore, increasing the cold season portion of the recharge into aquifers (Raidla et al., 2016). Modern groundwater $\delta^{18}O$ content varies in the BAB from -9.0 to -13.0 per mil as a latitude effect of precipitation. The most depleted values are observed in the northern part (Estonia), while modern groundwater is more isotopically enriched in Kaliningrad, Poland, and the southern Lithuania. However, this modeling includes only 20 years of temperature change, while shallow groundwater in the BAB may often be older (Samalavičius & Mokrik, 2016; Štuopis et al., 2012). Evaporation of groundwater in the BAB vadose zone and from the unconfined aquifer water table could have a significant role in a stable isotope enrichment, as was shown by Skuratovič, 2013. Therefore, the average meteoric water stable isotope composition is by far the most reliable reference point.

This reference could also be applied to paleogroundwater, but it is necessary to emphasize the climatic changes in the Holocene and Pleistocene. Paleoprecipitation (paleometeoric water) stable isotope content was generally more depleted compared to the present. Approximate paleoprecipitation content could be calculated using the mean annual temperature and stable isotope values relationship expressed in equation (Dansgaard, 1964). During the Holocene, the average temperature in the northern hemisphere deviated from the current ±1° C (Borgatti & Soldati, 2013), which accounts for oxygen-18 content in precipitation -9.8 to -11.2 per mil. This value range could be applied as a background for groundwater up to ~10 ka old. During the Pleistocene, the average temperature drop from the present could be down to -8° C (de Schepper et al., 2013). This temperature could result in a mean oxygen-18 in precipitation values as low as -15 per mil.

Table 2.2. Weighted annual mean of stable isotopes oxygen-18 and deuterium. Data obtained using database (IAEA/WMO, 2019).

State	Weighted annual mean	
	Oxygen-18, ‰ VSMOW	Deuterium, ‰ VSMOW
Belarus, Brest	-9.8	-71.1
Lithuania, Vilnius and Zarasai*	-10.6	-75.3
Latvia, Ramata	-10.2	-71.1
Estonia, Tartu	-10.7	-76.5
Estonia, Vilsandi	-10.2	-73.3
Russia, St. Petersburg	-11.5	-87.4

*(Skuratovič, 2013)

Groundwater formation and origin are usually associated with sources of recharge. These sources are often considered end-members in groundwater formation scenarios and diagrams, valuable for analysis and interpretation. They may be internal - groundwater from other aquifers, saline, brine, or freshwater with various isotope-geochemistry compositions. The data of the present groundwater is, in most cases, included in datasets. Paleogroundwater composition was reconstructed using various formation scenarios and models, such as Br/Cl and Na/Cl diagram, which shows chemical evolution; paleoprecipitation $\delta^{18}O$ content is deduced from the paleotemperatures (Dansgaard, 1964). Talik zones reveal a possible way for uranium isotope ratio, helium-4, and REDOX condition variations (Mokrik & Samalavičius, 2022). External recharge sources are mainly meteoric water, glacial meltwater, and the Baltic Sea water (Table 2.3.). The Pleistocene or Holocene seawater and paleometeoric water isotope-geochemistry composition could have been different from the present situation for a couple of reasons: colder climate conditions influence stable isotope content in precipitation (Clark & Fritz, 1997; Jouzel et al., 1994), glacial meltwater and seawater used to mix during multiple ice sheet transgression and regression cycles in the Pleistocene; seawater evolution in the Holocene, lower salinity in the Late Pleistocene-Early Holocene (Andrén et al., 2000; Grigoriev et al., 2011).

Permafrost formation affected the isotopic content of the paleogroundwater. The data of permafrost collected from Siberia, Canada, and Alaska sites reveal that $\delta^{18}O$ values vary from -17 to -28 ‰ and -14 to -37 ‰ in the Holocene and the Late Pleistocene dated samples, accordingly (Brosius et al., 2012). Groundwater studied in Canadian shield (down to depth of 1,300 m) was cryogenically altered as well (Stotler et al., 2012).

Fractionation curve (Clark & Fritz, 1997; Michel, 1986) (Figure 2.7.) shows that freezing affects groundwater isotopic composition in two directions. For residual fraction from 1 to ~0.4, groundwater is isotopically enriched, 0.4> depleted in reference to the initial composition (oxygen-18, -15 per mil). The residual fraction represents the unfrozen volume portion of the water unit. The example presented in Figure 2.7. represents a possible freezing curve of *in situ* isotopically depleted groundwater (oxygen-18, -22 per mil). Such effect of *in situ* freezing must be taken into account while evaluating possible end-members in the context of the northern BAB. The cryogenic EM manifests itself at the depths of permafrost propagation, which covers the shallow and intermediate levels of the BAB.

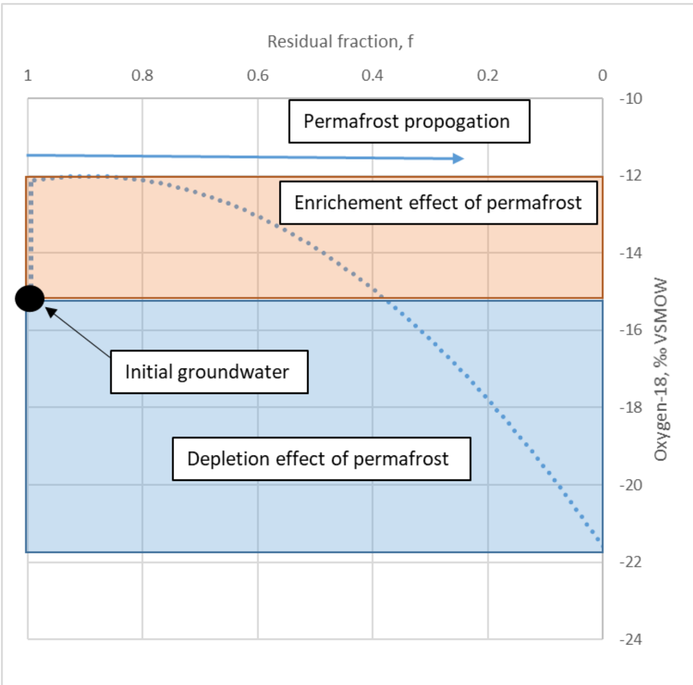

Figure 2.7. Rayleigh distillation effect on oxygen-18 content in the fixed water reservoir. The black circle represents the initial groundwater composition ((oxygen-18, -15 ‰). After (Clark & Fritz, 1997; Michel, 1986).

A generalized dataset of end-members collected from various sources is presented in Table 2.3. Some parameters are estimated according to the collected data (SI calcite and halite).

Table 2.3. Approximate values of the isotopic and geochemistry data of end-members relevant for the BAB groundwater. Chemical parameters of the Baltic Sea water and meteoric modern water were obtained from the Lithuanian database B. Oxygen-18 data of the Baltic Seawater obtained from Jefanova et al., 2020, meteoric water from IAEA/WMO, 2019 database resources. Glacial meltwater $\delta^{18}O$ and hydrochemical data obtained from the published material by Ferguson & Jasechko, 2015; Grootes & Stuiver, 1997; Johnsen et al., 1989; Jouzel et al., 1997; Lhomme, 2005; Mix & Ruddiman, 1984; Murozumi et al., 1969; Vasil'chuk, 2007; Yde et al., 2014). Precipitation at northern altitudes (Clark & Fritz, 1997).

<table>
<tr><th>Source</th><th></th><th>Oxygen-18, ‰ VSMOW</th><th>TDS, g/L</th><th>Chloride, mg/L</th><th>Sulfate, mg/L</th><th>SI calcite/ halite</th><th>pH</th></tr>
<tr><td rowspan="3">Glacial meltwater</td><td>MIN</td><td>-40</td><td rowspan="3"><0.1</td><td rowspan="3"><100</td><td rowspan="3"><5</td><td rowspan="3"><-1/<-8</td><td>4.5</td></tr>
<tr><td>AVG</td><td>-27.5</td><td>5 to 7</td></tr>
<tr><td>MAX</td><td>-15</td><td>9</td></tr>
<tr><td rowspan="3">Baltic Sea</td><td>MIN</td><td>-8</td><td rowspan="3">10</td><td rowspan="3">6000</td><td rowspan="3">850</td><td rowspan="3"><-0.7/<-3.5</td><td rowspan="3">7.5</td></tr>
<tr><td>AVG</td><td>-6</td></tr>
<tr><td>MAX</td><td>-4</td></tr>
<tr><td rowspan="3">Meteoric origin modern BAB</td><td>MIN</td><td rowspan="3">-10.4</td><td rowspan="3">0.4</td><td rowspan="3">10</td><td rowspan="3">10</td><td rowspan="3">1/<-9</td><td rowspan="3">7.5</td></tr>
<tr><td>AVG</td></tr>
<tr><td>MAX</td></tr>
<tr><td colspan="2">Precipitation at northern altitudes</td><td>From -25 to -18</td><td></td><td></td><td></td><td></td><td></td></tr>
</table>

3. MATERIALS AND METHODS

3.1. Groundwater Sampling and Analysis

Most of the data used in this study were obtained from previously published material and databases. A detailed explanation of the gathered data is given in the paragraph *Used datasets and data filtration*. The author of this study participated in field works in 2017 for groundwater sampling in Lithuania along with the staff of the Department of Hydrogeology and Engineering Geology (HEG) of VU and the Lithuanian Geological Survey. Fifteen groundwater samples were collected, eight from shallow Quaternary aquifers in Mickūnai (Well No. 172, 186), Trinkuškiai (487), Kaniūkai (2276), Elektrėnai (10597), Salininkai (47520), Rūdiškės (26368), Alanta (403) and seven from intermediate-deep aquifers in Likėnai (11978, 21965), Birštonas (4913), Palanga (47543), Telšiai (26418), Anykščiai (12350), Rokiškis (12349). Alanta sample was faulty, therefore, the obtained data is not valid. Sampling and analysis were the same for all groundwater levels: shallow, intermediate, and deep, except for tritium, which was measured in the Quaternary aquifer (shallow) groundwater samples. Various sampling techniques were applied according to the requirement for laboratory analysis.

Sampling procedures of the 2017 campaign. Groundwater for major chemical composition was sampled into 0.5 L plastic bottles. Trace element analysis requires a sample to be acidified - nitric acid was added into a plastic vessel (50 mL) according to the protocol (AntonParr, 2014). Water for stable isotope (deuterium and oxygen-18) analysis was sampled into 50 mL plastic bottles. For tritium volumetric activity determination, 1 L of groundwater was collected into plastic bottles. For helium analysis using the INGEM-1 device, samples were taken into glass bottles (0.33 L), airtight sealed with rubber corks. Excess air was removed from bottles with the help of a metal wire while tightening the cork (Levina et al., 1975). For noble gas analysis at IAEA Isotope Hydrology Laboratory, samples were collected in copper tubes. A steady flow of groundwater was released through the copper tube, both ends clamped without stopping the water stream. It ensures that groundwater is without air contamination according to the procedure described in Aeschbach-Hertig, 2020; Aeschbach-Hertig & Solomon, 2013; Beyerle et al., 2000.

Analysis of the 2017 campaign samples. The laboratory of the Lithuanian Geological Survey conducted major ion composition analysis using spectrophotometer Genesys 20 and Jemway PFP7. The error for this analysis is ±10%. Necessary parameters pH; Eh (redox potential), mV; and the temperature were measured during the sampling with portable devices Multi-Line F/Set 3 or VWR MU6100H.

Trace element analysis was executed at the Department of Hydrogeology and Engineering Geology, Hydrochemistry laboratory using inductively coupled plasma optical emission spectrometer (ICP-OEC) Perkin Elmer Optima 7000 DV (BerkeleyRausser, 2014; PerkinElmer, 2008; UOV, 2019). The error for this analysis is ±6%.

Stable isotopes deuterium and oxygen-18 were analyzed using Mass Spectrometer Picaro Isotopic Water Analyzer at the Department of Geology of Tallinn University, Technology laboratory. The typical uncertainty for this analysis is $\delta^{18}O$ ±0.1‰ and δD ±1‰ (Brand et al., 2009; Pärn et al., 2016; Vaikmäe et al., 2020).

Tritium was measured at the laboratory of the Nature Research Center, using Quantulus Tri-Carb 3170 Tr/Sl; the errors for electrolytically enriched samples are ±0.2 TU, while a direct measurement is ±2.4 TU (Mažeika, 2007).

Noble gases (He^3/He^4, He, Ne, Ar, Kr, and Xe) were measured at the Isotope Hydrology Laboratory at the International Atomic Energy Agency (IAEA). Sample extraction system, mass spectrometer MM5400, and two quadrupole mass spectrometers (QMS) were used to determine noble gas content in groundwater samples (Matsumoto et al., 2017; Suckow et al., 2007). The uncertainties calculated from the NG dataset (He^3/He^4 ±5 %, He±5 %, Ne±4 %, Ar±1 %, Kr±6 %, and Xe±10 %) (Vaikmäe et al., 2020).

3.2. Used Datasets and Groundwater Age Calculations

Two major sources of data were used in this study.

Dataset A. A dataset of the BAB groundwater published by Estonian scientists with the cooperation of Latvian and Lithuanian researchers (Vaikmäe et al., 2020) - in this study referred to as Dataset A. Lithuanian groundwater sample data obtained in the 2017 campaign was published in this dataset. Yet, the Estonian database lacks deep and intermediate-depth isotope-geochemistry data from Lithuania.

Dataset B. The first step of the alternative data base development occurred during 1976-2000 and was conducted by the Lithuanian Geological Institute (in this study referred to as Dataset B). Later on, it has been compiled at the Department of Hydrogeology and Engineering Geology of Vilnius University during the past 40 years. It includes necessary Lithuania deep and intermediate groundwater isotopic and chemical data. Vilnius University, the Estonian Geological Survey, the Institute of Geology, and Tallinn Technical University published material that served as a data source during the second period of database creation. A number of sample and data positions overlap in both databases as they were developed separately but by using the same published material in many cases. Neither exclusive data in dataset B, nor the database itself had been published before. However, numerous generalized or actual data was analyzed in the following:

- Published material (Banys et al., 1979; Gerber et al., 2017; Klimas & Plankis, 2007; Mažeika, 1999; Mažeika et al., 2013; Mokrik, 1997, 2003; Mokrik et al., 2009; Mokrik et al., 2021; Mokrik & Samalavičius, 2022; Štuopis et al., 2012; Vaikmäe et al., 2020; Yezhova et al., 1996; Zuzevičius et al., 2007).
- Manuscripts, theses (Bujanauskas, 2016; Dzikaitė, 2003; Samalavičius, 2015; Samalavičius & Mokrik, 2016; Skuratovič, 2013).

Database B is supplemented with the calculated values of mineral saturation indices (SI), which are not included in database A. Saturation states of minerals were calculated with the help of the program code Phreeqc, wateq4 database. Initial parameters were applied where actual data was unavailable: the temperature - 10° C, electron activity (pe) - 0, density - 1 g/cm^3. Wateq4 code is developed for calculating mineral solubility as a possible derivative of the chemistry of natural waters. It uses multiple input parameters: field measurements (temperature, pH, Eh, dissolved oxygen), alkalinity, major and minor dissolved constituents, ion activities, chemical reaction database (Appelo & Postma, 1993; Ball & Nordstrom, 1991).

Due to the high number of data entries in databases A and B, a reduction in the analysis is necessary. For each task, data filtration was applied to collect adequate information and establish representative samples without losing any crucial details. A total of **5 datasets** were derived from databases A and B. Principles of data filtration are explained further.

1. **The noble gas dataset** was used from database A samples in which at least helium, neon, argon, krypton, or xenon was measured (Vaikmäe et al., 2020; Weißbach, 2014). The dataset consists of 48 entries. In most of them, oxygen-18 and chemical data are available. Air excess was calculated for neon, argon,

krypton, and xenon. The dataset includes data obtained during the 2017 campaign.

2. **The selective isotope-geochemistry dataset** was compiled from databases A and B. Samples should have at least some major ion composition (sodium, potassium, magnesium, calcium, chloride, sulfate, bicarbonate) and oxygen-18 isotope records. Dating results, physical-chemical parameters were included as well where available. A total of 215 entries are in this dataset. The dataset consists of shallow (<300 m), intermediate (300-1000 m), and deep (>1000 m) aquifer groundwater from Lithuania, Estonia, Latvia, and Kaliningrad District. Such depth subdivision and terminology (deep, intermediate, shallow) were used in this study unless stated otherwise. The dataset includes data obtained during the 2017 campaign.
3. A separate **dataset of oxygen-18 and deuterium** was extracted from the described isotope-geochemistry dataset to develop Craig diagrams (Figures 2.5., 2.6.). There are 174 entries in this dataset. The dataset includes data obtained during the 2017 campaign.
4. **A dataset of groundwater age results** of intermediate and deep groundwater dated with conventional radiokrypton and helium methods was compiled, accompanied by estimated particle travel times, from dataset A. The numerical model used in this study was developed by the staff of the Department of Hydrogeology and Engineering Geology of Vilnius University. A total of 12 entries are in this dataset (Tables 4.5., 4.7., 4.8.). The dataset includes data obtained during the 2017 campaign.
5. **Dataset for cryogenic anomaly** study in Estonia was created from Databases A and B. Estonia’s groundwater is subdivided into sub-regions to make a more precise analysis of the anomaly in the Cm-V aquifer. This dataset involves 102 entries.

Additional data were used in Table 4.1. and the analysis of talik environments in the paragraph *Estonia Homocline Anomaly*. Specific data for ^{14}C and ^{4}He in Estonia’s groundwater were collected during the sampling campaign in 1974-1975 (14 wells) by the Lithuanian Geological Institute and analyzed at its Radiocarbon Laboratory (Mokrik & Samalavičius, 2022). Additional sampling from Tallinn and Pärnu sites (15 wells) was conducted in 1981-1982 by the Estonian Geological Survey. Samples were analyzed at the Isotope Laboratory of the Institute of Hydrogeology and Engineering

Geology (Moscow) (Mokrik & Samalavičius, 2022). Radiocarbon was measured using counting liquid scintillation, $\delta^{18}O$, and $\delta^{2}H$ - mass spectrometers in the VSMOW system, $\delta^{13}C$ according to PDB standard. The activity of ^{234}U and ^{238}U were measured using an α-spectrometer after electrolytic precipitation at the Institute of Hydrogeology and Engineering Geology, Moscow (Yezhova et al., 1996). Helium gas content was measured using the INGEM-1 device at the Lithuanian Geological Institute (Banys et al., 1979; Mokrik, 1997; Mokrik et al., 2002).

As mentioned before, numerical 3D steady-state and transient groundwater model of the BAB was developed in 2016-2019 (abbreviated as BABHEGM). Numeric models were created using Groundwater VISTAS 6 Pro user interface and the code with a program for groundwater modeling (MODFLOW). Differential equations of the groundwater flow in the schematized underground environment are applied (Rumbaugh & Rumbaugh, 2011). The BAB flow model was calibrated with the actual hydraulic heads of the wells. The modeled area is approximately 500,000 km^2, covering the BAB and its boundaries with other significant basins. The total number of cells is 614,823, grid size 5x5 km. Hydro stratigraphic subdivision includes 31 separated layers (aquifers and aquitards) from the crystalline basement aquifer to the Quaternary aquifer system (Mokrik et al., 2021). Modeled groundwater ages were obtained using MODPATH simulation for particles tracking.

Calculation of conventional helium age (t_{He}) requires multiple parameters to be considered and known while using Equations 3.1., 3.2., 3.3. Uranium and thorium content should be known in the continental crust (crystalline basement) and aquifer matrix, if available. Helium production rate J' was calculated (Equation 3.1.) (Torgersen & Stute, 2013), using average thorium (1500 ppm) and uranium (440 ppm) values from the rocks of the crystal basement in Estonia (Mokrik et al., 2021; Raudsep, 1997). Rock density (ρ=2.5 g/cm^3), the porosity of aquifers matrix ($n_{e=}$0.15), and release factor Λ_{He}1 (Mokrik et al., 2021) were used for the corrected helium accumulation rate J (Equation 3.2.) (Torgersen & Stute, 2013).

$$\mathbf{J' = 0.2355 \times 10^{-12} \times ([U]\left(1 + 0.123\left(\frac{[Th]}{[U]} - 4\right)\right))} \quad \textbf{(3.1.)}$$

$$\mathbf{J = J' \times \left(\rho \times \Lambda_{He} \times \left(\frac{1-n}{n}\right)\right)} \quad \textbf{(3.2.)}$$

$$\mathbf{t_{He} = \frac{C_{He}}{J}} \quad \textbf{(3.3.)}$$

Helium content in groundwater (cm^3STP/g) and corrected helium production rate J (cm^3STP/(g×a)) are used to obtain the conventional helium age (a) (Equation 3.3.) (Torgersen & Stute, 2013). The uncertainties of the conventional helium age calculations in this study are ±20 %.

Considering that radiokrypton ages were not calculated in this study, no detailed methodic information will be detailed in this section. Reference to sources, including data, description, analysis, and calculations, are found in Gerber et al., 2017; Vaikmäe et al., 2020. A short sampling and analysis of radiokrypton in groundwater timeline then follows. Radiokrypton sampling campaign took place in 2013-2017 (Gerber et al., 2017; Mokrik et al., 2021). Fieldwork, sample collection, and preparation were accomplished by a cooperation of the Laboratory for Radiokrypton Dating, Argonne National Laboratory; University of Bern; Tallinn University of Technology; and Vilnius University (Mokrik et al., 2021; Mokrik et al., 2022) According to the sampling procedure, groundwater is being pumped through the degassing unit. Extracted gases are separated and collected in a steel container (Gerber et al., 2017; Lu et al., 2014). Isotope ratio ^{81}Kr/Kr was analyzed using the Atomic Trap Trace Analysis (ATTA) technology at the Laboratory for Radiokrypton Dating, Argonne National Laboratory (Gerber et al., 2017; Mokrik et al., 2021). The uncertainty of radiokrypton obtained ages is ±23 %.

4. RESULTS AND DISCUSSION

The analysis of the BAB groundwater isotope-geochemistry must begin with the establishment of the background and anomalous groundwater plots. The anomaly term used throughout this study is a deviation from the site's background isotope-geochemistry values. In most cases, anomalies are considered any significant deviation (groundwater composition, age, location, depth, aquifer rock lithology) in the context of the same category (background) groundwater.

The isotopic and chemical parameters of groundwater vary in space and their origin often cannot be easily explained by existing geological and hydrogeological information or other environmental assessment factors. Anomalous groundwater is formed as a result of specific geological-hydrogeological conditions, lithological features of sediments or physical factors that determine changes in the composition of groundwater at a variety of relevant boundary conditions for groundwater flows. Each groundwater must be evaluated in various contexts: amounts of comparable data (resolution); chemical and isotopic composition; local and regional scale; aquifer position, depth range, and various dating techniques.

4.1. General Characteristic of the BAB Groundwater Anomalies

Many anomalies had been observed in previous studies, which is very helpful in identifying them. In these cases, the analysis could proceed further - by explaining the anomaly's origin, formation, or evolution in the light of the gathered data and known parameters. In other cases, a new formation model of anomalies is proposed during the analysis. These anomalies have been described and interpreted. It was not always certain what caused these anomalies; therefore, more than a few explanations of their origin was presented. Erroneous data could be mistakenly described as an anomaly as well. It was mentioned in the text where such suspicions arise to the author or are described in other publications. The source of inaccurate data could be explained for many reasons: wrong borehole parameters recorded in databases, insufficient water pumping from the aquifer before the sampling, data collection process, deviation from protocol, analytical errors obtained in laboratory measurements, etc.

4.1.1. Spatial Distribution Schemes of the BAB Groundwater Framework and Anomalies

The driving force of the hydraulic gradient determines groundwater distribution and zonality. Hydrodynamic network is necessary to follow the general term flow systems recharge and drainage sites divided into **regional** and **local** within shallow, intermediate, and deep intervals. These intervals are distributed spatially by fresh, brackish, saline, and brine water exchange zones.

Groundwater structural framework of the BAB features and anomalies systematic analysis revealed such schemes:

1. **The basin scale Estonian regional flow system anomaly of shallow and intermediate depth** of the O-Cm and Cm-V groundwater (Figure 4.1.). A new conceptual model suggests that this anomaly formed in the periglacial environment. Talik system and freezing-induced cryogenesis are the most important evolution factors. The evidence of these theses are discussed in the following topics:
    a. Talik system and permafrost influence on groundwater formation.
    b. Isotope-geochemistry aspects of anomalous groundwater.
    c. Thermodynamics of water-rock system, saturation indexes of calcite and halite.
    d. Noble gas content evidence of *in situ* groundwater freezing.
2. **Anomalies caused by deep and intermediate depth regional flow systems interaction in the central and southern BAB** (Figure 4.1.):
    a. Helium distribution and migration in the BAB multilayered system.
    b. Differences in groundwater dating results. Problems, causes, and alternative solutions.
    c. Deep-intermediate groundwater anomalies.
    d. Anomalies' occurrence in the regional flow systems interface boundaries (lowlands and slopes of elevated areas).
3. **Anomalies caused by local shallow and intermediate depth flow systems interaction** (Figure 4.1.):
    a. The southern Lithuanian injection type local anomalies caused by upward injection near tectonic lineament zones at rivers valleys.

b. Central BAB Devonian evaporitic (carbonate-sulfate) facies with brackish groundwater sub-regional anomaly in the fractured rocks.

Figure 4.1. Hydrogeological anomalies scheme of the BAB. Local injection anomalies and boundaries – after (Juodkazis et al., 1997). Sulfate groundwater, Ca-Cl facies anomalies, oxygen-18 data in Lithuania and Latvia – after: (Mokrik, 2003), in Estonia after talik scheme (Mokrik & Samalavičius, 2022). TFZ– Telšiai Fault Zone, after (Suveizdis, 1994, 2003).

There are two main trends of **shallow-intermediate groundwater** composition: the central and the northern part of the BAB (Estonia-Latvia, part of the northern Lithuania). $\delta^{18}O$ values are depleted from recharge regions toward discharge zones, and in the southern BAB - enriched. Chloride and oxygen-18 distribution in the BAB groundwater depends on the depth of the aquifer, and planar features on sub-basin levels.

In the central BAB (the westside Latvia and the northern Lithuania) territory, the Devonian aquifers groundwater is mostly of modern meteoric origin with slightly depleted $\delta^{18}O$ values (Figure 4.4., green arrow). This is presented in the profiles of the Figures 4.2., 4.3.: 4. Riga-Kemeri-Jūrmala site; 8. West Lithuanian site; 9. Panevežys-Biržai-Likėnai site. The anomalous $\delta^{18}O$ (-13 to -12 per mil) content in the areas is depleted compared to the overlying aquifer groundwater (-10 to -11 per mil). The depth where such anomaly is observed is at the intermediate level (300-700 m), D_{2-1} (Riga, Likėnai), and D_2 aquifer in Telšiai (Figures 4.2., 4.3.). However, this anomaly in each site differs in its geochemical characteristics as groundwater content results from sandstone cement, carbonate, and sulfate mineral dissolution. The recharge mechanism of paleoprecipitation is not clear; hydraulic head distribution should have been different from the present for substantial groundwater volume to recharge the intermediate level. Near the large Lielupe River valleys with intermediate and shallow discharges, this type of anomaly possibly results in $\delta^{18}O$ depletion of groundwater (Mokrik, 2003).

A depletion tendency formed by paleoprcipitation and cryogenesis anomaly is observed in North Estonia's Cm-V and O-Cm aquifer levels (shallow <300 m) as well as intermediate-depth groundwater in the southern Estonia (300-700 m). A cryogenic alteration can be deduced in a chloride-oxygen-18 plot – isotopically depleted groundwater (Rayleigh distillation) is more saline due to brine rejection (Figure 4.4.) (Mokrik, 1996, 1997, 2003; Mokrik & Samalavičius, 2022; Mokrik & Vaikmäe, 1988). Brown dashed arrows represent cryogenic evolution in Estonian groundwater. The talik associated processes enabled some meteoric water recharge (Mokrik & Samalavičius, 2022). The initial pre-cryogenic composition of the northern Estonian coastal groundwater is most likely a mix of seawater and Ca-Mg-HCO_3 freshwater. Part of it could be diluted with glacial meltwater recharge (Figure 4.4.) (Pärn et al., 2018; Raidla et al., 2009; Vaikmäe et al., 2001). An evident depletion of $\delta^{18}O$ could be observed along with the flow trajectory (Figure 4.2., profile 2-1). In these profiles, present hydraulic head distribution indicates depletion tendency toward the depth where vertical percolation predominates. However, the opposite hydraulic situation is on

Häädemeeste site (Figure 4.2., profile 3). The case of the previously described Devonian aquifer anomaly could take place in the D_{2-1} $\delta^{18}O$ ~-13 per mil. The Cm aquifer $\delta^{18}O$ ~-16 per mil content should be attributed to cryogenic type formation scenario. A depletion tendency of $\delta^{18}O$ towards the main discharge zone in the Baltic Sea predominate, with the sporadic enrichment near the buried valleys.

An inversion of hydraulic heads in the local injection points of the southern BAB results in $\delta^{18}O$ enrichment tendency toward the discharge zone near the river valleys (Figure 4.4., red arrow, Figure 4.2., profile 5). Saline groundwater injections occur close to the tectonic faults, connecting shallow and intermediate groundwater. Intermediate depth *in situ* saline groundwater is usually enriched with $\delta^{18}O$; therefore, mixed shallow groundwater in these areas is also affected (Gregorauskas et al., 2017; Mažeika, 1999; Mokrik, 2003; Zuzevičius et al., 2007). An analogous situation is on the Druskininkai site where the intermediate level $\delta^{18}O$ is -7 per mil. Near the seacoast, located sites could be influenced by seawater (Mokrik, 2003). The Palanga site's (Figure 4.3., profile 8) intermediate groundwater $\delta^{18}O$ is -9.5 per mil; shallow groundwater -10 per mil. Groundwater's main discharge area of the D_2šv-ar is in the Baltic Sea. The southern part of the BAB intermediate level groundwater discharging leads to enrichment tendency.

The differences of the shallow-intermediate groundwater in the BAB are due to different groundwater origin and paleoenvironments during the Late Pleistocene according to radiocarbon, helium, and other dating techniques (Banys et al., 1979; Mokrik & Samalavičius, 2022; Pärn et al., 2018, 2019; Raidla et al., 2012). Shallow groundwater $\delta^{18}O$ values vary little (except for Estonia) and mainly depend on meteoric water composition. Intermediate level groundwater is in a delayed exchange zone, where it originates from multiple sources and is significantly older than the modern one (meteoric). The groundwater age is a non-direct evidence of the present groundwater flow direction as during the Holocene-Pleistocene it could have been different. The anomalies in the intermediate groundwater are heterogeneous in all of the BAB, resulting in the varying isotope-geochemistry.

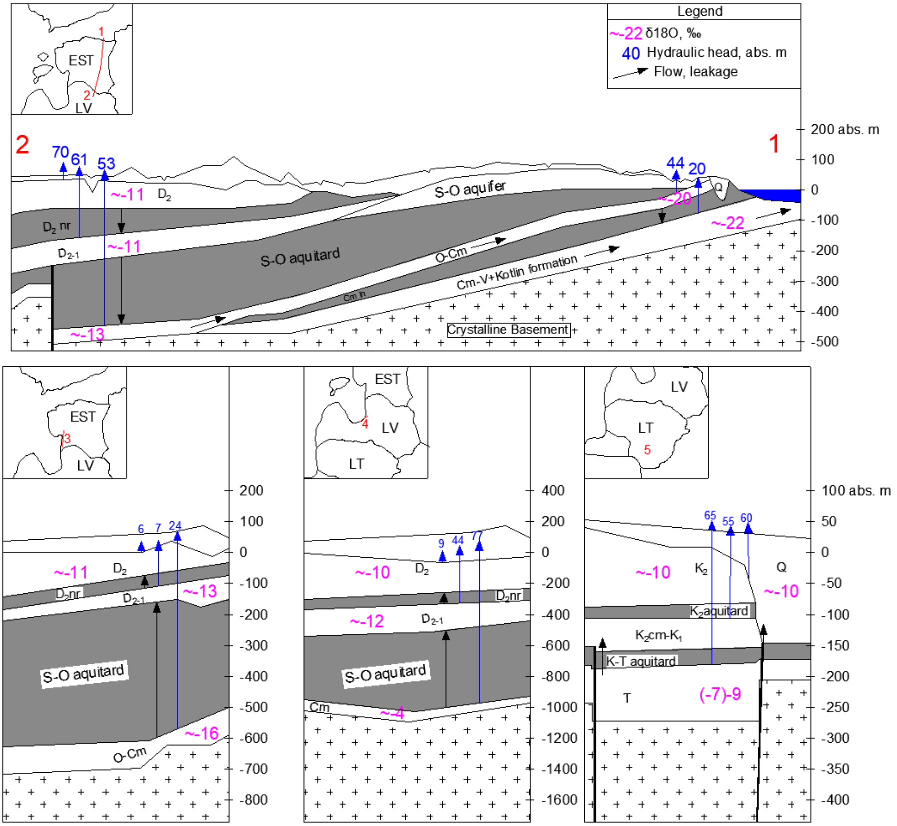

Figure 4.2. Schematized intermediate and shallow level groundwater interaction in the BAB. Flowlines, leakage in aquitards, and hydraulic heads are collected from the BABHEGM, except for the Birštonas site, where the data was obtained from Zuzevičius, 2010. Oxygen-18 values are approximate from dataset 2 entries [The selective isotope-geochemistry dataset] and the published maps (the Estonian Sites) (Pärn, 2018). 1-2. Cross-section from the northeastern to southern Estonia, the scheme after (Mokrik & Samalavičius, 2022). Profiles 3, 4, and 5 represent sites Häädemeeste, Riga-Kemeri-Jūrmala, Birštonas – accordingly.

Regional aquitards are the main factor for analyzing **intermediate-deep groundwater** interaction. Confining properties of the aquitards vary across the BAB: hydraulic conductivity (m/d) of S-O – $1E^{-9}$-0.001; D_2nr – $1E^{-8}$-$1.7E^{-5}$; T_1-P_2pr – $1E^{-8}$-$1.7E^{-5}$) (Table 2.1.). Hydraulic head distribution in the southern and central part of the BAB shows the process of the vertical discharge through the regional aquitards (Figure 4.3. profiles 7, 8, 9, 10). A similar situation is with the vertical helium flow. However, anomalies of helium content derived helium-4 ages and isotope-geochemistry are present. The main reason for this is a fault zone setting in the BAB, which constitutes highways for helium vertical emanation, dislocations limiting from the lateral flow (helium migration accordingly). Stagnant groundwater flow often does not coincide with the helium content expressed in the mean residence time. The differences in dating results obtained using various techniques (in this study: MODPATH simulation, conventional helium, and radiokrypton) illustrate this phenomenon. The isotope-geochemistry features should accompany these results to distinguish anomalies. The proven tool for this task is analyzing $\delta^{18}O$.

In the major part of the BAB, the S-O aquitard confines the Cm or O-Cm aquifer system where isotopically enriched brines ($\delta^{18}O$ -6 to -4 per mil) are located at 1-2 km depth. A very rigid inversion occurs in the southern Estonia ($\delta^{18}O$ -16 to -12 per mil) (Figure 4.2., 4.3. profiles 2, 3, 6-7). This inversion coincides with the inversed hydraulic heads in the southcentral Estonia, where vertical downward flow predominates. Helium ages in the southern Estonia O-Cm aquifer is 80-150 ka and is significantly younger than radiokrypton (timescale ~0.5 Ma). Helium and $\delta^{18}O$ reveal an anomaly in this region.

D_{2-1} aquifer confined with the Devonian Narva regional aquitard shows $\delta^{18}O$ depletion tendency along with the flow trajectory (Figure 4.3. profiles 6-7). $\delta^{18}O$ on Klaipėda site is -5 changing to -13 per mil in the southern Estonia along the cross-section; the significant decrease in the northern Lithuania (-12 per mil) (Figure 4.3. profiles 9-10). The helium age of the Klaipėda and Värska sites are ~600 and 35 ka, accordingly. The isotopic inversion occurs at depths 700-900 m. The helium age in Klaipėda is almost twice younger as compared to radiokrypton (1.2 Ma).

Latvian groundwater $\delta^{18}O$ data distributions reveal an inversion: a slight depletion (to -13.6 ‰) toward 0.5 km depth (Figure 4.4. green arrow, Figure 4.2. profile 4), and reverses to deep brines at 1 km depth (oxygen-18 above -5 ‰). A similar tendency can be observed in the chloride distribution, the inversion point seems to be around 10 gCl/L, but due to a data gap, it could be in the range of 10-50 gCl/L (Figure 4.4.). More data on Latvia's groundwater at the depth ranging 0.5-1.0 km could help to clear out this inversion. Helium age is three times younger than radiokrypton's, 0.3 and 0.9 Ma, accordingly.

An extreme anomaly is observed in Telšiai (Figure 4.3. profiles 9). Helium age is 5 ka, MODPATH's - 200 ka. A major isotope-geochemistry inversion occurs on the Telšiai-Šatrija sites separated with D_2nr aquitard.

Seawater intrusion is especially obvious for the Kaliningrad District - the groundwater is close to SDL (Seawater Dilution Line), (Figure 4.4. blue line). Shallow groundwater $\delta^{18}O$ is -9 per mil, intermediate level -7 per mil. The hydraulic head distribution indicates the vertical percolation going upwards (Figure 4.3. profiles 7); therefore, the leakage from the underlying aquifers could also affect the isotopic composition. A low volume of data on this site is insufficient to conclude any of the scenarios.

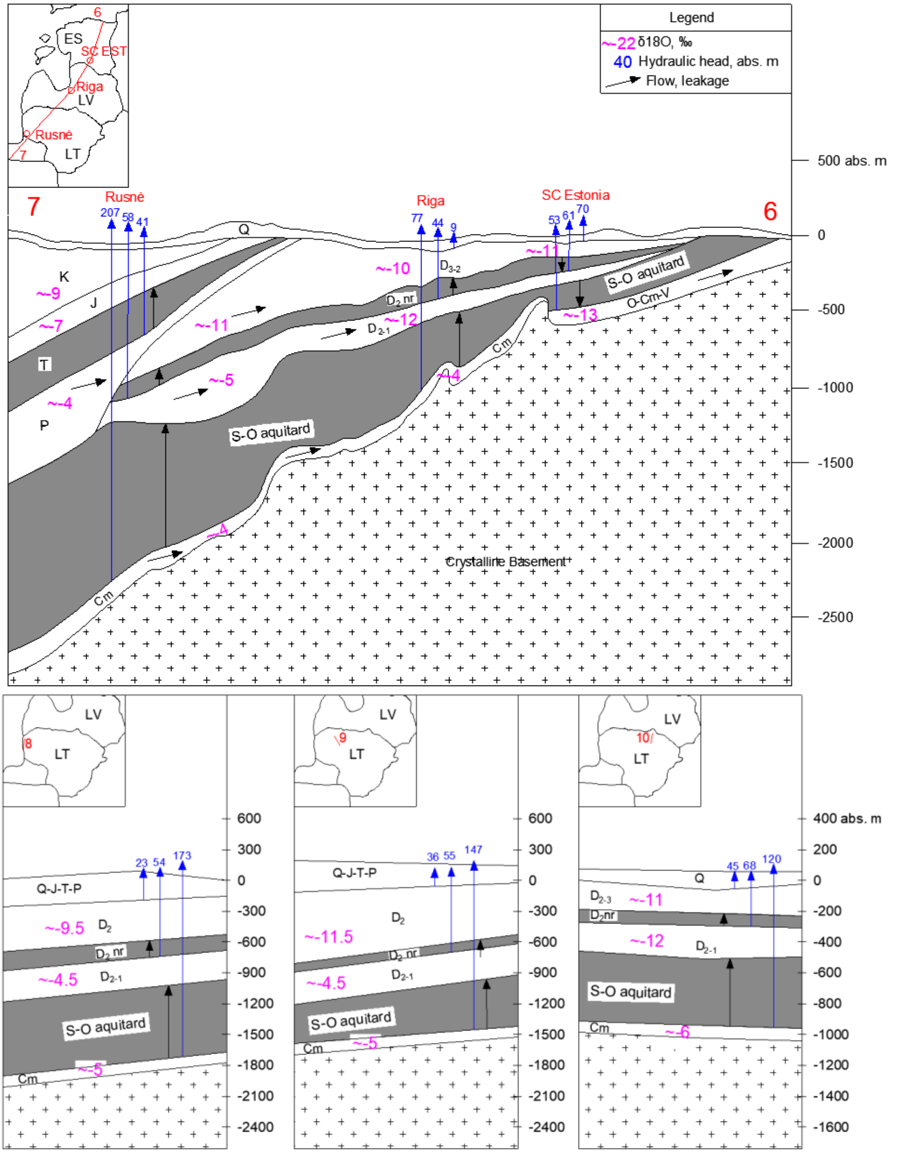

Figure 4.3. Schematized deep and intermediate level groundwater interaction in the BAB. Flowlines, leakage in aquitards, and hydraulic heads are collected from the BABHEGM. Oxygen-18 values are approximate from dataset 2 entries [The selective isotope-geochemistry dataset], except for Estonia, where the data was obtained from the published maps (Pärn, 2018). 6-7. Cross-section from the N.E. Estonia to Kaliningrad, layers geometry based on Juodkazis, 1980a, 1980b; Mokrik et al., 2021; Pärn et al., 2016; Virbulis et al., 2013. Profiles 8, 9, and 10 represent the Klaipėda-Palanga, Telšiai, Likėnai sites, accordingly.

These anomalies and inversions are a result of major regional aquitard settings. The shallow-intermediate-deep level groundwater is effectively confined from each other and could evolve separately. It leaves a specific signature of isotope-geochemistry, noble gas, and age in each zone or level. Nevertheless, the problem of groundwater composition in aquitards remains open. It requires specific study and data of isotope, major and trace distribution in the confining formations, and thorough analysis. It is often difficult to extract and sample groundwater from the aquitards. Therefore, databases often lack this type of content. The same problem stands with crystalline basement groundwater. Most of the data comes from sedimentary aquifer groundwater, while a few samples are taken from the basement. Data inconsistency should be accounted for in future campaigns and research emphasizing sampling from the less explored geological formations.

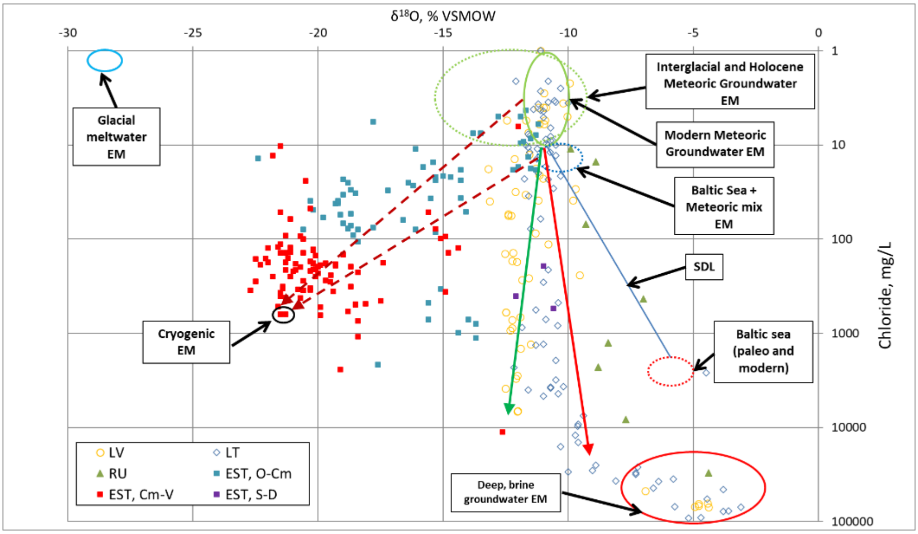

Figure 4.4. Chloride and oxygen-18 graph of the BAB groundwater. Groundwater samples: LT - Lithuania, LV - Latvia, EST - Estonia (S-D, Cm-V, and O-Cm aquifers, accordingly), RU - Russia (the Kaliningrad District). End members - EM. Blue line - SDL Seawater Dilution Line. Brown dashed arrows - cryogenic alteration trendline, red and green arrows - shallow-intermediate groundwater interaction in Lithuania and Latvia, accordingly.

4.1.2. Anomalies of Regional Groundwater Flow Systems Interface

Regional groundwater flow is in general distinguished by recharge areas at the highlands. This statement is relevant for the BAB as a sedimentary cover body structure located at the seaside. Shallow and intermediate groundwater flows are directed and discharged at rivers valleys, onshore lowlands, and submarine layers outcrop areas (Mokrik, 1997, 2003). On the contrary, deep groundwater flow is oriented from the central basin towards the periphery of marginal basin part and highlands slopes. On the slopes of homocline, anteclise, or other elevated areas, the hydrochemical and hydrodynamic barrier of shallow and intermediate groundwater flows occur. As a result, the transitional brackish and saline groundwater is formed (Mokrik, 1997, 2003).

On these barriers, **specific groundwater anomalies** could emerge. On the marginal parts of structural basins or near the slopes (between highlands and lowlands) exclusively, **brackish mineral** water types form. A similar transition is observed near the northern part of the Polish-Lithuanian Trough, where intermediate and deep groundwater connects. This phenomenon occurs in the deepest parts of the West Lithuania Lowland and the southern part of the Middle Lithuanian Lowland. Groundwater transition towards higher TDS takes place (Mokrik, 1997, 2003). Hydrogeologically active faults strongly influence Belt-like anomalies. The main faults in Lithuania are Telšiai together with the Klaipėda's zone; the South and East Baltic Fault (Baltic Fault Zone), which includes the Druskininkai-Biržai-Likėnai Faults; in the southwest Lithuania, the Nemunas Fault at the Sūduva High heading towards Nida (Figure 4.5.). In the territory of Latvia, the Liepaja-Riga-Pskov Fault Zone is located. A significant Pregol Fault Zone is found in the Kaliningrad District. In the Estonian Homocline,Middle (sometimes called Central) Estonian Fault Zone, Pärnu-Tapa Zone, and Vihterpalu Fault are situated (Figure 4.5.).

Close to these faults, anomalies with brackish water within a few kilometers belt are located, where the alteration coefficient is 12-100 (Mokrik, 2003). These bands extend on the basin margins and geostructure slopes. Such anomalies were observed in Cm-V and O-Cm aquifer systems around the Dzūkija High, along the river valleys of the Nemunas-Neris-Vilija, the southern slope of the Estonian Homocline close to the Central Estonian Fault Zone. In the middle-lower Devonian aquifer system, anomalies occur on the Mazury-Belarus Anteclise slope and Valmiera-Moniste-Lokno High. The Nemunas and Pregol Faults influence and predetermine anomalies for the Jurassic and Cretaceous aquifer systems. Two brackish areal anomalies in the Central BAB are the D_{2-1} aquifer system in the Jelgava-Riga-Pskov Zone (brown hash, figure) and the Cm-V aquifer system in Estonia, where groundwater TDS increase from 1 g/L at the Central Estonian Fault to 10 g/L at the Lokno High. A more detailed description of the boundaries and structures of these anomalies can be found in Mokrik, 2003.

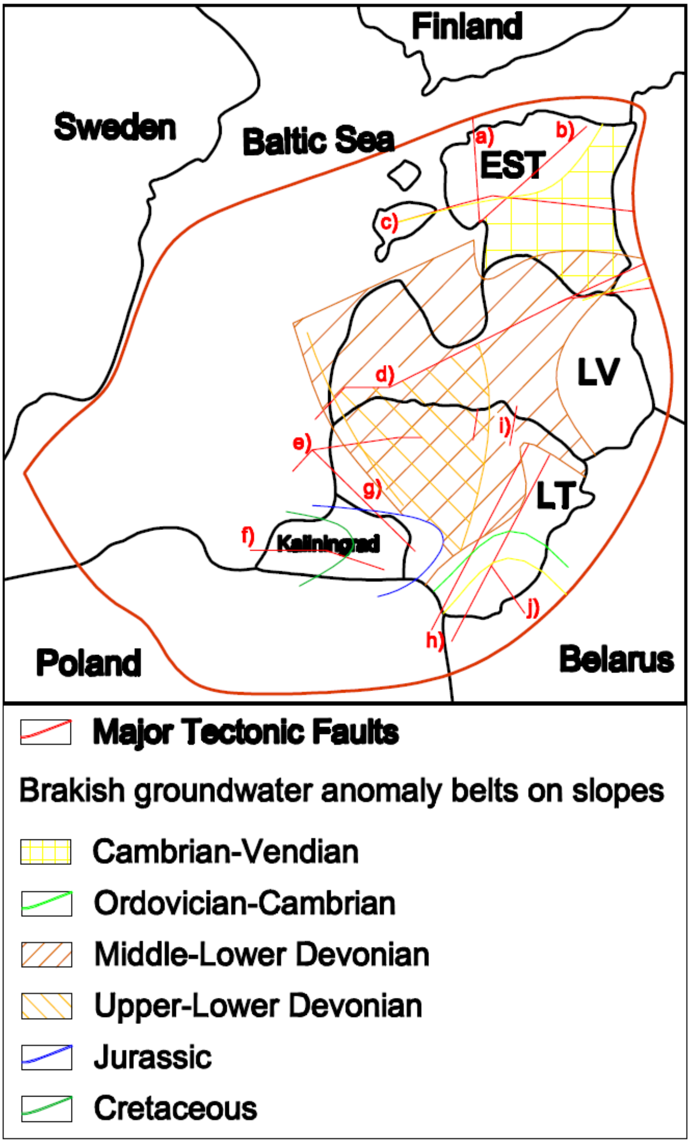

Figure 4.5. Brakish groundwater anomaly bands and major tectonic fault zones of the BAB. Faults and fault zones (red lines): a) Vihterpalu, b) Pärnu-Tapa, c) Middle Estonian, d) Liepaja-Riga-Pskov, e) Telšiai, f) Pregol, g) Nemunas, h) Southern Lithuanian, i) Baltic, j) Ashmyanski (Mokrik, 2003).

At the depth ranging 600-800 m, vertical interaction of deep-intermediate level groundwater occurs. A general vertical upward flow predominates, with the discharge areas covering the Baltic Sea Lowland area and river valleys (Juodkazis, 1980a, 1989, 2003; Juodkazis & Mokrik, 1981; Kondratas et al., 1969; Mokrik, 1997, 2003) (Figure 4.5.). The groundwater interaction in western coastal territory also depends on the Baltic Sea bottom's bathymetry. It influences shallow water discharge down to intermediate level and on brines where upward advective flow occurs.

The classification of anomalies of deep-intermediate flow system interface poses multiple problems. Hydrochemical, hydrodynamic and spatial distribution aspects are all valid as a basis distinguishing anomaly groups. However, each of them has significant shortcomings. Isotope-geochemistry parameters are essential to establish anomaly and background groundwater differences. However, the chemical data is difficult to analyze without additional information on groundwater flow path, depth, and age.

On the contrary, the spatial distribution, zoning, groundwater flow peculiarities do not provide specific information on the possible formation of anomalies without groundwater content. Therefore, the classification of anomalies could be done in the following order: 1. establish isotope-geochemistry peculiarities; 2. classify filtered data by their occurrence in planar and profile sections, areal or linear distribution, and association with structural elements. Attempts to do the general classification of intermediate-deep flow systems interaction results in five groups.

Southern Estonian areal anomaly group. The planar distribution covers the southern and a part of the eastern Estonian Cm-V and O-Cm aquifer systems groundwater. The aquifer overlays a crystalline basement on the Estonian Homocline, at the depths of 400-600 m. The main fault zones which affect flow conditions are Pärnu-Tapa and Middle Estonian (Figure 4.5.). Groundwater is brackish (TDS 1-4 g/L, Värska 18 g/L), oxygen-18 varies from -19 to -12 per mil, and pH is mostly alkaline up to 8.3. The key parameter which makes this groundwater anomalous is a strongly depleted oxygen-18 content.

Central BAB areal anomaly group. The anomalous brackish groundwater occurs in the D_{2-1} aquifer system at the depths of 400-800 m. Main fault zones may be attributed to the formation of this anomaly: in Latvia - Liepaja-Riga-Pskov, in the northern Lithuania - Telšiai, and the Baltic fault zones (Figure 4.5.). Groundwater chemical type is influenced by evaporite mineral (gypsum, carbonate minerals) dissolution, which makes water Ca-SO4 facies in extreme cases. Due to the anomaly's location at the deep-intermediate interface, deep saline and brines influence through faults. This results in an elevated sodium and chloride content near the tectonic lineaments. Oxygen-18 content is from -13 to -11 per mil, TDS 1-11 g/L, pH is slightly alkaline 7-8. The slightly depleted oxygen-18 content and evaporite mineral dissolution are the main parameters of determining the anomaly.

Southern Lithuanian local anomaly group. These anomalies are observed near the tectonic faults (Figure 4.5.) and large river valleys. They occur locally in the Triassic, Cretaceous aquifers at the depths of 300-400 m and strongly influence shallow groundwater. In some places, upward injection forms brackish groundwater up to the ground surface. The groundwater is enriched with Na and Cl and slightly with oxygen-18 (varies -11 to -9(7) per mil). Brackish groundwater TDS is 1-15 g/L, however, could be higher if the site was close to the saline water injection point. Helium anomalies are also observed in these places and indicate hydrogeologically active faults. The composition of groundwater is anomalous; however, it occurs locally within the proximity of the faults.

Western Lithuanian and Kaliningrad onshore and offshore's anomalies group. This part of BAB is significantly deeper - the Polish-Lithuanian Trough. Brackish-saline groundwater anomalies occur in the Jurassic aquifers in Kaliningrad and the Upper-Middle Devonian aquifers in Lithuanian part. Multiple major faults (Telšiai, Pregol, Nemunas) intersect this area; therefore, the brine groundwater effect on the intermediate-deep interface level is more significant. Intermediate level groundwater TDS is up to 20-30 g/L, oxygen-18 from -10 to -7 per mil, pH is close to neutral 6.5-7.2. Helium content, oxygen-18, and chlorides (TDS) are the main parameters indicating anomaly. The anomaly itself should be considered areal, but it is strongly influenced by the flux from the deep aquifers. Deep groundwater characteristics in this area (down to 2 km) determine the anomaly on the interface level. Another important factor distinguishing this regional anomaly from others is an elevated geothermal flux.

Eastern Lithuanian anomaly group. This anomaly group is located on the slope of the Mazury-Belarus Anteclise. The southern Lithuanian and the Ashmyanski Faults affect deep-intermediate interface anomalies. The Cambrian, Ordovician, and Middle-Lower Devonian aquifers in this area contain brackish-saline groundwater with TDS 1-10 (30) g/L. The groundwater freshening occurs in the southeastern direction on the Mazury-Belarus slope. The oxygen-18 content is -12 to -10 per mil; however, the value is -7.2 per mil on the Ignalina site. Due to the elevation of the slope, the groundwater TDS drop gradient is high. Therefore, the brackish groundwater area (1-10 g/L) is narrow, forming a band on the periphery of the BAB southeastern part (Figure 2.1. b). Oxygen-18 and chloride (TDS) are the main indicators of anomaly in this place.

Groundwater residence time is a critical factor determining the isotope-geochemistry content of anomalies. Multiple isotope-geochemistry anomalies could be observed on the Cl^-- $\delta^{18}O$ diagram (Figure 4.6.). An apparent trendline (dashed line) of all data is set on the plot to distinguish possible anomalies visually. A few anomalies could be revealed: elevated salinity in the southern Lithuania (Birštonas and Druskininkai), $\delta^{18}O$ depleted Pärnu, and Kuressaare groundwater. The Jurassic aquifer Svetlogorsk ($Na\text{-}SO_4$ facies), the Permian Svetlogorsk, $D_{2\text{-}1}$, Vepriai, and other samples are relatively enriched with oxygen-18 compared to their chloride content (Figure 4.6., red dashed line). A sub-regional anomaly may be associated with geothermal anomaly (up to 4-5°C/100 m) in the southwestern part of Lithuania and the Kaliningrad District onshore and offshore. Elevated temperature in local sites groundwater may increase oxygen-18 and deuterium fractioning towards enrichment (red arrow). The Vepriai site anomaly is placed in the impact crater. A single record of oxygen-18 (-3.1 per mil) exists in the database; therefore, it is difficult to make any conclusions. More data is required to elaborate on this topic. The Šatrija site's reading of oxygen-18 is significantly shifted from the BAB isotopic trend and should be reestimated.

Cation exchange caused the variation of calcium content in Lithuanian intermediate-deep brines from 21 to 54 %eq. Both extreme cases of chloride type groundwater are from $D_{1\text{-}2}$ aquifer: the Velaičiai groundwater is Ca-dominant Ca (54 % eq.)-Na (32 % eq.), Klaipėda is Na-dominant Na(67% eq.)-Ca (21 % eq.) type. These samples are taken from similar depths with TDS 83 and 92 g/L, accordingly. They are reflected in oxygen-18 values, which differ by 1.9 per mil. A factor leading to such a drastic difference in calcium content should be associated with an aquifer matrix mineral composition, which could be a key to a cation exchange rate and affect the hydrochemistry accordingly. However, the Klaipėda borehole groundwater was used for geothermal energy extraction, during which sulfates precipitated from solution and may have caused depletion of Ca content in groundwater (Brehme et al., 2019). Calcium content in brine samples from deeper O-Cm or Cm aquifers is consistent, varying 35-41 %eq.

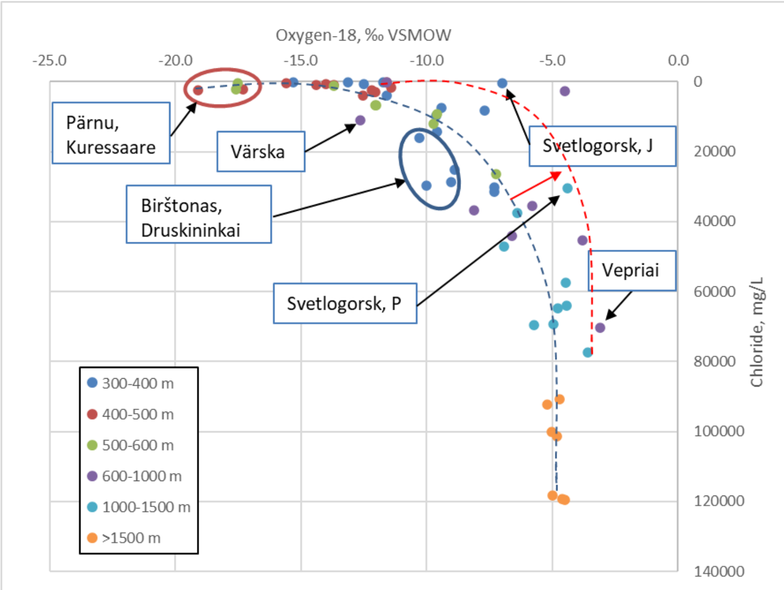

Figure 4.6. Oxygen-18 and chloride content diagram of the BAB deep-intermediate groundwater. Subdivided into smaller depth increments. Anomalies of the Telšiai, Šatrija, Velaičiai, Võisiku, Vepriai, and Svetlogorsk (the Jurassic and Permian aquifers) sites; the southern Estonia (red circle) and the southern Lithuania (blue circle) are marked separately. The blue dashed line represents the background values of the BAB groundwater. The red dashed line and red arrow represent isotope-geochemistry content shift due to geothermal anomaly in the southern part of the Baltic Basin.

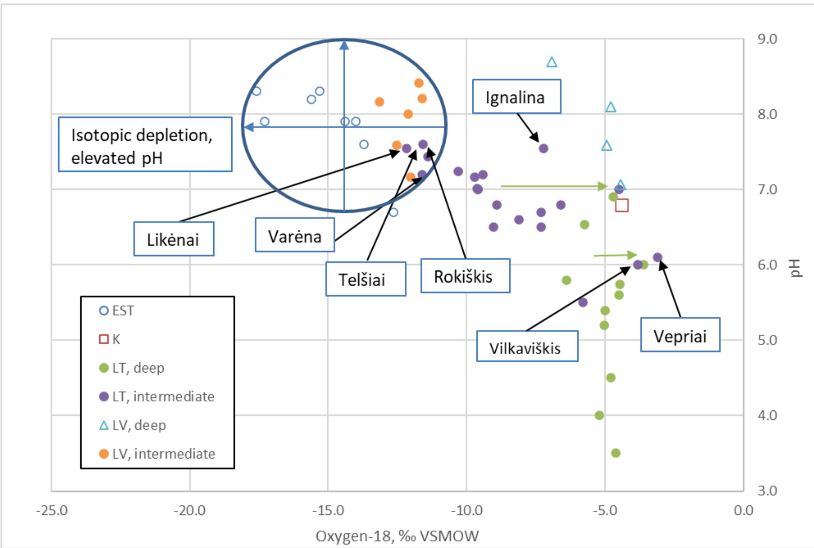

Figure 4.7. Oxygen-18 content and pH diagram of the BAB deep-intermediate groundwater. Subdivided into states. Anomalies of Telšiai, Likėnai, Varėna, Rokiškis, Šatrija, Vilkaviškis, Vepriai, and Ignalina are represented separately on the plot. Blue circle and blue arrows represent isotopically depleted pH elevated anomaly. Green arrows represent isotope enriched anomaly at intermediate depth range.

As mentioned before, the main subdivision of deep-intermediate level groundwater could be done based on oxygen-18 and deuterium isotopic fractioning by the reference of modern groundwater. The Estonian and Latvian intermediate groundwater is depleted as well as a few samples from Lithuania, in particular: Rokiškis, Likėnai, Varėna, and Telšiai (Figure 4.7.). These anomalies are not extreme (lowest $\delta^{18}O$ value in the Likėnai -12.2 ‰ and Telšiai wells -13 ‰) (Mokrik et al., 2009). Almost all isotopically depleted groundwater samples' pH is above 7, except for Värska pH=6.7. In Figure 4.7., isotopic depletion and increase in pH are represented by a blue circle and two arrows inside it. The depleted isotopic signature indicates that this groundwater could be exposed to a few chemistry altering factors, meteoric water recharge, *in situ* mixing, cryogenic alteration, dominant winter precipitation recharge, etc. The increase of pH values above 8, in this case, is due mainly to carbonate saturation or mineral precipitation during the Pleistocene evolution of the groundwater. The other part of the BAB intermediate and deep groundwater is neutral or acidic (pH<7.2) (Figure 4.7.). A decrease of pH in intermediate and deep aquifer groundwater is associated with the gradual accumulation of CO_2 gas, which forces carbonate equilibrium and pH accordingly toward acidic values. The exceptions are the Latvian deep groundwater (pH up to 8.7) and the Lithuanian sample from Ignalina (pH=7.6) from 500 depth O-Cm aquifer.

Overall, the anomalies in the deep-intermediate interaction interface are challenging to analyze, classify, and interpret. The isotopic data record is often very limited; chemical analysis alone is insufficient for such a task. The problem arises from the grey areas in the BAB where isotope-geochemistry data is scarce. The research was in most cases conducted in relevant places, leaving big territories unexplored. This should be accounted for future research and sampling campaigns. A more even spatial distribution of data records would significantly benefit the resolution of the background and anomalous groundwater content. The noble gas analysis is necessary for a deeper understanding of groundwater origin. The current record especially lacks data from Latvia, Poland, and the Kaliningrad District. Isotopic groundwater dating should be applied in many intermediate flow systems to obtain more records and identify patterns and tendencies ideally sufficient for mapping. The least explored part of the BAB is a crystalline basement and regional aquitard groundwater. The data from these objects would enable to clarify deep-intermediate groundwater interaction on many topics.

4.2. Basin Scale Anomaly of the Estonian Homocline

There are two main hypotheses on the Estonian groundwater isotope-geochemistry anomaly formation. A three end-member (EM) mixing (glacial meltwater, modern and saline groundwater (Pärn et al., 2018; Raidla et al., 2009; Vaikmäe et al., 2001)) and cryogenic alteration due to permafrost formation in the Pleistocene (Mokrik, 1996, 1997, 2003; Mokrik & Vaikmäe, 1988). Considering this anomaly, it is crucial to establish the age of the Estonian groundwater. This data were presented in the previous research stating that isotopically depleted groundwater in the northern Estonia could be dated to the Late Pleistocene (20-30 ka) (Banys et al., 1979; Pärn et al., 2018, 2019; Raidla et al., 2012) in the southern Estonia (Värska and Häädemeeste) 400-600 ka (Middle Pleistocene) according to radiokrypton (Gerber et al., 2017; Pärn et al., 2019). Radiocarbon age interpretation is supported with the data provided by tritium activity, radiogenic helium-4 amount, and stable isotope composition in the groundwater of the O-Cm aquifer system (Pärn et al., 2019). According to this data, O-Cm aquifer system groundwater seems to originate from mixing multiple source water with different ages. Radiocarbon, helium, and previously published radiokrypton ages suggest that groundwater most likely formed before the LGM period. It means that periglacial groundwater is currently present in the deepest aquifers of the northern part of the BAB.

Another important factor to consider is the influence of modern and paleoprecipitation recharge and mixing. The reconstruction of paleotemperature variation in the Holocene and Pleistocene shows that the annual average isotopic content $\delta^{18}O$ of precipitation in the Baltic region could have been -9.8 – -11.2 and down to -15 per mil, accordingly. Since the groundwater in North Estonia is isotopically depleted ($\delta^{18}O$ >23 per mil), the paleoprecipitation recharge could not have been a single factor of the groundwater formation. In this study, the analysis of the Estonian groundwater anomaly involves a few topics: isotope-geochemistry features in the context of the whole BAB groundwater, subdividing Estonia into zones or sub-regions to observe anomalies more thoroughly, talik distribution scheme, noble gas patterns of depleted isotope origin determination in groundwater.

4.2.1. Talik System and Permafrost Influence on Groundwater Formation

The conceptual talik scheme reconstructed in the northern BAB supports an opinion about the groundwater isotope-geochemistry features discussed in this chapter (Figure 4.8.). Talik distribution scheme is based on the present seabed and land depressions. The main lineament zones-taliks are the Gulf of Finland, the North-Central Baltic Proper, the Gulf of Riga, the Liivi Lowland, the Alutaguse-Peipus Lake Lowland. Talik system provides means for lateral flow in sub- and supra-permafrost aquifers as well as vertical flow (Figure 4.9.). However, in most cases, an upward groundwater flow was strongly confined by regional aquitards (Kotlin and Lontova) and permafrost terrains. The talik introduction into the groundwater formation scenario may suggest a mechanism to form various isotope-geochemistry content and chemical facies of the O-Cm and Cm-V groundwater. Aquifer recharge with meteoric and surface water could recharge aquifers near the taliks (Mokrik & Samalavičius, 2022).

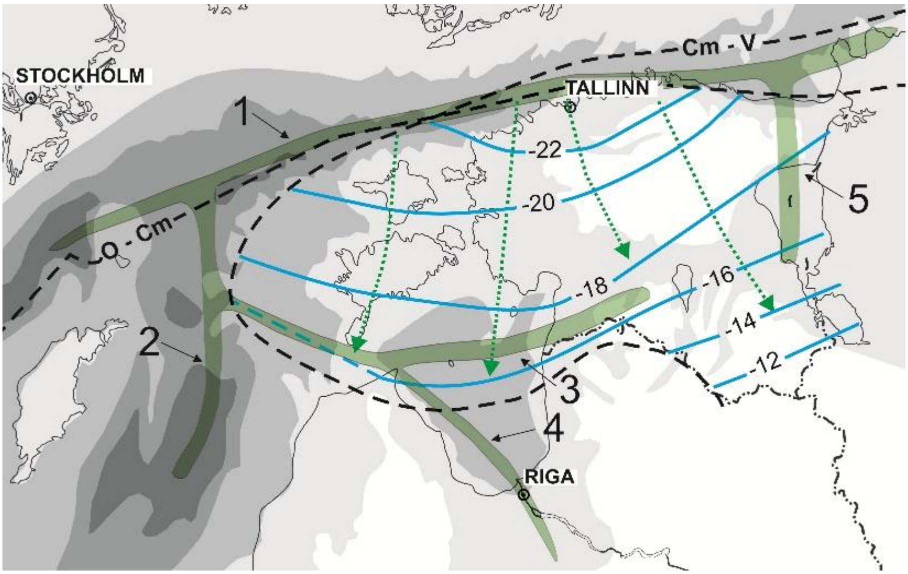

Figure 4.8. Talik zones' reconstruction scheme for the Pleistocene Epoch on the northern part of BAB. Numeration of taliks on the scheme: 1. Gulf of Finland Talik, 2. North-Central Baltic Proper Talik, 3. Liivi Bay Northern Talik, 4. Liivi Bay Southern Talik, 5. Alutaguse-Peipus Talik (Mokrik & Samalavičius, 2022).

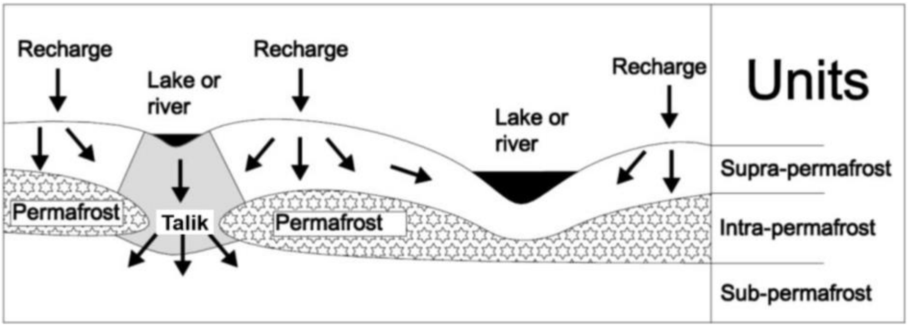

Figure 4.9. Talik zones' principal cross-section schemes based on Kurylyk et al., 2014; Mokrik & Samalavičius, 2022; Walvoord & Kurylyk, 2016.

Strongly depleted $\delta^{18}O$ content on the Tallinn sites (Kopli and Viimsi Peninsulas) coincides with the elevated uranium isotope ratios due to permafrost (Mokrik, 1997; Yezhova et al., 1996). The prolonged effect of permafrost on the groundwater in the Cm-V aquifer and the hydraulically connected upper basement part resulted in a substantial increase of ^{234}U in frozen rocks (Yezhova et al., 1996). Uranium isotope ratio $^{234}U/^{238}U$ may suggest cryogenic alteration via the formation of permafrost. In closed systems, this ratio is >1, while in open ones ~1 (Fujikawa et al., 2000). Permafrost traps uranium isotopes in the ice lattice; therefore, ^{234}U cannot escape. During the permafrost thaw, leaching of ^{234}U increases (Tokarev et al., 2006). In the northern Estonia, the Cm-V aquifer groundwater $^{234}U/^{238}U$ ratio was as high as 26 (Yezhova et al., 1996). The increasing uranium isotope ratios show the growing permafrost age (Ewing, O'Donnell, et al., 2015; Ewing, Paces, et al., 2015). Seasonal variation-induced permafrost thaw flow paths could also be studied using $^{234}U/^{238}U$ (Bagard et al., 2011; Hindshaw et al., 2018; Koch et al., 2013). Elevated uranium-234 and helium-4 production may be associated with rock fracturing while glacier retreat induced pressure release (Mejean et al., 2017). The study of St. Lawrence Lowland aquifer groundwater revealed that the release rate of helium might be up to 30,000 times higher than the local production rate (Mejean et al., 2017). This situation may have increased the uranium isotope ratio and overestimated helium ages in Cm-V aquifer groundwater.

The eastern part of the Gulf of Finland within the upper Cm-V layer consists of clays, siltstones, and sandstones. Groundwater on the close-by sites: $^{234}U/^{238}U$ ratio vary Lontova clays – 0.85, basement rocks – 0.75, Cm-V aquifer groundwater – 0.48-0.65 (Table 4.1.) (Bondarenko et al., 1981). Modern precipitation recharge may elevate the uranium isotope ratio up to 1.1. The Vendian aquifer in the Arkhangelsk-Severodvinsk-Novodvinsk site study area was covered with non-continuous permafrost (Malov, 2017).

Deeper layered brackish Vendian Mezen aquifer groundwater discharge upwards to the overlaying Vendian Padun aquifer bearing freshwater. The deeper (reduced Eh) groundwater uranium isotope ratio varies 4.8-7.2, the adjusted ^{14}C age range 17-33 ka, $\delta^{13}C$ -15.5 to -16.6 ‰, $\delta^{18}O$ content -14.4 ‰, TDS values 4.3 to 9 g/L (Table 4.1.). Meteoric water recharged upper part (oxidized Eh) freshwater $\delta^{13}C$ is -11.7 ‰, $\delta^{18}O$ -13.8 ‰ (Table 4.1.). Pleistocene glaciations, marine transgressions affected the Arkhangelsk region's groundwater isotope-geochemistry significantly (Malov, 2017). At seacoast line, shallow groundwater is slightly enriched with $\delta^{18}O$ = -7.7 ‰ and δ^2H = -98.9 ‰ (Malov & Tokarev, 2019). The elevated uranium ratios are found in the reduced groundwater.

Table 4.1. Isotopes and chemistry of the Tallinn and Sosnovy Bor intakes for Cm-V aquifer system modified after (Bondarenko et al., 1981; Malov, 2017; Malov & Tokarev, 2019; Mokrik & Samalavičius, 2022; Yezhova et al., 1996), (Poljakov unpublished, 1988 from DHVU).

Well No.	**TDS, g/L**	**$\delta^{18}O$, ‰**	**δ^2H, ‰**	**$\delta^{13}C$, ‰ PDB**	**$^{234}U/^{238}U$, (AR)**	**^{14}C, pmC**	**Adjusted ^{14}C and uranium decay ages, ka.**	**Depth, m b.s.l.**
Kopli Peninsula,								
14	0.95	-19.4	-150	-15.0	8.0	9.4	18.4	100-125
22	0.92	-20.6	-156	-16.2	3.3	16.8	15.4	50-120
17	0.43	-15.2	-110	-15.0	5.1	24.0	11.8	115-130
18	0.42	-15.1	-111	-12.5	3.0	43.0	5.5	116-135
19	0.44	-21.1	-160	-16.2	16.0	7.8	21.7	112-136
20	0.43	-21.3	-165	-16.2	26.0	7.1	22.5	90-140
Viimsi Peninsula								
21	0.46	-21.5	-160	-15.0	4.0	16.7	14.8	45-115
27	0.84	-22.5	-170	-12.4	15.1	33.6	7.5	60-125
26	0.35	-12.0	-90	-12.6	2.7	54.7	3.6	80-122
25	0.53	-14.4	-105	-13.4	11.5	53.2	4.3	60-110
66	0.7	-15.0	-111	-11.2	-	48.1	3.7	59-125
67	0.8	-16.3	-125	-14.7	-	39.2	7.6	56-120
1A	9.3	-11.6	-	-	-	-	-	110-120
Rakvere Deposit area, Kabala site								
606 O_2 kk	0.4	-13.7	-	-15.7	1.6	53.0	5.7	45
513 O-Cm	0.47	-16.9	-	-10	4.1	3.5	24.4	90
1433 O-Cm	0.45	-16.9	-	-13.9	4.8	14.0	15.7	115
3752	0.55	-19.8	-	-20.0	8.2	3.6	29.9	165
Sosnovyi Bor site								
P9	1.5	-15.5	-	-	1.1	-	5.5	-
P6	-	-12.6	-86	-	0.63	-	-	180

Well No.	TDS, g/L	$\delta^{18}O$, ‰	$\delta^{2}H$, ‰	$\delta^{13}C$, ‰ PDB	$^{234}U/^{238}U$, (AR)	^{14}C, pmC	Adjusted ^{14}C and uranium decay ages, ka.	Depth, m b.s.l.
P14	2.4	-18.8	-	-	-	-	9.0	160
П4	2.7	-15.7	-108	-	0.48	-	-	191
П2	2.9	-13	-98	-	0.64	-	13.0	240
Northern Dvina River delta site								
8mz	22.25	-12.2**	-94.4**	-	2.97	-	460*	120
La5	15.7			-	6.19	-	110*	200
No1	8.9	-7.7**	-58.3**	-	6.72	-	80*	90
Mi	5.3	-14**	-107**	-14.6	7.16	1.7	33.0	150-201
B1	9.14			-15.6	5.41	5.79	26.1	105
Lo	0.79	-13.8**	-100**	-11.2	5.94	37.03	5.4	80
W6	0.732			-9.6	2.86	25.3	4.0	80-90
3e	0.138			-12.3	2.26	34.18	2.1	20-25

Note: Borehole 1A is located on the Aegna Island (Tallinn Bay offshore); Sosnovyi Bor site is located on the eastern coast of the Koporye Bay (Leningrad district); for the Kabala site above layered aquifers are marked with stratigraphic unit; *- uranium (^{234}U-^{238}U) isotopic dating of age; ** - $\delta^{18}O$ and $\delta^{2}H$ stable isotopes average value.

In shallow Cm-V aquifer system groundwater at the Tallinn site, the uranium isotope ratio varies from 3.6 to 26 (Table 4.1.). Uranium AR and TDS slightly correlate, especially on Viimsi Peninsula. It is likely that during the Holocene, Eh, in the Cm-V aquifer, groundwater was -150 – -250 mV. Redox inversion to the oxidizing environment is mainly due to meteoric water recharge near buried valleys (Mokrik et al., 2009). During the periglacial before LGM, the drop in the sea level opened up an elevated cliff in the Estonia's western and northern parts resulting in the landscape altitude change toward eroded seabed-taliks. It established a new recharge and discharge boundary for groundwater flow paths. A redox part of the Cm-V aquifer could only be oxidized near taliks, where supra-permafrost recharge occurred (Figure 4.8.) (open Liivi Bay and Alutaguse-Peipus talik systems). The accumulation of the ^{234}U occurred in the sub-permafrosted aquifer due to α-recoil from ^{238}U in the aquifer for 10-20 ka duration. In these conditions, a similar accumulation of helium could occur *in situ* from α-recoil. Groundwater with high uranium isotope values started to flow from the original formation locations. A deviation from an equilibrium of $^{234}U/^{238}U$, can be observed in the O-Cm, and Cm-V aquifer groundwater (Figure 4.10). The highest AR values (40-56) are measured in samples from Saaremaa Island and Viimsi Peninsula (Yezhova et al., 1996).

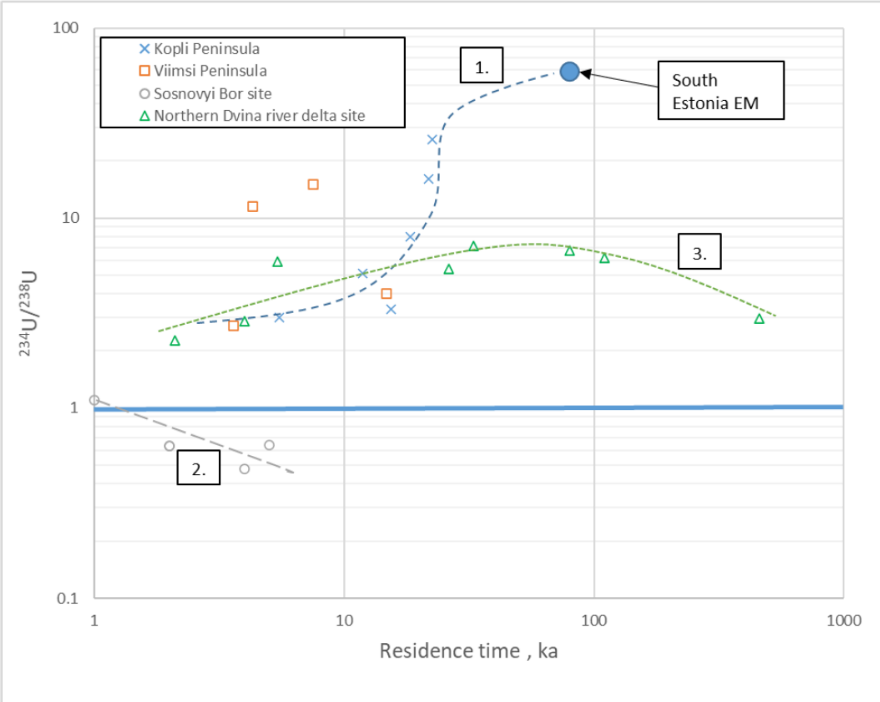

Figure 4.10. Residence time and $^{234}U/^{238}U$ activity ratio diagram. 1. Tallinn intake, 2. Sosnovyi Bor intake, 3. Northern Dvina site. Data after: (Bondarenko et al., 1981; Malov, 2017; Malov & Tokarev, 2019; Mokrik & Samalavičius, 2022; Yezhova et al., 1996; Poljakov unpublished, 1988 from DHVU.

Groundwater radiogenic ^{4}He ages of the southern part of Estonia, Värska site (close to Alutaguse-Peipus Talik), are 81 ka for O-Cm (463 m) and 86 ka Cm-V (545 m) for aquifers; Häädemeeste site (close to Liivi Bay Northern Talik) is 150 ka for O-Cm (610 m) (Mokrik et al., 2021). In the eastern Estonia, groundwater in the middle part of Alutaguse-Peipus Talik is significantly younger (^{14}C adjusted age is 26.8 ka, TDS is 1.5 g/L) in comparison with the northern part of the Pandivere Highland 33.1 ka, TDS is 0.5 g/L (Mokrik, 1997). Such inversion may be caused by the talik environment and prolonged permafrost occurrence on the Estonian Homocline.

Helium-4 and uranium-234 content in groundwater is associated with periglacial environment studies (Mejean et al., 2017). The opening of new additional fractures in aquifer rocks results in a bigger surface area for a more rapid ^{234}U and ^{4}He transition into the water (Mejean et al., 2017). This scenario could be observed in the Estonian Homocline (EH), ^{234}U, and ^{4}He anomalies found in the North Estonian coastal plain, the West Estonian Lowland, the Alutaguse-Peipus Lake Lowland coinciding with the major taliks (Figure 4.8.). In the sub-permafrost O, Cm, V formations, and basement fractures were joined to a single hydraulic unit. The correlation of the ^{234}U and ^{4}He excesses in the groundwater is evident for establishing a boundary between near talik supra- and sub-permafrost units.

Modern groundwater recharge in paleo valleys results in lowering of uranium isotope ratio. Similar depletion occurs from the seawater intrusion with the end-member being yet higher in TDS compared to modern water. In this case, the uranium isotope ratio could be used to distinguish elevated salinity sources in the isotopically depleted waters: seawater with close to equilibrium values, cryogenic water with >1 activity ratio. Sea intrusion influence could be deduced in wells No. 14, 22 (Kopli Peninsula), and No. 27 (Viimsi Peninsula) (Table 4.1.). Alteration of the chemical content in this groundwater includes an increase in TDS and SO_4/Cl during 1977-1988 (Mokrik, 1996), supporting evidence of seawater influence. The rest of the salinity in groundwater samples of Estonia most likely originate from cryogenic alteration.

Disequilibrium of $^{234}U/^{238}U$ AR, REDOX conditions, ^{4}He ages supports the theory of groundwater formation in a periglacial environment where talik system development and permafrost formations are the main factors for the northern BAB anomaly formation.

4.2.2. Isotope-Geochemistry Aspects of Anomalous Groundwater

Two main processes of cryogenic water alteration are salt (brine) rejection (Starinsky & Katz, 2003; Tsironi et al., 2020) and isotopic Rayleigh distillation (Gragnani R et al., 1998; Lehmann & Siegenthaler, 1991; Souchez et al., 1987). Due to the increasing major ionic content in groundwater, oversaturation of minerals resulting in their precipitation occurs (Jessen et al., 2014; Kononova, 1979; McEwen & Marsily, 1991).

Cryogenic fractionation of stable isotopes ($\delta^{18}O$ and δD) depends on the freezing velocity at the ice-water boundary (Lehmann & Siegenthaler, 1991). Fractionation constants (under equilibrium condition) published in research material vary $\delta^{18}O$ 2.8-3.0 ‰ (Clark & Fritz, 1997; O’Neil, 1968; Suzuoki & Kimura, 1973). Freezing velocity influences naturally occurring cryogenic fractionation either under kinetic or non-equilibrium conditions (Gragnani R et al., 1998; Souchez et al., 1987).

Hydrochemical stratification of the groundwater in the aquifer itself indicates cryogenesis. Water chemical type gradually evolves with the increasing depth from bicarbonate to chloride dominant. Salt rejection causes mineral precipitation (calcite, dolomite, gypsum, and pyrite). It decreases bicarbonate, magnesium, calcium, and sulfate content and shifting pH to alkaline (Alexeev et al., 2007; Alexeev & Alexeeva, 2002, 2003; Jessen et al., 2014; Kononova, 1979; Lacelle et al., 2006; Starinsky & Katz, 2003).

Diagram of Na/Cl and Br/Cl ratios revealed the cryogenic influence on the chemical composition of groundwater in Estonia (Figure 4.11.). The diagram is supplemented with groundwater data from Äspö and Palmottu sites in Scandinavia (Zhang & Frape, 2003). Two lines representing the alteration and evolution of seawater during evaporation and freezing processes are presented in Figure 4.11. The evaporation trend was determined experimentally, while the seawater freezing line is predicted (Herut et al., 1990; Starinsky & Katz, 2003). Evaporation and predicted freezing trends of seawater may not be the same for Estonia's groundwater the initial (pre-cryogenic) composition did not necessarily match the one of seawater. Cryogenic salt rejection has multiple impacts on groundwater chemical composition: increased dissolved solids content, oversaturation with major ions - mineral precipitation, and selective concentration of dissolved species may occur. These processes affect Na/Cl and Br/Cl ratios manifesting in a specific distribution of groundwater on the plot (Figure 4.11.). Groundwater evolution trends are different for calcium and sodium dominated initial water, significantly changing Na/Cl ratio values (Stotler et al., 2012).

Such trendlines may be observed in the groundwater of Estonia's O-Cm and Cm-V aquifers (Figure 4.11.). It is necessary to mention that groundwater evolution trends are entirely different for Cm-V and O-Cm groundwater, indicating distinct formation scenarios and environments, initial water composition, or both these factors.

The groundwater of the O-Cm aquifer Na/Cl and Br/Cl ratios tend to increase, showing either an elevation of sodium and bromide content or a decrease of chloride. Differences in Br/Cl ratio coincide with the slight evolution of chemical facies: Na-HCO_3-Cl groundwater Br/Cl vary from 0.002 to 0.004; sample with ratio >0.004 chemical type is Na-HCO_3. The stable isotope content of Na-HCO_3 groundwater is -19.0 to -18.5 per mil of $\delta^{18}O$. The transition of chemical types may be due to carbonate mineral precipitation, resulting in the depletion of calcium, magnesium, and bicarbonate species in groundwater. Hypothesizing that the initial water in the O-Cm aquifer was calcium-dominated, the precipitation of carbonate minerals could have resulted in Na-HCO_3-(Cl) water facies. It would support the theory of the influence of cryogenic processes on groundwater chemical composition; therefore, the freezing trend could be deduced (Figure 4.11.).

The setting of O-Cm aquifer groundwater Na/Cl and Br/Cl ratios match the data from Scandinavian Shield, Äspö, and Palmottu sites (Zhang & Frape, 2003), which are likely influenced by cryogenesis. Sodium-calcium cation exchange with minerals (illite, glauconite, etc.) in the Estonian O-Cm aquifer groundwater was considered to explain the formation of Na-HCO_3-(Cl) facies (Kirsimae & Jorgensen, 2000; Pärn et al., 2019). Yet, the cation exchange may increase sodium content rather than the Br/Cl ratio elevation, both of which are anions.

The alteration of Cm-V aquifer groundwater follows the trendlines of seawater freezing and evaporation. An increase in the Br/Cl ratio in Cm-V groundwater occurs toward the lower Na/Cl ratio, different from O-Cm (Figure 4.11., red and blue freezing lines, accordingly). Calcium-sodium-chloride facies groundwater Br/Cl ratio exceeds 0.004, with $\delta^{18}O$ varying from -21.5 to -20.7 per mil. Groundwater may have evolved either following the evaporation trend or the freezing trend. The evaporation process could not be the significant factor in the Cm-V groundwater alteration as it contradicts previously established statements: groundwater age averages the Late Pleistocene, colder annual temperature causing freezing rather than evaporation. The groundwater evaporation tends to enrich heavy stable isotope content ($\delta^{18}O$ and $\delta^{2}H$) while Cm-V aquifer groundwater is depleted. Seawater freezing trendline may fit better, explaining Cm-V groundwater chemistry and isotopic composition. As stated before, the initial water composition in the Cm-V aquifer could result from meteoric and seawater mixing. This mixture may have been less calcium-dominant and more saline than O-Cm initial groundwater. Mineral precipitation from this groundwater may have had a different product compared to the O-Cm case. Carbonate mineral precipitation could happen on multiple occasions, strongly depleting the groundwater of bicarbonate, therefore effectively preventing further fallout. From this point, a brine rejection could concentrate the solute without any loss of dissolved solids. Moderate sulfate mineral precipitation may be a reason for the low SO_4 amount in Cm-V groundwater. Cryogenic alteration increases chloride, calcium, and sodium amounts, resulting in Ca-Na-Cl chemical facies groundwater, which follows the Cm-V groundwater freezing trend (Figure 4.11., blue line). The evolution and formation of O-Cm and Cm-V groundwater strongly depend on the initial chemical composition of groundwater. It is safe to assume that the initial water and groundwater of both aquifers were distinct; therefore, cryogenesis resulted in different chemical facies, TDS, and other parameters. The source of the initial groundwater is most likely to be meteoric water, seawater, and in some cases, glacial meltwater. The mixture of seawater and the Pleistocene meteoric groundwater could have resulted in the $\delta^{18}O$ value ranging from -15 to -9 per mil, depending on each portion percentage. Isotopic depletion due to the Rayleigh distillation of the freezing fraction of aquifer groundwater should have been significant to decrease by 7 or more per mil $\delta^{18}O$ (cryogenic Cm-V aquifer groundwater is down to -23 per mil of $\delta^{18}O$). The permafrost should have penetrated >0.5 of the aquifer for isotope depletion to occur. Therefore, the influence of isotopically depleted glacial meltwater could have caused lower stable isotope values in the initial groundwater composition or affected them after cryogenesis. Some of O-Cm and Cm-V aquifer groundwater is affected by modern meteoric recharge. These samples are plotted near the modern groundwater member on the diagram (Figure 4.11.).

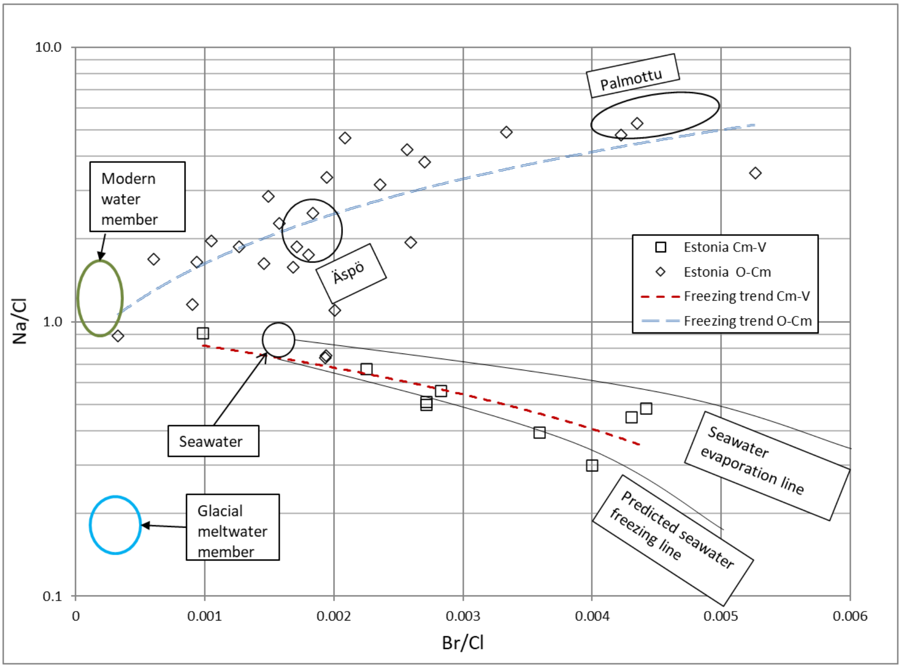

Figure 4.11. Sodium, chloride, and bromide ratio diagram (Mokrik & Samalavičius, 2022) of the BAB groundwater, predicted seawater freezing (Herut et al., 1990), and seawater evaporation (McCaffrey et al., 1987) lines are supplemented. Äspö and Palmottu groundwater data is provided as a reference for cryogenic alteration in the Fennoscandian shield (Zhang & Frape, 2003).

One of the most important chemical parameters for evaluating the permafrost effect on groundwater is the Ca/Mg ratio (eq/L). Cryogenic water, which undergoes periodic precipitation of calcite, eventually becomes depleted of calcium. Therefore, the Ca/Mg ratio drops to the value range 1-2 (Alexeev & Alexeeva, 2002). This case is observed in O-Cm shallow groundwater, particularly Na-HCO_3 facies, which are plotted in the range of

1.08-1.38. O-Cm groundwater has the lowest Ca/Mg ratio in the BAB, making it exclusive.

An opposite trend is observable for the Ca/Mg ratio ranging 3.31-5.42. This groundwater is found in the shallow Estonian Cm-V aquifer and crystalline basement. Strongly isotopically depleted ($\delta^{18}O$ -22.7 to -21.3 ‰) groundwater is Ca-Na-Cl or Na-Ca-Cl-HCO_3 facies. The most extreme case is found on Tallinn sites (Well No. 646, 1151), where the Ca/Mg ratio is above 4.5. It seems that the groundwater on these sites is purely cryogenic in origin. The pH value of Viimsi site groundwater is 8.5, and SI calcite is oversaturated. However, after that the water was repeatedly concentrated due to multiple freezing-thawing cycles.

The rest of the shallow Estonian Cm-V and O-Cm groundwater have a Ca/Mg ratio of 1.5 to 3. Their chemical facies vary but mainly include sodium, calcium, chloride, and bicarbonate. These chemical types fall between previously discussed Na-HCO_3 and Ca-Na-Cl. This groundwater may be affected by salt rejection and carbonate precipitation resulting in a series of groundwater chemical facies but not modeling marginal forms with anomalous Ca/Mg ratio.

4.2.3. Thermodynamics of Water-Rock System, Saturation Indexes of Calcite and Halite

Simple moving averages (SMA) of calcite saturation data were calculated in the diagrams of SI calcite versus $\delta^{18}O$ (Figure 4.12.) to emphasize the general tendency and eliminate background noise. SMA is obtained from the specifically arranged data sequence divided into intervals. An average value for each interval was calculated (Schneider et al., 2013). The obtained data intervals overlap with the required increment (in this calculation, the increment is 1). To illustrate the process, a sequence (1, 2, 3, 4, 5, 6, 7) with an interval 3, and an increment 1 results in the following data sets: (1, 2, 3), (2, 3, 4), (3, 4, 5), (4, 5, 6), (5, 6, 7). The average value of each obtained data set is then calculated. An array of these averages is SMA. Data was sorted on ascending $\delta^{18}O$ values. Simple moving averages were calculated with two intervals (2 and 10). Accordingly, intervals of 2 and 10 represent a more precise and generalized distribution of calcite saturation in each area.

An increase in SI Calcite SMA correlates with the depletion of $\delta^{18}O$ ranging -22 to -19 ‰ in the northcentral part of Estonia (Figure 4.12.b, red arrow). Calcite saturation increased from -0.7 to 0.2, reaching its maximum at the most depleted $\delta^{18}O$ value range. Saturation of 0.2 means that the groundwater is close to equilibrium or is oversaturated slightly. Depending on calcium, magnesium, and bicarbonate resources in groundwater, cryogenesis-induced mineral precipitation should effectively deplete groundwater from these components and maintain SI equilibrium value (0±0.2). In the northeastern part (Figure 4.12.a), oxygen-18 enrichment from -21.5 to -19.5 ‰ correlates to an increase in saturation from -0.5 to 0.3 accordingly. Meteoric groundwater influence may be the reason for an opposite trendline direction (black arrow) at the oxygen-18 interval from -19.5 to -18.0 ‰ and SI Calcite increase from -0.5 to 0.6, accordingly. The Kotlin aquitard present in the northeastern Estonian part may be a barrier for permafrost; therefore, the Voronka aquifer groundwater is being cryogenically altered during more cycles than the confined Gdov aquifer. Isotope-geochemistry in such situations may be diverse in both sub-aquifers of the Cm-V. It could also be two distinct groundwater fractions – cryogenically altered toward isotope enrichment in the first instance of freezing and a follow-up depletion at a greater depth.

The cryogenic trendline is not apparent in the northwestern area (Figure 4.12.c, red arrow). It is noticeable in the green series (SMA interval of 10) with $\delta^{18}O$ ranging from -22.4 ‰ to -20.0 per mil. Saturation with calcite in this isotope range is in equilibrium, possibly due to mineral precipitation caused by cryogenic salt rejection. Cryogenic alteration of groundwater was most likely different in the northwestern region compared to other parts of North Estonia. In this area, Cm-V and O-Cm aquifers are hydraulically connected without a considerable confining layer between them. It allows cryogenesis-induced calcite precipitation to be more substantial. While propagating downward permafrost, brine rejection may result in multiple mineral precipitation cycles, depleting the groundwater of calcium, magnesium, and bicarbonate.

In Tallinn, oxygen-18 ranging from -22.4 to -20.0 ‰ correlate to SI Calcite ranging from -0.8 to 0.6 (Figure 4.12.d). An apparent cryogenic trendline could be deduced from the green series (SMA interval of 10). It is well established that the groundwater in the Tallinn area was significantly altered by multiple factors: modern meteoric water influence, seawater intrusion, glacial meltwater recharge, and cryogenic alteration. The exploitation of the Cm-V aquifer strongly affected its composition by changing the natural flow paths. A net of buried valleys in the Tallinn region is where modern groundwater leakage from O-Cm, S-O occurs (Mokrik, 1996; Mokrik et al., 2005; Raidla et al., 2009; Vaikmäe et al., 2001; Yezhova et al., 1996). Many groundwater formation factors lead to diverse isotope-geochemistry, including variations in SI calcite. Some groundwater in the Tallinn area is cryogenic: elevated pH, high chloride content, depleted isotopically, in equilibrium, or oversaturated with calcite. Groundwater marginal value of $\delta^{18}O$ >-16 per mil in calcite SMA is due to modern groundwater influence (Figure 4.12.).

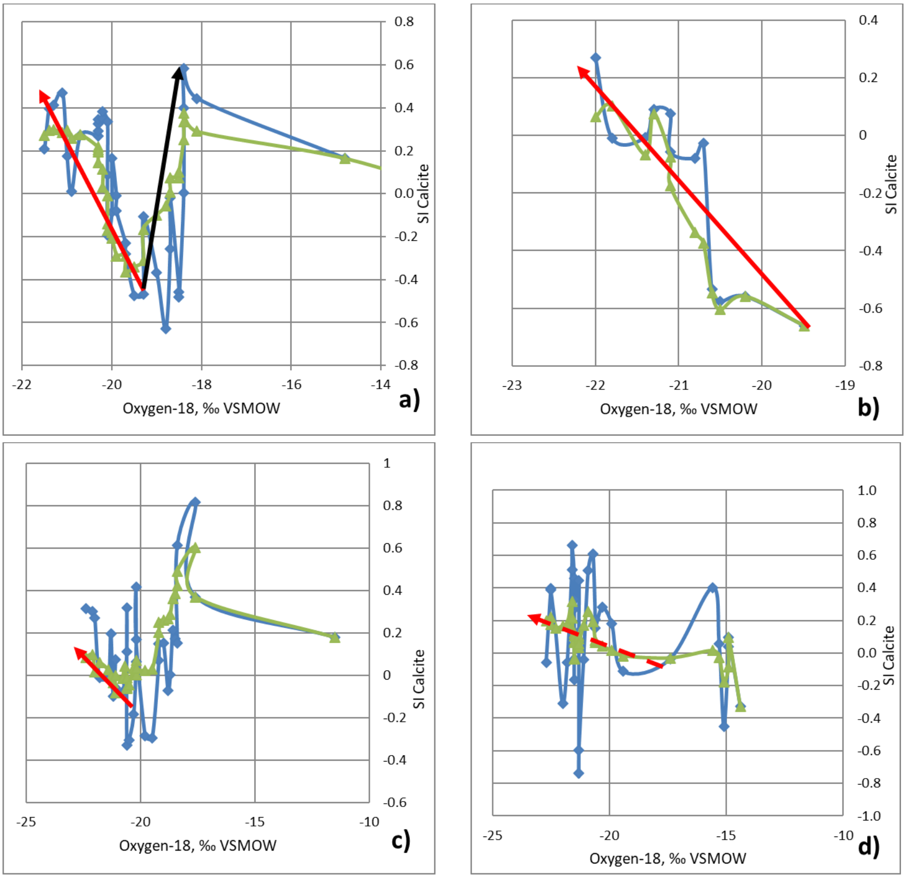

Figure 4.12. Calcite saturation and $\delta^{18}O$ diagram of North Estonia Cm-V aquifer groundwater. a) Northeastern part, b) Northcentral part, c) Northwestern part, d) Tallinn site. The blue line represents SMA with interval 2, green line - 10. Red arrows show salt rejection.

The Estonian anomaly could be observed in the context of the whole BAB groundwater variety. Two background lines in the TDS vs. SI Halite diagram represent the general increase of TDS in Lithuania-Latvia (Figure 4.13. blue dashed line) and Estonia (red dashed line). On average, the Estonian groundwater is more saturated (~1 unit of SI) with halite than the Lithuanian-Latvian groundwater with identical TDS (Figure 4.13.). Higher saturation with halite means an elevated content of sodium and chloride. Brine rejection caused by cryogenesis could alter the chemical composition of the Estonian groundwater by increasing Na and Cl amount in the groundwater. However, the same salt rejection forces the precipitation of calcium, magnesium, and carbonate species into the solid-state. Relative depletion of Ca, Mg accompanied by increased Na and Cl results in higher halite saturation without a loss of TDS amount. Some Estonian groundwater has either modern chemical composition or it is influenced by a meteoric origin water recharge (green arrow).

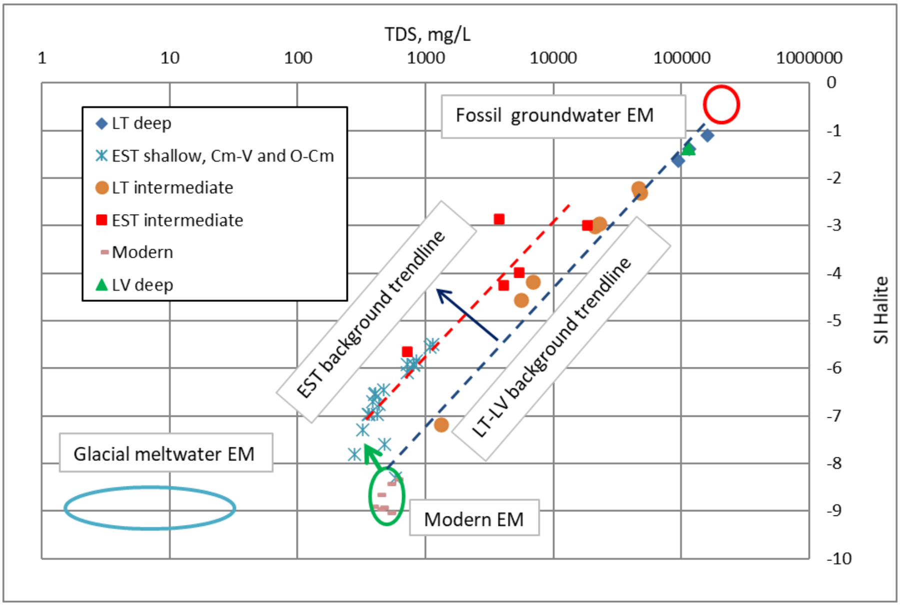

Figure 4.13. TDS and SI halite diagram of the selectively picked BAB groundwater. Modern, glacial meltwater and fossil (brine) end-members are presented. The blue dashed line represents the chemical evolution of the Lithuanian and Latvian groundwater. The red dashed line represents the chemical content background values of the Estonian groundwater. The blue arrow represents shift due to cryogenic brine rejection or different thermodynamic conditions in aquifers.

Saturation with calcite mineral in the northern Estonian groundwater correlates with $\delta^{18}O$ depletion, which complements previously stated brine rejection during freezing. This observation solidifies the theory of this anomaly's chemical evolution. However, isotopic content variation ($\delta^{18}O$) could be proved additionally, extending toward the noble gas signatures of the groundwater.

4.2.4. Noble Gas Content Evidence of *In Situ* Groundwater Freezing

Noble gases Ar, Kr, Xe content, and their ratios are used in ground ice and permafrost origin determination (Utting et al., 2016). Excess air in the

Estonian samples was hypothesized to be originated from air bubbles trapped in the glacial ice and, due to compression, increased the noble gas content in meltwater which recharged aquifers (Weißbach, 2014). However, the Canadian permafrost and ground ice study reveal that noble gas content should be close to atmospheric content (Utting et al., 2016). On the contrary, frozen groundwater noble gas content must be closer to AEW at STP. Noble gas ratios in the delta notion (Table 4.2.) are being used to evaluate the origin of underground ice (Utting et al., 2016). A similar approach was made with other dissolved gases (O_2, N_2, CO_2, CH_4), which are less reliable due to their reactive nature (Utting et al., 2016). This theory may suggest an approach for reconstructing paleoenvironments as well as present permafrost-snowpack / ice-sheet glacier distinction.

Noble gas ratios in δ notation were calculated for the Estonian samples: δ(Ar/Xe) and δ(Kr/Xe) (Equation 4.1.). The main objective of these ratios was to evaluate the origin of isotopically $\delta^{18}O$ depleted groundwater in Estonia, based on similar research of the Canadian cryogenic samples (Utting et al., 2016).

$$\delta(^{Ar(Kr)}/_{Xe})_{sample} = \left(\frac{sample(^{Ar(Kr)}/_{Xe})}{atmosphere(^{Ar(Kr)}/_{Xe})} - 1\right) \times 100\ \% \qquad (4.1.)$$

In equation 4.1.: δ(Ar or Kr/Xe) sample, %; sample (Ar or Kr/Xe) - noble gas ratio of the sample; atmosphere (Ar or Kr/Xe) - noble gas ratio in the atmosphere (Table 4.2.) (Utting et al., 2016).

Table 4.2. Noble gas composition of atmosphere air and air equilibrated water (Aeschbach-Hertig et al., 1999; Aeschbach-Hertig & Solomon, 2013; Potter & Clynne, 1978; Sano et al., 2013; "Solubility Data Series, Argon," 1980; "Solubility Data Series, Helium and Neon," 1979; "Solubility Data Series, Krypton, Xenon and Radon," 1979; Stute & Schlosser, 1993; Weiss, 1970, 1971; Weißbach, 2014). Isotope ratios in delta notation are shown based calculation procedure in Utting et al., 2016.

Gas	Atmosphere, cm^3STP/g	AEW at 0 °C, cm^3STP/g
Helium $\times 10^{-6}$	5.2	0.049
Neon $\times 10^{-6}$	18.2	0.25
Argon $\times 10^{-4}$	93	4.98
Krypton $\times 10^{-6}$	1.14	0.125
Xenon $\times 10^{-8}$	8.6	1.91
Ratio	**Atmosphere, %**	**AEW at 0 °C, %**
δ(Ar/Xe)	0	-75.9
δ(Kr/Xe)	0	-50.7

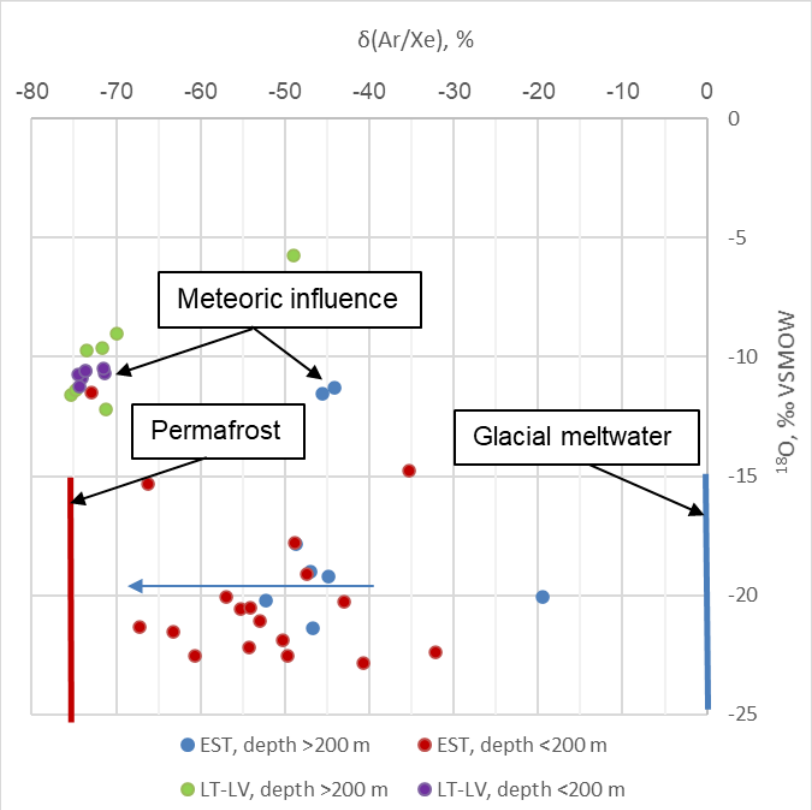

Figure 4.14. Delta argon/xenon and oxygen-18 diagram. Data is subdivided into the Lithuanian-Latvian and Estonian regions at depths over and below 200 m. The blue line represents the glacial meltwater's end-member and the red line - permafrost's end-member. The blue arrow represents the increase of Ar-Xe toward atmospheric content.

According to Figures 4.14., 4.15., the Estonian groundwater $\delta^{18}O$>-15 per mil is almost exclusively originated from groundwater freezing; most of the samples are closer to a permafrost noble gas end-member (blue arrows) (Samalavičius & Mokrik, 2021). Most samples of argon, krypton, and xenon content are insufficient to be of a glacier, firn, or snowpack origin. A few sites (Nõva, Harju-Risti) (Figures 4.15., yellow circle) are considered to obtain depleted $\delta^{18}O$ values from glacial meltwater, which is supported with the low TDS content described previously. Canada's example on the Eagle River site (Figures 4.15., green circle) contains the lowest amount of noble gases from the research (Lauriol et al., 2010; Utting et al., 2016), yet it is proven to originate from frozen groundwater. Almost all Estonian samples contain less argon, krypton, and xenon (Figures 4.15., blue arrow), meaning that the atmospheric signal is low or absent. Therefore, permafrost is the predominant factor of this groundwater formation.

Excess air in the Estonian samples could be explained by gas rejection during freezing in the Pleistocene. This would support the depleted $\delta^{18}O$ content, probably due to Rayleigh distillation during the freezing. Rejection of gases was observed to be stronger than dissolved solids (Lipp et al., 1987; Loose et al., 2009).

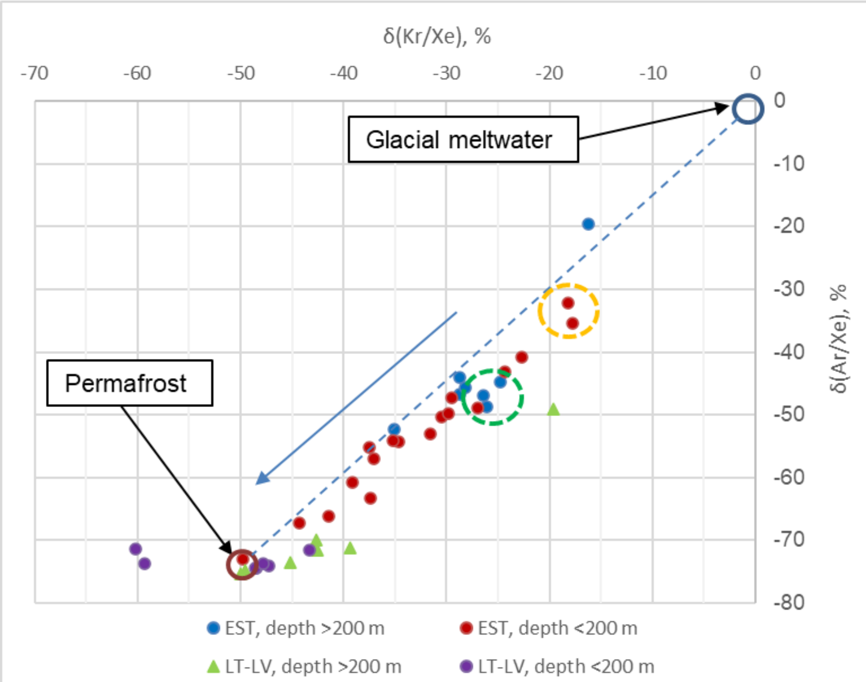

Figure 4.15. Delta argon/xenon and delta krypton/xenon diagram. Data is subdivided into the Lithuanian-Latvian and Estonian regions at depths over and below 200 m. The blue dashed line represents the mixing line of glacial meltwater (blue circle) and the red circle - permafrost's end-member. The blue arrow represents a noble gas content evolution toward permafrost EM for water $\delta^{18}O$ (<-15 per mil). The yellow dashed circle - the Estonia groundwater recharged with glacial meltwater. The green circle - Canada, the Eagle River frozen groundwater (Lauriol et al., 2010; Utting et al., 2016).

The excesses of noble gas in the Estonian groundwater depleted with $\delta^{18}O$ (<-15 per mil) is mainly caused by *in situ* freezing. Heavy noble gas δ(Ar/Xe) and δ(Kr/Xe) ratios range toward the permafrost EM, with little possible influence of glacial meltwater (Samalavičius & Mokrik, 2021). A few samples deviate from this tendency, indicating the meltwater as a source. However, they are exceptions to the general trend.

4.3. Interaction of Deep and Intermediate Depth Regional Flow Systems

4.3.1. Differences in Groundwater Dating Results

Three conventional intermediate and deep groundwater dating techniques were used in this study: radiokrypton, helium-4, and modeled particle track (Mokrik et al., 2021). The research group at HEG Department of VU calculated most sampled helium-4 and particle track groundwater ages as a part of an IAEA Research Project F33022. The obtained results were published in a book and report (Mokrik et al., 2021; Mokrik et al., 2022). Hydraulic ages were determined on sites where helium and radiokrypton dates had been calculated. The particle travel time option was employed using MODPATH simulation. Recharge areas were established in regional highland areas. In the case of a few separate particle track paths crossed on site, two of the most significant recharge areas were selected (cases: Riga Well No. 50194 and Likėnai Aukštaitija Well No. 21965) (Figures 4.16., 4.17.). Therefore, two-particle travel times were obtained and recorded (Figures 4.16., 4.17., Table 4.5.). The examples of particle travel tracks and apparent hydraulic ages are presented in three aquifers O-Cm, D_{2-1}, and D_2šv-ar (Figure 4.16. a, b, c). Radiokrypton ages were obtained from the previous research of the BAB (Gerber et al., 2017; Vaikmäe et al., 2020).

A few dating techniques combined allow to verify groundwater age results, include necessary corrections, and evaluate possible groundwater mixing and other features of aquifer systems that can alter the results (IAEA, 2013). The distribution of helium in multilayer systems is helpful in assessing numeric modeling both in vertical and horizontal directions, especially in deep aquifers (Zhao et al., 1998). The lack of necessary structural features in regional-scale models eliminates the possibility of helium diffusing vertically in overlaying aquifers; therefore, the hydraulic age seems older than the one calculated using the helium method (Zhao et al., 1998).

Aquitards significantly influence the helium age of deep groundwater in the Great Artesian Basin, Australia, as helium accumulates in the top of aquifers altering ^{4}He residence time. Helium amount in multilayered system aquifers can be useful in evaluating vertical flow rates of recharge and discharge (Bethke et al., 2000). A vertical flow through regional-scale aquitards is generally slow; for example, in the Arckaringa Basin, Australia, it is calculated using helium and chloride tracers to be 0.7 mm/a (Priestley et al., 2017). Radiokrypton is considered an almost ideal tracer due to its nonreactive nature, a constant and steady source in the atmosphere

(Aeschbach-Hertig, 2014). The $^{81}Kr/Kr$ ratio decreases due to radioactive decay, therefore enabling groundwater dating. The half-life of radiokrypton is 229 thousand years; an old (150-1500 ka) groundwater, polar ice, and thermal fluids can be dated using this isotope. Younger water lacks the $^{81}Kr/Kr$ ratio resolution necessary for measuring, while >1500 ka groundwater krypton ratios are below uncertainty due to technical limitations (Lu et al., 2014). Latest studies reveal that geogenic krypton-81 production is possible (Purtschert et al., 2021).

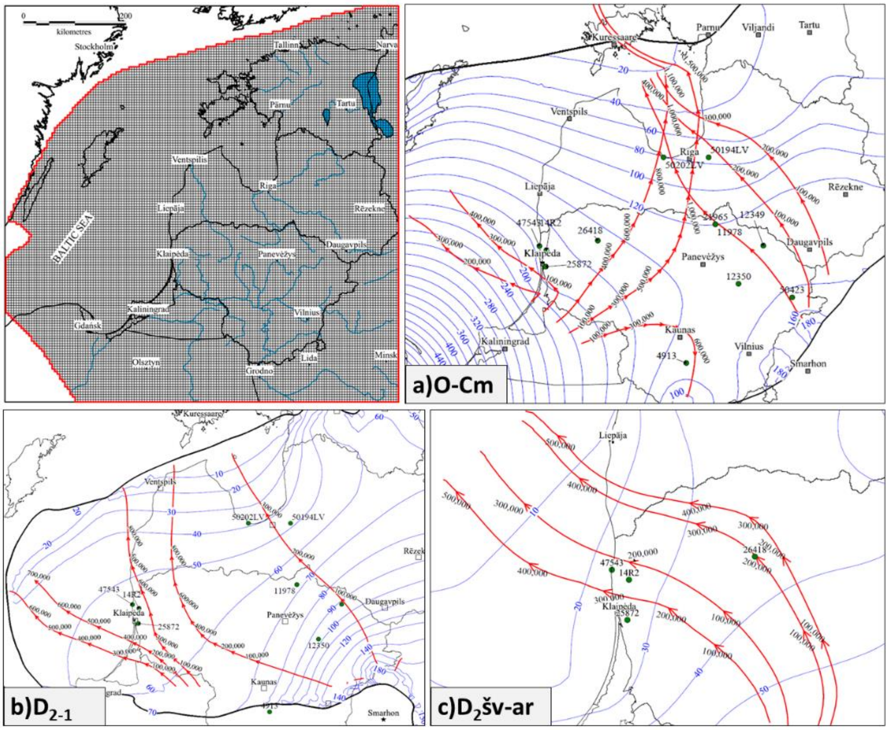

Figure 4.16. Numerical 3D steady-state and transient groundwater model grid of the BAB. An illustration of MODPATH modeled particle tracks for a) O-Cm, b) D_{2-1}, c) D_2šv-ar aquifer. The particles were released in two recharge areas: the eastern Lithuania and the northern part of the Kaliningrad District. Blue lines and numbers represent hydraulic heads in meters above sea level. Red arrows and black numbers represent particle track and time in years, accordingly. Partly based on Mokrik et al., 2021.

Groundwater dating results in deep (>1000 m) aquifer groundwater show the most significant difference among the three dating techniques (Figures 4.17.). Groundwater age obtained by the radiokrypton method is >2 times older compared to helium and modeling results. Aquifers on these sites (Klaipėda, Riga) are confined with regional scale aquitards and, in some cases, overlaid by a few semi-permeable layers. Low helium amount in aquifer results in young age. It is possible that helium diffuses through faults upwards and accumulates under the aquitards in places not disrupted by tectonic dislocation.

Particle travel time is lower than the radiokrypton age and slightly higher than the helium residence time. Krypton-81 and particle track pathways should mostly coincide, but groundwater ages differ significantly. Aquifers in the numeric model are smooth; the parameters which affect the flow are: hydraulic conductivity, porosity, and boundary conditions. Faults and similar geological structures are not digitized; therefore, the radiokrypton ages are significantly older. The particle track migrates more easily in a modeled setting compared to the radiokrypton in a natural environment.

Helium and particle travel time ages are similar in the intermediate aquifer groundwater of Lithuania (Figure 4.17., Table 4.5.). On the contrary, helium shows that the intermediate-depth Estonian groundwater is very young compared to ages obtained with other techniques. The Lithuanian-Poland Trough's intermediate aquifer isolation by structural aquitards sealing features result in an elevated helium accumulation in groundwater. At the eastern part of the Saldus-Riga-Pskov Fault Zone (Latvia) and the south-eastern Estonian Highlands the situation is opposite; therefore, a significant amount of helium escapes from intermediate-depth aquifers (Häädemeeste and Värska). The data of two wells of Lithuania (Likėnai and Rokiškis) in the Lower-Middle Devonian aquifer groundwater show 3-fold younger helium age compared to the modeled groundwater flow alternative. Meteoric water recharge is a possible cause of low helium content values here as well. The elevated content of radioactive elements is found in basement rocks in many places of the BAB basement, including Latvia and Estonia (Mokrik et al., 2021).

Helium distribution in the multilayered aquifer system of a particular site reveals that older groundwater may be found in a more shallow aquifer compared to deep brines as a result helium age inversion occurs. For example, close to the Klaipeda-Telšiai Fault Zone, the immense helium value was fixed according to Mokrik et al., 2002, in the D_{1-2} aquifer system because of the Narva aquitard sealing. This anomaly contradicts the isotope-geochemistry data distribution by depth, contrary to the BAB groundwater tendency of older groundwater in deeper aquifers. Such occurrences reveal that the tendency is not valid in principle. Therefore, such on-site occurrences in hydro stratigraphy must be considered while interpreting helium ages.

Table 4.3. Aggregate ^4He age on the Klaipėda site's multilayered aquifer systems (Mokrik et al., 2021; Mokrik et al., 2022). Helium content was obtained in Gerber et al., 2017; Juodkazis & Tibar, 1989; Mokrik, 2003; Mokrik et al., 2002.

System	He, ccSTP/g	Age, ka
T	Regional aquitard	-
P_2	4.56E^{-8}	Modern
D_2	3.06E-^{4}	225
D_2nr	Regional aquitard	-
$D_{1\text{-}2}$	8.12E^{-4}	597
O-Cm	9.00E^{-4}	662
Σ	2.02E^{-3}	1484

Table 4.4. Aggregate ^4He age on the Värska site's multilayered aquifer systems (Mokrik et al., 2021; Mokrik et al., 2022). Helium content was obtained in Gerber et al., 2017; Juodkazis & Tibar, 1989; Mokrik, 2003; Mokrik et al., 2002.

System	He, ccSTP/g	Age, ka
D_2nr	Regional aquitard	-
$D_{1\text{-}2}$	4.75E^{-5}	35
O-Cm	1.10E^{-4}	81
V_2vr	1.17E^{-4}	86
V_2gd	3.09E^{-6}	2
Σ	2.78E^{-4}	204

The significant effect of upward helium diffusion through aquitard fractures may suggest a specific vertical distribution together with inside sources in multiple aquifers on one site. Therefore, aggregate helium age is a total of all aquifer helium content in an area or site of a multilayered aquifer unit (Tables 4.3., 4.4.) (Mokrik et al., 2021; Mokrik et al., 2022). The summing-up of all ages could be of great benefit to the analysis and interpretation of groundwater dating results. The sum of accumulated helium in aquifers should be equal to its total emanation from the crystalline basement and inner sources. The primary helium accumulation occurs in the aquifer reservoirs up to the most shallow major regional aquitard. Above this confining layer, helium escapes into the atmosphere; therefore, the amount found in the shallow groundwater is low, usually close to equilibrium with the air content.

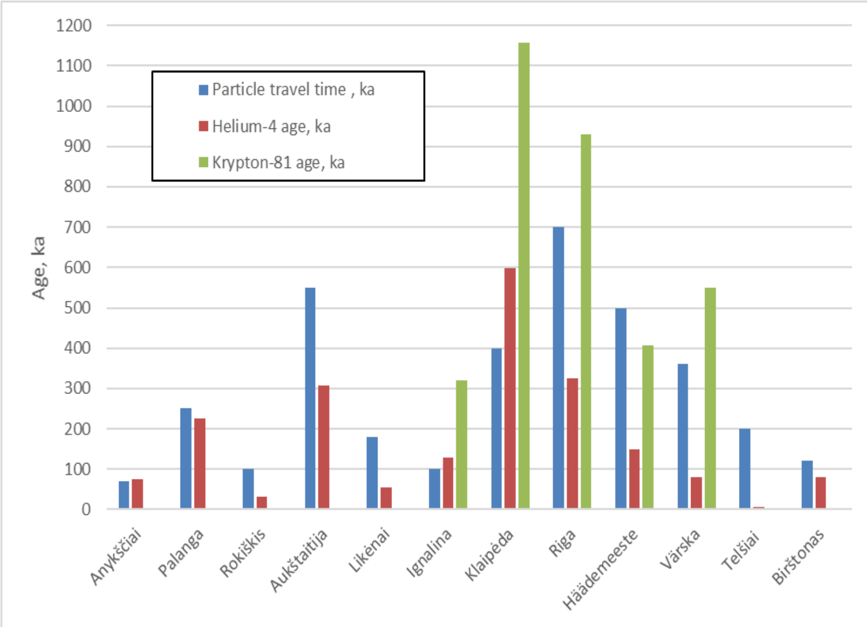

Figure 4.17. Intermediate and deep BAB groundwater age according to conventional helium, radiokrypton, and particle travel time techniques. Data is presented in Table 4.5.

The results of conventional helium age and aggregate helium age are presented on two sites of the BAB regions (Tables 4.3., 4.4.): Värska and Klaipėda. In a cross-section of the Klaipėda site, which is located near the Lithuanian coastline with the Baltic Sea, helium content in the aquifer is O-Cm – 9.0E^{-4}, D_{2-1} – 8.1E^{-4}, D_2 – 3.1E^{-4}, P_2 – 4.6E^{-8} (ccSTP/g). The total amount of accumulated helium is 20.2E^{-4} ccSTP/g. The calculated aggregate helium age on the Klaipėda site is 1,484 ka. Aggregate helium age could suggest a way to interpret and obtain a reliable residence time of the deepest aquifer. In the Klaipėda area, it is O-Cm. The radiokrypton measured age in the overlaid D_{2-1} aquifer dates the groundwater to approximately 1.2 Ma. The aggregate helium groundwater age (1.5 Ma) is a more likely scenario in the O-Cm aquifer system than 0.66 Ma calculated by conventional helium dating (Mokrik et al., 2022).

A site in the southern Estonia (the case of Värska) presents an even more peculiar situation where age inversion (anomaly) is observed (Mokrik et al., 2022). The deepest sedimentary aquifer (V_2gd) groundwater is depleted with helium more than 40 times compared to overlaying V_2vr (Table 4.4.). These aquifers in a major part of Estonia are united, yet separated by the Kotlin aquitard in this area. Helium amount distribution in the aquifers of Värska site is the following: V_2gd - 3.1E^{-6}, V_2vr - 1.2E^{-4}, O-Cm - 1.1E^{-4}, D_{2-1}- 4.8E^{-5} ccSTP/g. The sum of accumulated helium on the Värska site is 2.8E-04 ccSTP/g, the aggregate helium age is 204 ka. Similar to the Klaipėda case study, the estimation of the deepest aquifer V_2gd groundwater age could be made using the aggregate helium age - 0.2 Ma. Compared to conventionally helium-dated groundwater (0.002 Ma), the results differ almost 100 times.

Hydrogeological age inversions using aggregate helium age were partially corrected. Yet, it is important to emphasize that this method may be insufficiently accurate, and not covering all aspects of helium dynamics underground. For example, the groundwater of the Värska O-Cm aquifer dated with the radiokrypton technique reveals the age of 0.6 Ma, which is significantly (3-fold) older than the aggregate helium age. This discrepancy may occur due to the loss of helium from the whole multilayered aquifer unit. It is likely that a significant part of helium escapes to the atmosphere diffusing through aquitards or other pathways which lower the confining capacity of layers. In this case, the total bulk emanation is not equal to the sum of accumulated helium. The influence of confining regional scale aquifers is crucial while applying conventional and aggregate helium age techniques (Mokrik et al., 2022).

Table 4.5. Intermediate and deep BAB groundwater age according to conventional helium, radiokrypton, and particle travel time (modeled), recharge from south/east techniques (Gerber et al., 2017; Mokrik et al., 2021; Vaikmäe et al., 2020).

Well No.	Site	Index	Depth, m	State	Particle travel time	^{4}He age	^{81}Kr age
					ka		
12350	Anykščiai	D_{2-1}	360	Lithuania	70	76	-
47543	Palanga	D_2	522	Lithuania	250	225	-
12349	Rokiškis	D_{2-1}	440	Lithuania	100	31	-
21965	Likėnai (Aukštaitija)	O-Cm	1011	Lithuania	900/180	308	-
11978	Likėnai (Likėnai)	D_{2-1}	434	Lithuania	180	55	-
50423	Ignalina	O-Cm	500	Lithuania	100	129	320
25872	Klaipėda	D_{2-1}	1100	Lithuania	400	597	1,157
50194	Riga, Hospital	O-Cm	1027	Latvia	1,100/300	326	929
8021	Häädemeeste	O-Cm	610	Estonia	500	150	408
4613	Värska	O-Cm	600	Estonia	360	81	550
26418	Telšiai	D_2	715	Lithuania	200	5	-
4913	Birštonas	T_1-P_2	300	Lithuania	120	79	-

The differences in groundwater mean residence time obtained using isotopic and particle travel times are considerable. The general tendency of the groundwater ages is, on average, Krypton-81>MODPATH>Helium-4. The numerical model should be updated with the correction of hydraulic parameters and geometry to represent structural features such as fault zones. A different age modeling could be applied in the future, including mass distribution and transport (MT3D). Helium migration in the multilayered system is a proxy for future research on groundwater age determination, where more accurate porosity or double porosity parameters (porous-fractures conditions) should be applied for conventional helium dating.

4.3.2. Helium Distribution and Migration in the BAB Multilayered System

The role of the regional scale aquitards in the BAB groundwater age estimation and isotope-geochemistry formation is crucial. Hydraulic conductivity values of the BAB aquitards, which prevent meteoric water leakage into intermediate-depth aquifers on a regional scale, are below 5E-7 m/d. Other specific features which must be accounted for are the structures preventing the lateral flow of groundwater in the aquifer. Vertical faults offset could reach from 100 to 600 m, drastically slowing down groundwater flow (Mokrik et al., 2021). Major tectonic faults that could influence the groundwater flow are the Middle Estonian, Liepaja-Saldus-Riga, fault systems in the western Lithuanian, and Paldisk-Pskov. In the deepest aquifers of the BAB, these vertical dislocations isolate and separate areas where groundwater flow rates are fast or delayed from stagnant. The average velocity of the groundwater flow in intermediate depth aquifers at the peripheral part of the BAB may vary from 0.2 to 1 m/a (Mokrik, 2003).

The source of ^{4}He in the BAB is mainly crustal due to the decay of radioactive elements (uranium and thorium) found in minerals of the basement rocks (Figure 4.18., red circle). Neon generation in the crust is extremely low compared to helium; therefore, Ne/He ratio is close to 0 (Ozima & Podosek, 2002). Radiogenic ^{4}He amount in intermediate and deep aquifers is significantly higher than in the Lithuanian shallow groundwater, yet similar to the Estonian freshwater. It is probably due to a crystal basement depth higher in the northern Estonia by tens to hundreds of meters, while in Lithuania - by hundreds to thousands of meters. Because of this reason, helium flux in the Estonian shallow aquifers is higher compared to the Lithuanian ones. Major Rapakivi granite massifs in the Estonian region crust add a significantly higher content of helium as well. The origin of the

Lithuanian shallow aquifer groundwater helium seems to be crustal and atmospheric (Figure 4.18., green circle). This observation suggests that radiogenic crustal helium could accumulate in shallow Quaternary aquifer systems as well. The groundwater is enriched with ^{3}He through anthropogenic tritium decay (Figure 4.18., blue circle) - a considerable amount of tritium was found in the shallow groundwater (Mažeika, 1999; Mažeika et al., 2013; Mokrik et al., 2014; Samalavičius & Mokrik, 2016; Štuopis et al., 2012). The measured tritium content on these sites varies 4.7-5.4 TU. It elevates $^{3}He/^{4}He$ ratio values (Figure 4.18., red arrow) above helium equilibrium with the atmosphere. Neon is in equilibrium with atmospheric content. Deeper Quaternary aquifers lack anthropogenic ^{3}He as the anthropogenic tritium signal was considerably lower there.

Helium flow underground could be different from groundwater because the ^{4}He molecule diffusion coefficient is 3-10 times higher than H_2O molecule or dissolved chloride (Bethke & Johnson, 2008; Krynicki et al., 1978; Oelkers & Helgeson, 1988; Wise & Houghton, 1966). It should be especially noticeable in stagnant or delayed flow regimes. Therefore, helium may migrate through aquitards faster than water and give significant mass transport balance uncertainties. In some cases, the upward helium diffusion may be completely different from the general flow path of groundwater (Bethke & Johnson, 2008). The diffusion coefficient of chloride, helium, and water molecule depended on temperature. Due to this property, helium distribution in the groundwater is often unpredictable depending on the confining aquitards and structural features of the layers rather than on the groundwater flow (Juodkazis & Tibar, 1989; Mokrik et al., 2002). In reservoirs, the accumulation rate of helium could increase significantly, therefore resulting in older groundwater. The opposite situation occurs when helium escapes from deep and old groundwater and accumulates elsewhere. All these factors contribute to the helium amount variation in intermediate-deep groundwater of the BAB: $4.6E^{-8}$ up to $9.0E^{-4}$ccSTP/g (Mokrik, 2003). The distribution of thorium and uranium elements in the crystal basement differs in the whole BAB (Juodkazis & Tibar, 1989; Mokrik et al., 2002; Raudsep, 1997). The high content of these radioactive element's margins is found near large and small Rapakivi type granite massifs and other basement granitoids which can emit He migrating towards sedimentary cover. The main traps are on the Polish-Lithuanian Trough onshore in the O-Cm rocks, circuit water oil deposits; in the Lower Devonian aquifer system (800-1000 m deep); below the clayey Devonian Narva aquitard; in the deep-intermediate depths of the Riga Depression; the southwestern Estonian Coast, the northern part of the Mazury-Belarus Anteclise Slope. Fractured zones in the crystalline basement are usually associated with high helium content in groundwater reservoirs (Mokrik et al., 2002).

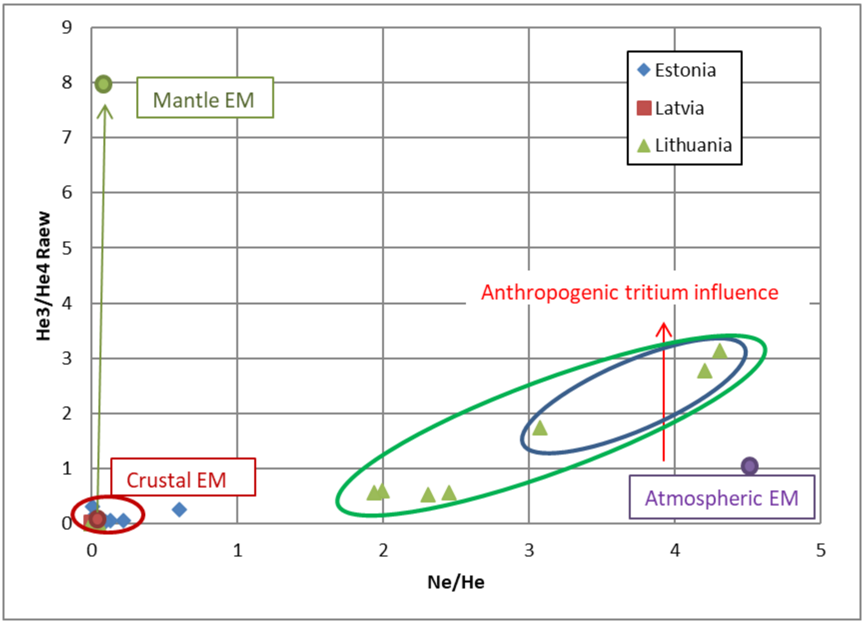

Figure 4.18. Helium origin in natural waters diagram. $^3He/^4He$ Raew - isotope ratio corrected for air equilibrated ratio, Ne/He - neon, and helium ratio.

The tectonic faults strongly determine helium and groundwater migration in the multilayered aquifer system in the BAB. The main lineaments are given in Figure 4.5. It is necessary to establish whether the intermediate-deep groundwater helium content appears from the tectonic faults as a highway for emanation or leakage through aquitards. According to the BABHEGM, the confining properties of the regional aquitards are usually very high; therefore, they isolate aquifers very well. A modeled parameters on the main studied sites are presented in Table 4.6. The increase in helium content could occur near the tectonic faults or along the flowline trajectory, passing high helium zones.

In the southern Estonia (Värska, Häädemeeste, South-Central Estonia sites), S-O aquitard hydraulic conductivity is from 1.0E^{-9} to 1.0E^{-5} m/d, thickness is 100-300 m, hydraulic head drop along the aquitard is 1-20 m (Table 4.6.). These parameters enable the calculation of the hydraulic velocity of leakage approximately 1E^{-11}-7E^{-7}-m/d. A modeled actual velocity (n=0.005) is 1E^{-4}-1E^{-8} m/d. However, the southern Estonian fault zones limit groundwater's lateral flow on the Värska site, Cm aquifer, and act as a hydraulic connection vertically - a head drop in the S-O top and bottom is

~2 m. The vertical helium leakage through the S-O aquitard would have resulted in significantly higher accumulation rates than observed; therefore, older groundwater according to the helium method. The fault allows some helium to migrate upwards faster. The role of the fault zone in this place could also be supported by comparing the helium content on the Häädemeeste site O-Cm (less fault influence, higher helium content) - Värska (fault influence, lower helium content). However, the situation was different during the permafrost conditions when helium accumulation could have been significantly higher.

The main difference in fault zone distribution in the central and southern BAB is that a higher density of dislocations is in the western part (Figure 4.5.). The sites of Klaipėda-Palanga, Riga, Telšiai, the Kaliningrad District (Rusnė) could be directly influenced by higher helium upwelling due to faults. Some helium could be distributed along the flow trajectory in the BAB. In the Cm and O-Cm aquifers, groundwater flow from the southern, deepest parts of the BAB and the southeastern recharge point towards the north (Figure 4.16.). Hydraulic conductivity is 0.2 m/d. In D_{2-1} aquifer recharge area is mainly in the western Lithuania with the general flow line directed toward the Baltic Sea (Figure 4.16.). Hydraulic conductivity is 1-2.4 m/d. The S-O aquifer on the sites is significantly thicker – 200-600 m, modeled k values are ~$1.0E^{-9}$ m/d. Such confining properties of the regional aquitard should limit the helium upwelling to the minimum at the intermediate-deep interaction level. S-O aquitard thickness and hydraulic head difference at bottom-top suggest that hydraulic gradient may vary 0.07-0.22. The leakage velocity may vary $1E^{-8}$-$1E^{-7}$ m/d, seepage velocity (n=0.005) is $1E^{-8}$-$5E^{-8}$ m/d. Such parameters make the aquitards almost impermeable. The role of the faults in the intermediate-deep level, in this case, is obvious. Without the loss through faults, helium content in the O-Cm aquifer should be significantly greater than measured and lower in the D_{2-1}. The tendency of the lowest helium ages compared to radiokrypton and MODPATH simulation indicates a fault's importance. The mass balance simulation may be an alternative solution to modeling groundwater ages in the BAB, which would account for groundwater mixing. The homogenous hydraulic parameters of the modeled regional aquitards S-O (k=$1E^{-9}$ m/d) and D_{2-1} (k=$1E^{-8}$-$1E^{-7}$ m/d) could be corrected to simulate the fault zones and represent a more accurate hydrogeological situation.

Table 4.6. Main sites hydrodynamical parameters of aquifers/aquitard according to the BABHEGM data. Parameters are approximate for the site region and are not actual wells.

Site (surface elevation, m abs.)	Index	Hydraulic heads, m abs.	Hydraulic conductivity (x-y for aquifers; z for aquitards) m/d	Thickness, m	Top elevation, m abs.
Värska (38)	Cm-V	70	0.5-1	150	-350
	Cmln	64	1.0E^{-7}	28	-322
	O-Cm	58	1	32	-290
	S-O	57	1.0E^{-5}	166	-124
	D_{2-1}	56	1.5	48	-76
	D_2nr	47	1.7E^{-6}	45	-31
	D_2	36	3	21	-10
Häädemeeste (11)	O-Cm	24	10	140	-363
	S-O	15	1.0E^{-9}	333	-30
	D_{2-1}	6	0.01	6	-24
South-Central Estonia (100)	O-Cm	53	1	130	-320
	S-O	57	1.0E^{-9}	197	-123
	D_{2-1}	61	1.5	37	-86
	D_2nr	66	1.0E^{-7}	26	-60
	D_2	70	3	87	27
Riga (20)	O-Cm	77	0.2	150	-962
	S-O	54	1.0E^{-9}	487	-475
	D_{2-1}	44	1	99	-376
	D_2nr	25	1.0E^{-7}	103	-273
	D_2	9	3	214	-59
Klaipėda-Palanga (10)	O-Cm	173	0.20	200	-1800
	S-O	60	1.0E^{-9}	520	-1280
	D_{2-1}	54	1.4-2.4	260	-1020
	D_2nr	40	1.0E^{-8}	215	-805
	D_2	23	0.5-1	168	-637
Telšiai (130)	O-Cm	147	0.20	70	-1730
	S-O	91	1.0E^{-9}	650	-1080
	D_{2-1}	55	1.40	274	-806
	D_2nr	46	1.0E^{-8}	130	-676
	D_2	36	1	196	-480
Likėnai (46)	O-Cm	120	0.20	150	-844
	S-O	81	1.0E^{-9}	391	-453
	D_{2-1}	68	1.00	133	-320

Site (surface elevation, m abs.)	Index	Hydraulic heads, m abs.	Hydraulic conductivity (x-y for aquifers; z for aquitards) m/d	Thickness, m	Top elevation, m abs.
	D_2nr	56	1.0E^{-7}	97	-223
	D_2	45	2.4	217	-6
Rusnė (2)	O-Cm	207	0.20	225	-2000
	S-O	131	1.0E^{-6}	840	-1160
	D_{2-1}	58	2.4	210	-950
	P	41	2	200	-750
Birštonas (55)	T aquifer	90	1	40	-180
	T aquitard	81	1.0E^{-6}	15	-165
	K_2cm-K_1	78	2	60	-105
	K_2	53	1.0E^{-4}	120	15

4.3.3. Helium Content and Isotope-Geochemistry Peculiarities

Helium content in the intermediate-deep groundwater varies from 1E^{-5} to 1E^{-4} ccSTP/g (Figure 4.19., Table 4.7.). The helium content strongly depends on depth, with higher helium values in the deeper aquifers. Analogically, helium content correlates with the chloride amount. A similar generalized tendency is for the TDS and oxygen-18. The enrichment of oxygen-18 correlates with the depth and chlorides, accordingly. Therefore, helium content is also observed to rise in this trend. As mentioned in previous chapters, helium content in the BAB groundwater is strongly predetermined by confining properties of the overlaying aquitard, fault zones, and other structural features of sedimentary cover and crystal basement. The highest amount of helium is found in the Cambrian aquifer system (Likėnai, Klaipėda, and Riga) at depths of >1 km (Table 4.7.). These sites coincide with the major Rapakivi massifs where the largest amount of helium is produced, such as the Riga massif. The Häädemeeste site also deviates from the He-Cl with elevated helium content near the western Estonian massif (Figure 4.19.) (Juodkazis & Tibar, 1989). The Veisiejai massif emanation may similarly influence the Birštonas site.

Groundwater residence time can be attributed to the helium content either directly (helium-4 ages) or indirectly compared to the radiokrypton and particle tracks. The Riga and Klaipėda sites' groundwater helium content may be attributed to the 1 Ma timescale. Ignalina, Häädemeeste and Värska are 0.3-0.6 Ma, according to radiokrypton. Other sites' groundwater is younger by <0.3 Ma. The insight in this generalization may suggest that the Likėnai Cm groundwater age should be close to Riga and Klaipėda, due to the similar helium content. An anomaly of the Telšiai site where low helium and chloride content is observed should be associated with shallow groundwater leakage, which dilutes groundwater *in situ*.

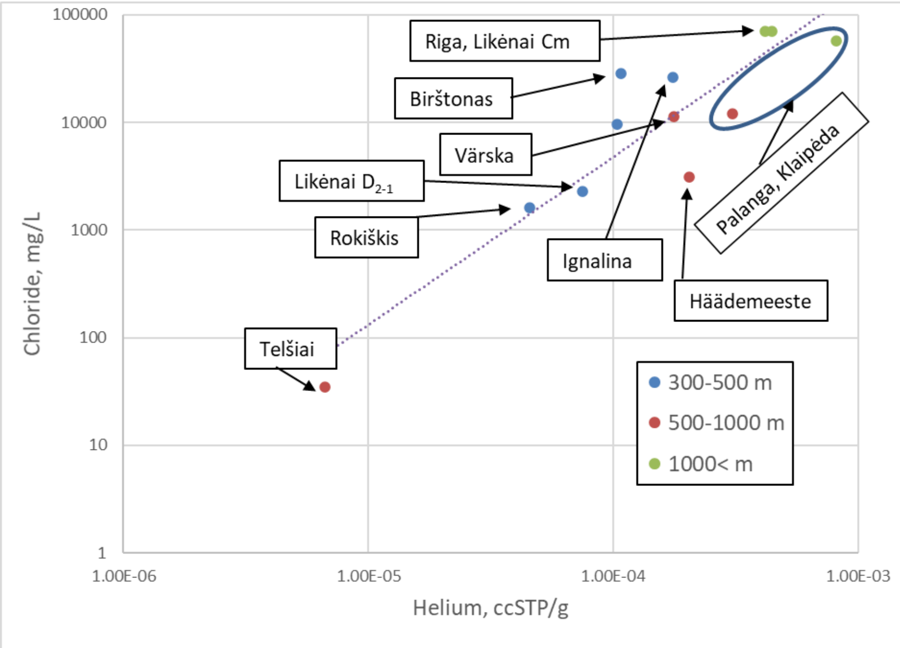

Figure 4.19. Chloride and helium diagram of intermediate-deep groundwater of the BAB.

Some of the isotope-geochemistry anomalies in basin-scale intermediate-deep levels could be observed in the light of groundwater age, especially obvious deviations from the established general trendlines of the BAB (Figure 4.20). The trendline slope of radiokrypton is 0.75x, particle track - 1.08x, and helium age - 1.29x (Figure 4.20.). These slope values mean that groundwater age differences using each method increase in deeper aquifers and data divergence occurs. The equations presented in Figure 4.20. could be used to roughly estimate the groundwater age at a certain depth of the BAB. It is necessary to mention that the equations are only valid for intermediate and deep aquifers with minimal depth criteria. The starting point of groundwater age is a depth function - a trendline transecting y-axis (x=0). According to equations, the criteria are radiokrypton at the depth of 260 meters, helium - 413 m, particle track - 319 m. It is necessary to mention that these depths, 0 annum age groundwater references, are close to the intermediate depth groundwater upper limit used in this work (300 m), and the previously established delayed exchange zone depth (360 m) according to Mokrik, 2003; Mokrik & Mažeika, 2006. However, in the western part of Lithuania on the Žemaitija High, the fresh groundwater anomaly reaches up to 400-500 m thickness (Juodkazis & Mikalauskas, 1994; Mokrik, 2003). This anomaly is possibly formed by an intensive percolation of meteoric water through fractured and high permeability rocks of the Devonian Formations during the Holocene-Pleistocene.

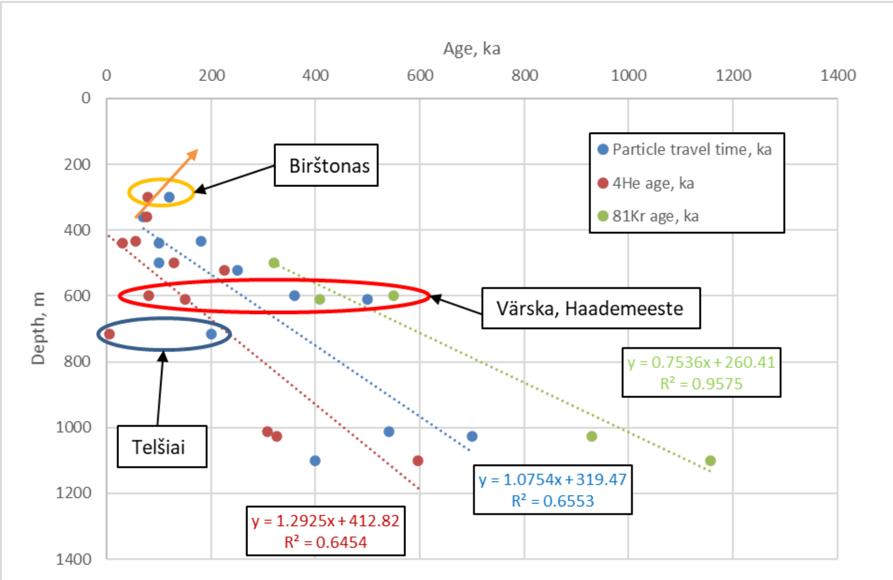

Figure 4.20. Intermediate-deep level groundwater age vs. aquifer depth based on Mokrik et al., 2021. Linear trendlines are plotted for helium, radiokrypton, and particle travel time dating results. The yellow circle and arrow represent the southern Lithuanian anomaly (the Birštonas site). The red circle represents the southern Estonian anomalies (the Värska and Häädemeeste sites). The blue circle represents the Telšiai site.

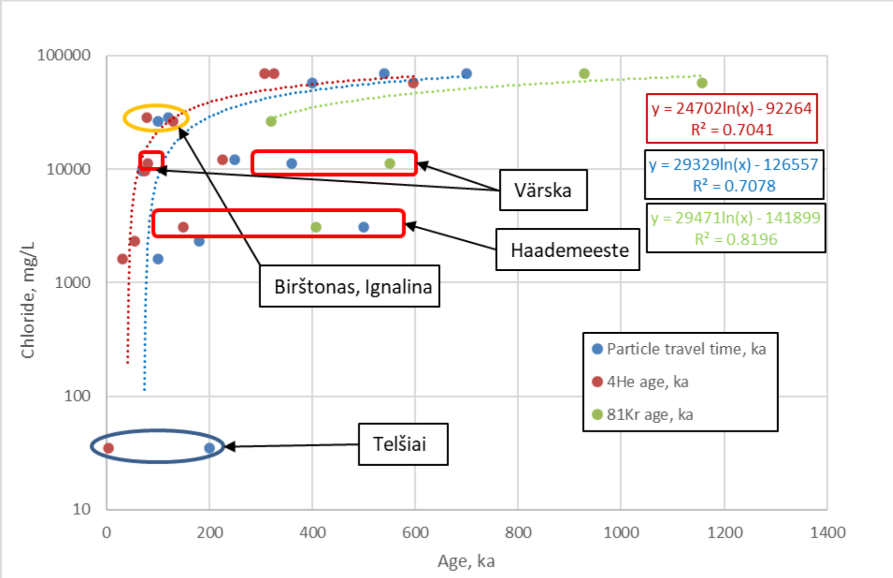

Figure 4.21. Intermediate and deep BAB aquifers groundwater age dependence on chloride content. Trendlines are plotted for helium, radiokrypton, and particle travel time dating results. The yellow circle represents the Birštonas and Ignalina sites. Red circles represent the southern Estonian anomalies (the Värska and Häädemeeste sites). The blue circle represents the Telšiai site.

Table 4.7. Isotope-geochemistry data of intermediate and deep BAB groundwater with determined ages (Mokrik et al., 2021).

Well No.	Site	$\delta^{18}O$, ‰	δ^2H, ‰	^4He content, ccSTP/g	TDS, g/L	SI calcite	SI halite
12350	Anykščiai	-9.6	-72.8	$1.04E^{-4}$	20.9	-0.40	-3.02
47543	Palanga	-9.7	-70.0	$3.06E^{-4}$	22.8	0.28	-2.95
12349	Rokiškis	-11.4	-83.8	$4.54E^{-5}$	5.6	0.33	-4.56
21965	Likėnai (Aukštaitija)	-5.7	-46.0	$4.19E^{-4}$	114.7	-0.42	-1.39
11978	Likėnai (Likėnai)	-12.2	-88.4	$7.47E^{-5}$	6.9	0.24	-4.18
50423	Ignalina	-7.2	-55.2	$1.76E^{-4}$	46.3	0.72	-2.22
25872	Klaipėda	-4.5	-34.7	$8.12E^{-4}$	94.2	-1.24	-1.64
50194	Riga, Hospital	-4.8	-42.7	$4.43E^{-4}$	114.2	0.86	-1.37
8021	Häädemeeste	-13.6	-100.7	$2.04E^{-4}$	5.1	0.31	-3.98
4613	Värska	-12.6	-92.8	$1.77E^{-4}$	18.4	0.34	-2.99
26418	Telšiai	-11.6	-85.5	$6.64E^{-6}$	1.3	0.20	-7.18
4913	Birštonas	-9.0	-66.0	$1.08E^{-4}$	47.6	-0.32	-2.31

Table 4.8. Isotope-geochemistry data of intermediate and deep BAB groundwater with determined ages (continued) (Mokrik et al., 2021).

Well No.	Cl^-, mg/L	SO_4^{2-}, mg/L	HCO_3^-, mg/L	Br^-, mg/L	Na^+, mg/L	K^+, mg/L	Mg^{2+}, mg/L	Ca^{2+}, mg/L
12350	9700	3500	69	19.4	6030	99	430	1010
47543	12100	2008	97	-	5790	196	500	2081
12349	1630	2064	116	-	850	54	163	745
21965	69600	1630	38	208.0	32450	308	2700	7780
11978	2300	2050	82	9.1	1480	42	158	772
50423	26348	2589	-	81.5	14535	190	764	1781
25872	57470	1712	-	368.9	24947	594	2319	6787
50194	69770	1379	-	287.1	33011	342	2567	6848
8021	3093	73	-	15.0	1648	36	78	175
4613	11240	249	-	53.6	5348	80	383	1006
26418	35	814	102	-	78	16	76	208
4913	28570	1540	74	-	11045	84	1570	4750

The case of the Telšiai groundwater in the D_{2-1} aquifer is significantly younger based on conventional helium and particle travel time modeling, 5 and 200 ka, accordingly (Figures 4.20., 4.21., blue circle). Using the established equations, the theoretical groundwater age at this depth should be 235 ka (helium equation), and 366 ka (particle travel time equation). A theoretical radiokrypton age can be calculated as well - 607 ka. The difference between actual and hypothetical ages is significant. It is also possible that for helium age calculation in the Telšiai groundwater, low porosity value should be reestimated; therefore, the groundwater age result differs from the modeled one 40 times.

The age results in the southern Estonian groundwater, the Häädemeeste and Värska wells, according to helium and radiokrypton is close to the general trendlines in the BAB (Figures 4.20., 4.21., red circle). On the contrary, the calculated particle travel time (Häädemeeste 500 ka, Värska 360 ka) is higher than the theoretical (~260 ka) at this depth. These results are calculated based on the same digital numeric model; therefore, the difference in groundwater age is a consequence of the multiple parameters and geometry coded into this simulation.

On the Birštonas site, a slight groundwater age inversion could be observed (Figures 4.20., 4.21., yellow circle arrow). According to previously established equations, the theoretical groundwater age should be modern. The equations are imperfect: the trendlines should intercept 0 on both axes -

the groundwater age starts from the recharge of soil at the ground surface. Therefore, the fit of the trendline is not necessarily linear.

It is difficult to establish any generalized relationship between groundwater age and chemical parameters. Geochemical anomalies and regional differences of groundwater isotope-geochemistry should be considered while analyzing and interpreting certain ages, groundwater chemical, and isotopic composition categories. For this reason, in Figure 4.21., four isotope-geochemistry anomalies are isolated and omitted from the calculation of trendlines and their equations: Birštonas (the southern Lithuanian anomaly), Värska and Häädemeeste (the southern Estonian anomalies), and Telšiai. The background trendlines of the BAB groundwater (Lithuania and Latvia) are established.

The major ion content in intermediate-deep level groundwater increases with the mean residence time due to multiple factors: initial water composition, water-rock interaction, evaporation, gravitational sink, ultrafiltration through confining layers. Groundwater alteration (or metamorphization) is usually a prolonged process; therefore, an increase in salinity (chloride) takes hundreds of ka. In case of increased chloride content, a certain solubility limit is reached (Figure 4.21., Table 4.8.). Solubility limit depends on the thermodynamic conditions in aquifers, which may vary across the BAB. The opposite situation is with sulfate. In intermediate-depth aquifers, the groundwater sulfate content is higher because it is not yet reduced to H_2S or other substances. The reduction of chemical species in groundwater occurs in succession; therefore, a sulfate could persist for hundreds of ka. The reduction strongly diminishes the sulfate content in million-year age (according to radiokrypton) groundwater. The southern Estonian groundwater lacks sulfate compared to other BAB groundwater of the similar age at least threefold. The cryogenic alteration which leads to sulfate precipitation and increases chloride content could partly explain both these anomalies.

The highest helium content is near the Baltic Sea coast and islands - in intermediate-deep level groundwater discharge areas. The deep and intermediate level groundwater flows are separated with the regional aquitards strongly confining the aquifers; therefore, the most significant leakage of helium should be associated with hydraulically active faults. However, vertical block dislocations may decrease the regional groundwater flow trajectory in the lateral direction. Helium has good conditions to accumulate below the regional aquitards in reservoirs bounded by screened faults and other dislocations. Helium content irregularities could often be considered an anomaly largely unsupported by isotope-geochemistry deviations.

4.4. Shallow-Intermediate Flows Interaction on the Evaporitic Succession Rocks Area and Tectonic Lineaments Local Sites

4.4.1. Intermediate Groundwater Upward Flow Injection on Local Anomalies Sites in the Southern Lithuania

The interaction of the shallow and intermediate groundwater occurs throughout the BAB, where leakage through aquitards or flow through tectonic faults occurs, in places where vertical inversed head distribution results in upward percolation (Juodkazis, 2003; Juodkazis et al., 1997; Mažeika, 1999; Mokrik, 2003). However, the southern Lithuanian groundwater anomalies are significantly pronounced, isotope-geochemistry alteration may reach the ground surface - spring discharge with saline groundwater. Such a phenomenon serves as a basis for considering anomalies in the area. The isotope-geochemistry peculiarities in the southern Lithuania are associated with sites where saline or brine groundwater discharges into shallow freshwater aquifers through tectonic faults. Intermediate-shallow groundwater interaction near the injection points results in a dome-shaped hydrogeological unit (Figure 4.22.). Therefore, isotope-geochemistry anomaly occurs in lateral and vertical dimensions. Hydraulic heads implicate a vertical upward discharge. Due to the low permeability of the Triassic aquitard (k=1E^{-8}-1E^{-5} m/d, 10-30 m thick according to BABHEGM), the main discharge occurs through the vertical faults, instead of leakage creating injection anomalies. This process was thoroughly studied in previous research; there are numerous observations and evidence of this phenomenon published (Juodkazis, 2003; Juodkazis et al., 1997; Mažeika, 1999; Mokrik, 2003; Zuzevičius et al., 2007). Hydraulically permeable tectonic faults can equally leak the helium from the intermediate zone and below. Chloride and helium content quantitatively correlate. Such observation supports the theory of deeper groundwater brine discharge and mixing with shallow freshwater (Gregorauskas et al., 2017; Juodkazis, 2003; Juodkazis et al., 1997; Mažeika, 1999; Mokrik, 2003; Zuzevičius et al., 2007). In the Figure 2.3., three main groundwater chemical facies could be derived: sodium-calcium-chloride (in some cases Ca-dominant), calcium-magnesium-bicarbonate, and freshwater end-member sodium-bicarbonate. A binary mixing line is presented between Na-Cl and Ca-Mg-HCO_3 type groundwater. There are no data points on this line concerning anomaly in this chapter as a TDS value of mixed groundwater should be between 1 and 2 g/L to make a chemical type that could manifest itself on PIPER plot, which is absent in the database. This is due to a significant difference in TDS values of end-members, freshwater <1 g/L, and saline groundwater up to 50 g/L. Therefore, a small portion (>5 % of total volume) of Na-Cl end-member is required to change calcium bicarbonate type into sodium chloride (Juodkazis & Mikalauskas, 1994).

The anomalous groundwater in this region is used as a mineral water resource; therefore, the most explored sites are Birštonas and Druskininkai. According to corrected radiocarbon dating, groundwater mixture on the Birštonas site's Cretaceous and Quaternary aquifer systems are up to 9,600 years old (Zuzevičius et al., 2007). Conventional helium and particle track ages of the Triassic aquifer saline groundwater members are 79 and 120 ka, accordingly. Based on tritium and radiocarbon data, a freshwater member is modern (Zuzevičius et al., 2007). Such on-site age distribution is logical and concurs with the previously established binary mixing. The theoretical age of mixed water should extend from the modern to ~100 ka timeframe, depending on freshwater-saline member portions. However, the dating methods are crucial at this point.

Helium content in the intermediate layer may be strongly affected by the tectonic fault vicinity, confining properties of aquitards, and helium production *in situ*, and crust. The sample for helium analysis was extracted near the tectonic fault in the Birštonas site's Triassic aquifer and could be depleted with upward emanation. It may cause an error in the dating results. The most likely solution would be to take additional samples from the intermediate level further from the anomalous site, avoiding any significant faults nearby. Such an approach may reveal the helium content in an aquifer without the disturbance of probable loss. Particle travel time modeling in this site shows 1.5 times older groundwater compared to helium. The previously stated fact that the digital model lacks structural features may be advantageous in this particular case. The groundwater age is not affected in any way apart from the intermediate aquifers' flow time and hydraulic properties. It may be a methodical problem for a solution for estimating a groundwater age distribution in anomalous sites. Other isotopic techniques, such as radiokrypton, may help estimate the age of groundwater in the intermediate zone. The radiokrypton method limit may not be sufficient if groundwater age is <150 ka (Lu et al., 2014). These problems should be addressed in future research of the injection type anomalies in the southern Lithuania.

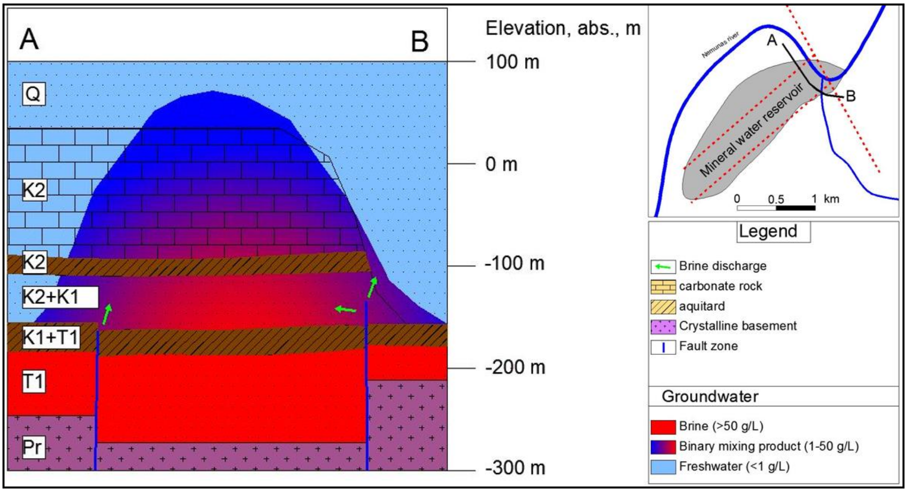

Figure 4.22. Druskininkai (Lithuania) mineral groundwater reservoir scheme. The black line A-B represent cross-section line, the red dashed lines are tectonic faults. After: Juodkazis, 2003; Juodkazis et al., 1997; Samalavičius, 2015.

The case study of natural and artificial processes which affect the southern Lithuanian anomalies was elaborated in the study (Gregorauskas et al., 2017). Groundwater modeling results in the Cenozoic-Mesozoic (Triassic, Jurassic, Cretaceous, and Quaternary aquifer systems) resources in the southern Lithuania are 893 thousand cubic meters per day. Most of it consists of meteoric water and lateral underground recharge. The primary discharge endpoints are river valleys and the Baltic Sea (Gregorauskas et al., 2017).

According to the authors, a natural process of binary mixing is catalyzed during the exploitation of freshwater. Due to the low permeability of aquifers and exploitation, the hydraulic head drops significantly; therefore, saline groundwater recharge from underlying aquifers intensifies. This process may alter the freshwater quality by increasing TDS and chloride content (Gregorauskas et al., 2017). The groundwater facies result from mixing modern meteoric, the Holocene Baltic Sea stages' recharge, and *in situ* saline groundwater leakage or injection. Water mixing results in Ca-Mg-HCO_3, Na-Ca-HCO_3-Cl, Na-HCO_3-Cl, Na-Cl-HCO_3, and Na-Cl facies (Gregorauskas et al., 2017; Mokrik, 2003). The increase of chloride content observed near the river valleys often indicates tectonic faults (Gregorauskas et al., 2017). According to chloride content modeling, significant anomalies are observed near the Šešupė River valley. A similar situation occurs in the proximity of the Nemunas River around Šakiai district (Figure 4.23.). A distinction of chloride anomalies found near tectonic faults correlates with geogenic helium emanation. This phenomenon can be observed in Figures

4.23., 4.24. In the Šešupė River valley, helium content varies 25-1,000 (10^{-5} mL/L), the Nemunas River near the Birštonas tectonic fault zone up to 2,000 (10^{-5} mL/L). Such an increase indicates favorable groundwater and helium upwelling conditions through tectonic faults into freshwater aquifers (Gregorauskas et al., 2017).

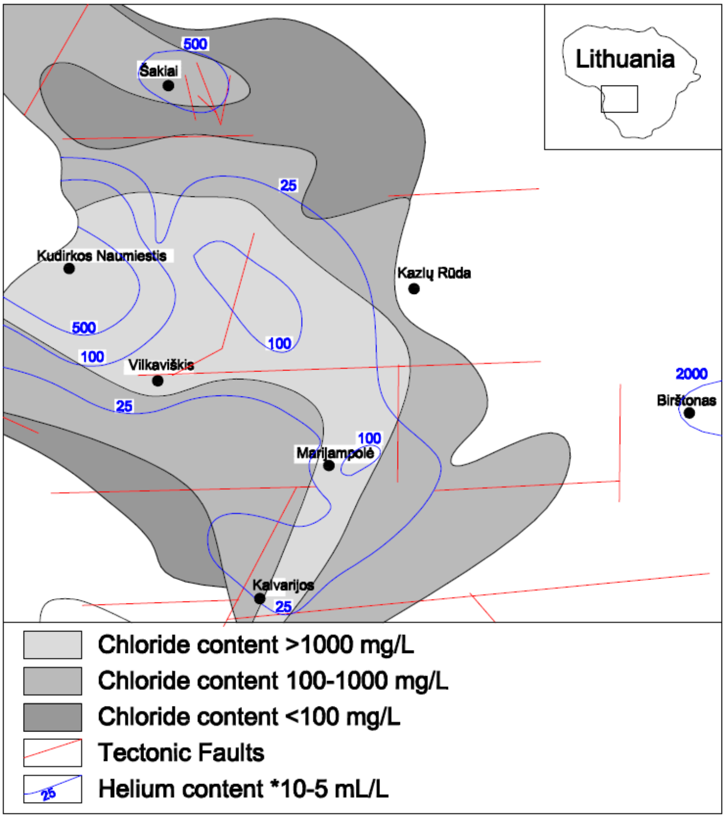

Figure 4.23. The scheme of helium and modeled chloride content in the groundwater of the Cretaceous aquifer system in the southwestern Lithuania. Modified based on Gregorauskas et al., 2017.

Isotope-geochemistry characteristics must be approached, focusing on the saline member of binary mixing. This statement is relevant concerning separate injection points in the southern Lithuanian area. Freshwater member is usually constant in their isotope-geochemistry composition - chloride content is <0.5 g/L, $\delta^{18}O$ ~-10.4 per mil. However, brine end-members differ on the sites. In the case of the Birštonas saline water, the chloride amount is 25-30 g/L, $\delta^{18}O$ content -9.0 per mil, the Druskininkai brine chloride content is >30 g/L, $\delta^{18}O$ value is -7.3 per mil. Chemical composition, pH values, and depth are similar in samples of the Triassic (T_1)

aquifer in Druskininkai and Birštonas. The distance between these locations is ~60 km. However, $\delta^{18}O$ values differ by 1.7 per mil. This difference is significant, keeping in mind that most other parameters are very similar. It could be explained by the influence of different types of brine by depth. Saline end-member could result from various brine mixing, such as discharge from the below. Vertical tectonic faults present on these sites could lead to multiple-level aquifer groundwater mixing. The shallow-intermediate interaction is as likely as multiple intermediate aquifer groundwater mixing as faults propagate towards the depth intersecting and hydraulically connecting them. Such phenomenon may be analyzed in the light of groundwater ages obtained in multiple site saline members. Noble gas signatures may reveal the origin and mix formation scenarios and provide crucial data where isotope-geochemistry is insufficient.

A clear correlation of chloride and helium content was observed in the Lithuanian groundwater at shallow-intermediate groundwater interface including the southern Lithuanian anomalies (Gregorauskas et al., 2017; Juodkazis, 2003; Juodkazis et al., 1997; Mažeika, 1999; Mokrik, 2003; Zuzevičius et al., 2007). This supports a widely observed binary mixing of intermediate-shallow groundwater in the BAB. However, groundwater helium deficit is observed on Druskiniai and Birštonas sites (Figure 4.24., blue circle). These anomalies most likely occur due to a few reasons. Intermediate groundwater with higher salinity (>5 gCl/L) could be sensitive to sample proximity to a fault zone. Groundwater near the hydrogeologically inactive tectonic dislocation may be effectively depleted of helium compared to the background by upward vertical emanation. The helium content of shallow aquifer groundwater is most likely controlled by the confining properties of aquitards in the saline groundwater discharge location. Chloride as a conservative constituent does not react to changes of geological setting, unlike helium. This phenomenon may have a crucial impact on the helium-4 dating results due to its loss. The importance of confining layers on helium content in groundwater was explicitly shown in Figure 4.18. where the Quaternary aquifer system aquitards collect a small amount of helium, contrary to other sites where almost all of He is lost to the atmosphere.

The $\delta^{18}O$ enrichment tendency toward the local discharge places is the opposite of Latvia and Estonia anomalies because of the upward outflow of isotopically heavier groundwater. The helium ages in these anomalies are less predictable than other intermediate-deep groundwater as He loss to the atmosphere is significant. It is essential to provide additional dating techniques to establish He loss in balance-reliable time frame at the injection points.

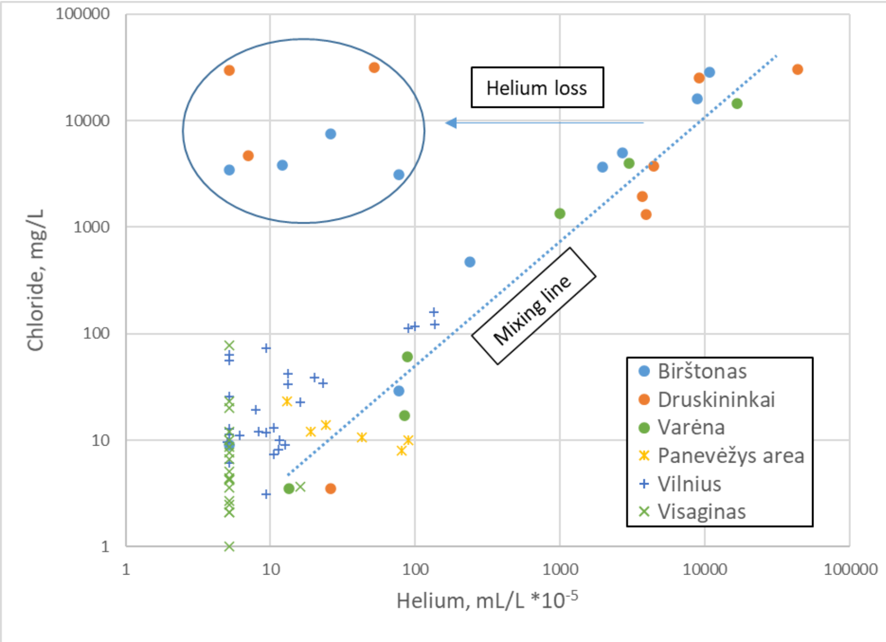

Figure 4.24. Chloride and helium diagram of shallow-intermediate depth groundwater in Lithuania supplemented with Birštonas, Druskininkai, and Varėna anomalies (Gregorauskas et al., 2017; Juodkazis, 2003; Juodkazis et al., 1997; Mažeika, 1999; Mokrik, 2003; Zuzevičius et al., 2007).

4.4.2. Central BAB Anomalies of the Devonian Evaporites Dissolution and Groundwater Leakages

Abundant shallow groundwater of Latvia and the northern Lithuanian isotope-geochemistry data shows an increase of chloride content correlating with a depletion in $\delta^{18}O$. Such an occurrence could suggest a previously mentioned cryogenic effect similar to the one observed in Estonia. Most of the isotopically depleted and elevated salinity samples are found at the depth ranging 150-300 m. However, in the Central BAB, the shallow groundwater may have modern recharge features according to many last decades' assessments. Groundwater tends to be slightly depleted with $\delta^{18}O$ in the Devonian aquifers at the intermediate-shallow level in the Middle Lithuanian Lowland (North Lithuania) and the Zemgale Plain (Latvia). The depletion near the coast correlates to groundwater chemistry alteration increase (Mokrik, 2003). A depletion with $\delta^{18}O$ is observable down to -11.5 -13.2 per mil. The predominant hydrochemical type is Ca-Mg-SO_4, associated with carbonate and sulfate mineral rocks dissolution in the Upper Devonian aquifers. Therefore, it is a sub-regional type of anomaly. Another anomaly is observed in the Kurzeme-Zemiatija Upland and the Middle Lithuania Lowland which from the south are bordered near transient zone from shallow to intermediate flow environment. Groundwater southwestward from this area has increased TDS values compared to the shallow depth background. This anomaly is connected with a northern part of the Middle Lithuania Lowland and the Zemgale Plain anomaly. However, here groundwater is more enriched with ^{18}O values from -10 to -11 per mil.

The interaction of shallow and intermediate groundwater manifests itself considering the Narva Formation regional aquitard. The inclination of the shallow aquifer formations indicates that the interaction occurs in both lateral and depth boundaries (Mokrik, 2003). The Ca-Mg-SO_4 groundwater is found at the depth ranging ~150-715 m. However, the sodium chloride facies are observed near the coast (Palanga) at ~500 m depth. The interaction of intermediate-deep level groundwater separated by the Narva regional aquitard must be elaborated on considering the transecting faults or by hydraulic conductivity of fractured lithologic rocks sequence. The areal anomalies study may include the sites near the Klaipėda-Telšiai Fault Zone, which may help to analyze this case.

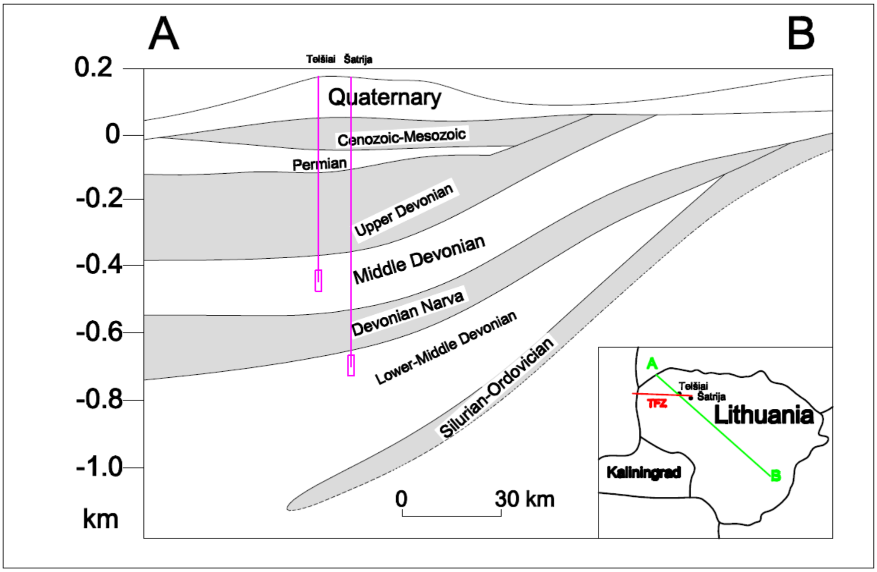

Figure 4.25. Telšiai and Šatrija sites in the cross-section of Lithuania. Upper Devonian, Devonian Narva, Silurian-Ordovician formations are regional aquitards. Modified based on Juodkazis and Mikalauskas, 1994.

Stable isotope depletion occurs in the shallow groundwater of the northern part of the Middle Lithuania Lowland-Zemgale Plain. There is an apparent $\delta^{18}O$ inversion towards the deep meteoric observed in the last decades (Figure 4.26., red arrows). The depletion trend of this anomaly of $\delta^{18}O$ occurs down to the depth of ~ 400 m with the value of -11.5-13.2 per mil, and chloride content up to a few hundred mg/L. At this point, the isotopic trend for the western-central site of the Liepaja-Riga-Pskov Antiklinal zone reverses toward a stable isotope enrichment indebted to the Kurzeme-Žemaitija Highland recharge area by modern precipitation, where mean annual $\delta^{18}O$ precipitation values are about 10.5 per mil. A slightly isotopically depleted Latvian groundwater at the Lielupe River valley on the Zemgale Plain is close to intermediate-shallow depth of <200-300 m, resulting from modern recharge on local land sites with winter season precipitation surplus in total balance. Calculations show that modern meteoric water percolation velocities can reach that depth in 30-50 years. Radiocarbon dating coupled with the tritium method also revealed that at this anomaly modern recharge occurs (Mokrik et al., 2009). The anomaly is likely related to wintertime depleted meteoric precipitation water mixing with the shallow groundwater of aquifer host rocks. Such winter seasonal precipitation has significantly increased in the last decades near sea lowlands and riverstream deltas on the Baltic coast (Jaagus et al., 2010; Kriaučiūnienė et al., 2012).

Global climatic variations shifts to winter season domination have probably caused isotopically depleted precipitation recharge. Available radiocarbon data at the sites of Renceni (Well. No. 9369, oxygen-18 -12.4 ‰, chloride 56 mg/L) and Baldone (Well. No. 1506, oxygen-18 -12.1 ‰, chloride 3022 mg/L) are 4.2 and 21.4, accordingly. This roughly (uncorrected carbon-14 data) could suggest the groundwater age of the Late Pleistocene or the Early Holocene Epoch. However, a significant amount of dissolved dead carbon in carbonate and evaporitic rocks may appear in the groundwater DIC. For the Baltic region, the Middle Lithuanian Lowland dead carbon content in groundwater is largely detected (Mokrik et al., 2009). A post-Pleistocene meteoric recharge most probably significantly affected the groundwater by diluting and depleting it in stable isotope content.

However, additional data is required to elaborate on the origin of the Devonian aquifer's isotopically depleted groundwater on the Baltic Sea islands, where regional discharge groundwater may be preserved.

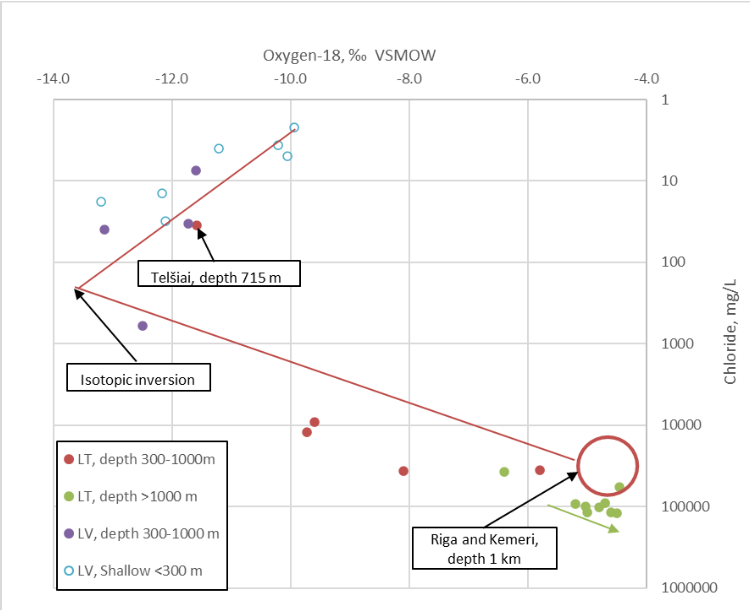

Figure 4.26. Oxygen-18 and chloride content diagram of the western Lithuanian and Latvian groundwater. The red lines represent isotopic inversion in the shallow-intermediate-deep groundwater multilayered system. The green arrow represents stable isotope enrichment in deep (>1500 m) brines.

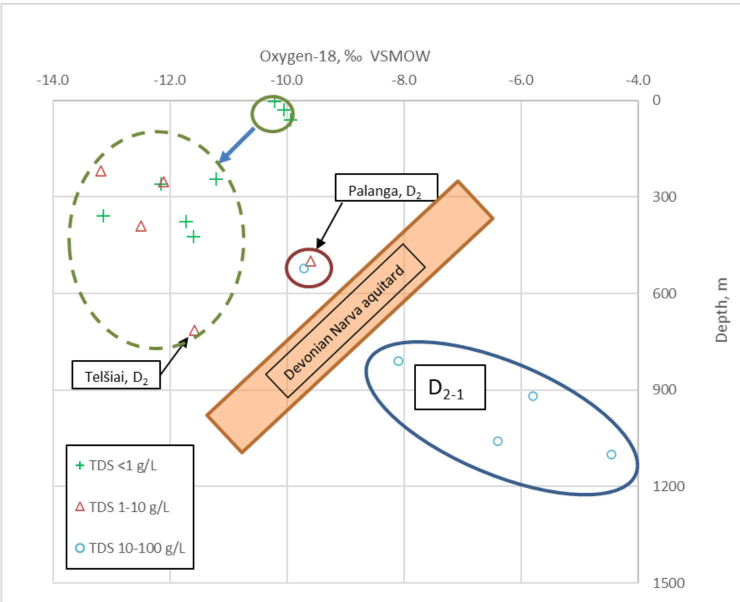

Figure 4.27. Oxygen-18 content and depth diagram of the western Lithuanian and Latvian groundwater in the Devoniain aquifers. The green circle represents modern meteoric origin groundwater, the green dashed circle - the Holocene Epoch groundwater, the red circle - the Middle Pleistocene Epoch, the blue circle - the lower-middle Devonian aquifer confined with regional aquitard. The blue arrow represents the formation of calcium sulfate facies, the red arrow - sodium (calcium) chloride.

The groundwater on the Telšiai site (Figure 4.25.) significantly deviates from the background according to its isotope-geochemistry content. The groundwater o the Telšiai site is in the Middle Devonian aquifer system: the depth is 650-715 m; TDS is 1.3 g/L, a slight depletion in $\delta^{18}O$ is from -11.6 to -13.2 per mil with Ca-Mg-SO_4 groundwater facies. A low helium content is observed on the Telšiai site and could be explained by a modern groundwater recharge influence from the overlying Frasnian Formation. It is quite possible that the pumping well is not properly sealed; therefore, leakage from shallow aquifers occurs. The Telšiai site is very similar to all Latvian evaporitic anomalies, according to the parameters mentioned before.

The groundwater dating results in the Devonian aquifers reveal that different groundwater facies evolve on each shallow-intermediate interaction level. Calcium sulfate groundwater in the D_2 aquifer most likely originates from the Holocene Epoch precipitation, according to radiocarbon ages and $\delta^{18}O$ depletion (Figure 4.27., blue arrow). However, the Telšiai site's groundwater dating results are controversial - according to the helium method, the age is ~5 ka, while particle track time is ~200 ka. The establishment of this site's groundwater age value requires additional studies. The Palanga D_2 aquifer's groundwater sample is entirely different from the Latvian groundwater (Figure 4.27., red circle). It has sodium chloride facies and ages 225-250 ka (Mokrik et al., 2021). For comparison, $\delta^{18}O$ content is slightly enriched in the Palanga sample. This groundwater most likely originates from altered seawater or mixing of meteoric, paleoseawater, and *in situ* saline recharge from underlying aquifers. The D_{2-1} groundwater is significantly older than the sample of the D_2 aquifer. According to radiokrypton dating of the Klaipėda site in D_{2-1} groundwater is >1.3 Ma, modeled and helium ages are 0.4-0.6 Ma (Gerber et al., 2017; Mokrik et al., 2021). Ages and isotope-geochemistry support the hypothesis that groundwater in both these aquifers differs in origin; the Devonian Narva aquitard is a significant controlling factor of this phenomenon (Mokrik, 2003).

The study of the Telšiai $\delta^{18}O$ depleted Middle Devonian aquifer groundwater would strongly benefit from the broader record of noble gas data. Such an approach may provide evidence of the groundwater origin, especially argon, krypton, xenon content, and excess air parameters. Multiple aspects could be cleared up: meteoric signal, recharge temperatures, and their relation to $\delta^{18}O$ source.

CONCLUSIONS

Groundwater anomalies found in the BAB are challenging to classify because of the variety of isotope-geochemistry content and their spatial distribution. From the scientific point of view, it often occurs that more than one formation scenario is possible; therefore, no definite conclusion could be made at this point. Nevertheless, some critical observations, theses, and suggestions could be made and proven with currently available data. The analysis supported the formation and origin of multiple previously stated anomalies by providing a new context of their occurrence. Some characteristic features are proposed in already established cases and sites. Other groundwater anomalies are, on the contrary, being reviewed and updated with an original conceptual model including entirely different explanations, hypotheses, and evidence. Spatial distribution sites of conceptualized BAB groundwater anomalies were based on the analysis of the flow formation models and origin. To reveal anomalies for shallow (<300 m), intermediate (300-1000 m), and deep (>1000 m) aquifers, the groundwater analysis of isotope-geochemistry data was executed. Additionally, the main factors, such as geological and hydrogeological settings and paleo-climate aspects during the Holocene and Pleistocene that influenced its formation were assessed. The establishment of a distinction within the background groundwater composition was made in the context of the local, intermediate, and deep flow system interaction for the formation of the surrounding lateral and depth-sequencing sites' groundwater anomalies by chemical and isotopic content.

The new conceptual model approach for the Estonian Homocline Cm-V and O-Cm aquifer systems groundwater shows that permafrost conditions occur on the boundary of the Fennoscandian and Northern Baltic regions. This approach is based on stable oxygen-18 isotope and thermodynamic data together with $^{234}U/^{238}U$ AR and helium ages. During periglacial cryogenic processes, the talik system influenced groundwater. Isotope-geochemistry of the Estonian Cm-V and O-Cm groundwater reveals that brine rejection (cryogenic concentration) and the Rayleigh distillation (depletion) formed these anomalies.

The saturation of the Estonian groundwater with calcite coincides with $\delta^{18}O$ depletion trendline and supports the previously stated brine rejection.

Permafrost-induced shifts in hydrochemistry (elevated ionic content and partial, selective mineral precipitation) lead to higher SI Halite (~1 unit) values in the Estonian groundwater compared to other BAB groundwater with the same TDS.

According to Na/Cl and Br/Cl ratios and the Pleistocene Epoch's mean annual temperature variations, the initial, pre-cryogenic groundwater composition should be close to meteoric, paleogroundwater, and seawater mix. Uranium $^{234}U/^{238}U$ isotope ratio AR and helium content suggest that the groundwater before LGM was frozen. However, some hydraulic pathways existed along the talik framework, allowing local flux on supra- and sub-permafrost levels.

Argon, krypton, and xenon gas content ratios in the Estonian shallow anomalous groundwater reveal that isotopic depletion originates from *in situ* groundwater freezing as it is closer to an air-equilibrated water composition's end-member than atmospheric air. Noble gas excess air, in this case, could be explained by gas rejection during the freezing.

A good linear relationship of chloride-helium values content exists in the BAB groundwater. In recharge areas on highlands, the shallow groundwater helium content is diluted with meteoric precipitation. Helium may escape intensively in the intermediate-shallow groundwater boundary; resulting in lowering its amount. This evidence is observed on sites near the deep fluid injection places close to the hydrogeologally active tectonic fault zones. Helium escapes to the atmosphere, where the confining properties of overlaying aquitards are insufficient for trapping.

Shallow-intermediate groundwater $\delta^{18}O$ composition change in the BAB toward discharge places forming two general trends:

a. In the central and northern parts of BAB, $\delta^{18}O$ values are getting depleted. Two distinct anomalies support this trend. In the Late-Middle Devonian shallow aquifer system on the coastline and the Lielupe River system, slightly $\delta^{18}O$ depleted groundwater may originate from modern winter season precipitation due to the increased atmospheric water balance during the last 30 years. The isotopically depleted groundwater trend of the northern and western Estonian coast in the Cm-V and O-Cm aquifers is due to cryogenesis and talik system in the Pleistocene.

b. The interaction of the shallow and intermediate groundwater flows in the vicinity of the tectonic lineaments on river valleys manifests by the changes of isotope-geochemistry where saline water discharge occurs. In the southern part of the BAB, an enrichment of $\delta^{18}O$ values occurs - saline groundwater injections into freshwater aquifers near the river valleys result in isotopic enrichment.

Deep and intermediate depth flows are separated by regional-scale aquitards, which is proved by the steady-state 3D groundwater flow model coupled with the noble gas residence times of the deep groundwater. In the deep-intermediate groundwater interaction zone, helium migration and distribution may not necessarily coincide with groundwater flow. The most critical factors on helium content in groundwater are confining regional scale aquitards and hydrogeological highways within tectonic zone fractures (faults).

Helium dating peculiarities in the BAB multilayered aquifer systems extend beyond a simple collection of data and parameters necessary for the calculation. The regional features of groundwater isotope-geochemistry composition, formation environments, and processes suggest various approaches to evaluate helium age validity. The knowledge of geological settings (aquifer and aquitard position, tectonic features, permeability hydraulic parameters, etc.) is crucial for assessing conventional helium ages. The coupled dating method, which includes MODPATH modeling and radiokrypton tracer, provides necessary data concerning helium distribution. Differences in dating techniques and results could be embraced based on the background trends and anomalies in the BAB or isolated flow systems. The aggregate helium method could be used to correct groundwater ages in the deepest aquifers, accounting for advection and diffusion of helium in depth.

The particle track trajectories revealed the lack of tectonic fracture zones' permeability in the numerical model, which significantly distorts the estimated modeled residence times compared to radiokrypton and helium ages. It must be solved by correcting hydraulic parameters and including fault geometry. An alternative groundwater mass transport modeling may also help with the reevaluation of groundwater ages. In many cases, the difference between radiokrypton, helium ages, and groundwater flow particle travel times are significant. The absence of fault zones' actual permeability characteristics in the numerical model may be substituted with the correction of hydraulic parameters in layers to reflect a natural hydrogeological internal boundary setting more accurately. It is also necessary to minimize discrepancies of ^{81}Kr and ^{4}He groundwater ages, improving methodical assessment aspects to actual porosity parameters of multi-layered porous-fractured media. An alternative groundwater mass transport modeling may also help with the reevaluation of groundwater ages, however, problems in defining initial boundaries arise as well.

REFERENCES

Aeschbach-Hertig, W. (2014). Radiokrypton dating finally takes off. *Proceedings of the National Academy of Sciences of the United States of America*, *111*(19), 6856–6857. https://doi.org/10.1073/pnas.1405830111

Aeschbach-Hertig, W. (2020). *Groundwater Sampling for Helium / Noble Gases*.

Aeschbach-Hertig, W., El-Gamal, H., Wieser, M., & Palcsu, L. (2008). Modeling excess air and degassing in groundwater by equilibrium partitioning with a gas phase. *Water Resources Research*, *44*(8), 1–12. https://doi.org/10.1029/2007WR006454

Aeschbach-Hertig, W., Peeters, F., Beyerle, U., & Kipfer, R. (1999). Interpretation of dissolved atmospheric noble gases in natural waters. *Water Resources Research*, *35*(9), 2779–2792. https://doi.org/10.1029/1999WR900130

Aeschbach-Hertig, W., & Solomon, D. K. (2013). The noble gases as geochemical tracers. In *The Noble Gases as Geochemical Tracers* (Issue September 2014). https://doi.org/10.1007/978-3-642-28836-4

Alexeev, S. v., & Alexeeva, L. P. (2002). Ground ice in the sedimentary rocks and kimberlites of Yakutia, Russia. *Permafrost and Periglacial Processes*, *13*(1), 53–59. https://doi.org/10.1002/ppp.408

Alexeev, S. v., & Alexeeva, L. P. (2003). Hydrogeochemistry of the permafrost zone in the central part of the Yakutian diamond-bearing province, Russia. *Hydrogeology Journal*. https://doi.org/10.1007/s10040-003-0270-8

Alexeev, S. v., Alexeeva, L. P., Borisov, V. N., Shouakar-Stash, O., Frape, S. K., Chabaux, F., & Kononov, A. M. (2007). Isotopic composition (H, O, Cl, Sr) of ground brines of the Siberian Platform. *Russian Geology and Geophysics*, *48*(3), 225–236. https://doi.org/10.1016/j.rgg.2007.02.007

Andrén, E., Andrén, T., & Kunzendorf, H. (2000). Holocene history of the Baltic Sea as a background for assessing records of human impact in the sediments of the Gotland Basin. *Holocene*, *10*(6), 687–702. https://doi.org/10.1191/09596830094944

AntonParr. (2014). *Application Report Total Digestion with HF in Multiwave GO Complexation of Fluorides Application Report*. Anton Parr.

Appelo, C. A. J., & Postma, D. (1993). Geochemistry, groundwater and pollution. In *Geochemistry, groundwater and pollution*. https://doi.org/10.1016/0016-7037(94)90585-1

Babre, A., Kalvāns, A., Popovs, K., Retiķe, I., Dēliņa, A., Vaikmäe, R., & Martma, T. (2016). Pleistocene age paleo-groundwater inferred from water-stable isotope values in the central part of the Baltic Artesian Basin. *Isotopes in Environmental and Health Studies*, *52*(6), 706–725. https://doi.org/10.1080/10256016.2016.1168411

Bagard, M. L., Chabaux, F., Pokrovsky, O. S., Viers, J., Prokushkin, A. S., Stille, P., Rihs, S., Schmitt, A. D., & Dupré, B. (2011). Seasonal variability of element fluxes in two Central Siberian rivers draining high latitude permafrost dominated areas. *Geochimica et Cosmochimica Acta*, *75*(12), 3335–3357. https://doi.org/10.1016/j.gca.2011.03.024

Ball, J. W., & Nordstrom, D. K. (1991). User's Manual for WATEQ4F, with revised thermodynamic data base and test cases for calculating speciation of major, trace, and redox elements in natural waters. In *U.S. Geological Survey Water-Resources Investigations Report* (Vols. 91–183). http://wwwbrr.cr.usgs.gov/projects/GWC_chemtherm/pubs/wq4fdoc.pdf

Ballentine, C. J., & Burnard, P. G. (2002). Production, release and transport of noble gases in the continental crust. *Reviews in Mineralogy and Geochemistry*, *47*(January), 482–538. https://doi.org/10.2138/rmg.2002.47.12

Banys, J., Juodkazis, V., & Mokrik, R. (1979). Regional regularities of radiocarbon distribution in groundwaters of the Baltic artesian basin. *Water Resources (in Russian)*, *6*(2), 243–248.

BerkeleyRausser. (2014). *Perkin Elmer ICP Instructions*.

Bethke, C. M., & Johnson, T. M. (2008). Groundwater Age and Groundwater Age Dating. *Annual Review of Earth and Planetary Sciences*, *36*(1), 121–152. https://doi.org/10.1146/annurev.earth.36.031207.124210

Bethke, C. M., Torgersen, T., & Park, J. (2000). The "age" of very old groundwater: Insights from reactive transport models. *Journal of Geochemical Exploration*, *69–70*, 1–4. https://doi.org/10.1016/S0375-6742(00)00115-1

Beyerle, U., Aeschbach-Hertig, W., Imboden, D. M., Baur, H., Graf, T., & Kipfer, R. (2000). A mass, spectrometric system for the analysis of noble gases and tritium from water samples. *Environmental Science and Technology*, *34*(10), 2042–2050. https://doi.org/10.1021/es990840h

Bondarenko, G., Gudzenko, I., & Kovalyukh, N. (1981). Formation of radioactive and stable isotope front in discharge area of artesian basin. *Nauka (in Russian)*, 157–164.

Borgatti, L., & Soldati, M. (2013). Hillslope Processes and Climate Change. *Treatise on Geomorphology*, *7*(March), 306–319. https://doi.org/10.1016/B978-0-12-374739-6.00180-9

Brand, W. A., Geilmann, H., Crosson, E. R., & Rella, C. W. (2009). Cavity ring-down spectroscopy versus high-temperature conversion isotope ratio mass spectrometry; a case study on delta(2)H and delta(18)O of pure water samples and alcohol/water mixtures. In *Rapid communications in mass spectrometry : RCM* (Vol. 23, Issue 12, pp. 1879–1884). https://doi.org/10.1002/rcm.4083

Brangulis, A., & Kaņevs, S. (2002). *Tectonics of Latvia [In Latvian]*. State Geological Survey.

Brehme, M., Nowak, K., Banks, D., Petrauskas, S., Valickas, R., Bauer, K., Burnside, N., & Boyce, A. (2019). A Review of the Hydrochemistry of a Deep Sedimentary Aquifer and Its Consequences for Geothermal Operation: Klaipeda, Lithuania. *Geofluids*, *2019*. https://doi.org/10.1155/2019/4363592

Brosius, L. S., Walter Anthony, K. M., Grosse, G., Chanton, J. P., Farquharson, L. M., Overduin, P. P., & Meyer, H. (2012). Using the deuterium isotope composition of permafrost meltwater to constrain thermokarst lake contributions to atmospheric CH4 during the last deglaciation. *Journal of Geophysical Research: Biogeosciences*, *117*. https://doi.org/10.1029/2011JG001810

Bujanauskas, M. (2016). *Sequence peculiarities of oxygen–18 stable isotopes and chlorides in the shallow aquifers of the Baltic artesian basin)*. Thesis.

Bujanauskas, M. (2018). *Assessment of groundwater resources of Upper – Middle Paleozoic aquifer systems in the Baltic region by numerical modeling*. Thesis.

Burnard, P. (2012). *The Noble Gases as Geochemical Tracers*. Springer Berlin Heidelberg. https://books.google.lt/books?id=GUHyDVBVCkEC

Cheban, E. (1966). Aquifer and aquifer systems characterization. In B. Archangelsky, E. Mustygi, & E. Cheban (Eds.), *Hydrogeology USSR. Estonia. Volume 30. [in Russian]* (pp. 65–193). Nedra.

Clark, I., & Fritz, P. (1997). *Environmental isotopes in hydrogeology*. Lewis Publishers. https://doi.org/10.1201/9781482242911

Dansgaard, W. (1964). Stable isotopes in precipitation. *Tellus*, *16*(4), 436–468. https://doi.org/10.3402/tellusa.v16i4.8993

De Schepper, S., Groeneveld, J., Naafs, B. D. A., van Renterghem, C., Hennissen, J., Head, M. J., Louwye, S., & Fabian, K. (2013). Northern Hemisphere Glaciation during the globally warm early late Pliocene. *PLoS ONE*, *8*(12). https://doi.org/10.1371/journal.pone.0081508

Delina, A., Kalvans, A., Saks, T., Bethers, U., & Valdis, V. (2012). *Highlights of groundwater research in the Baltic Artesian Basin*. University of Latvia.

Dzikaite, A. (2003). *Determination of hydrogeological activity of karst area tectonic fractures*. Thesis.

Ewing, S. A., O'Donnell, J. A., Aiken, G. R., Butler, K., Butman, D., Windham-Myers, L., & Kanevskiy, M. Z. (2015). Long-term anoxia and release of ancient, labile carbon upon thaw of Pleistocene permafrost. *Geophysical Research Letters*, *42*(24), 10730–10738. https://doi.org/10.1002/2015GL066296

Ewing, S. A., Paces, J. B., O'Donnell, J. A., Jorgenson, M. T., Kanevskiy, M. Z., Aiken, G. R., Shur, Y., Harden, J. W., & Striegl, R. (2015). Uranium isotopes and dissolved organic carbon in loess permafrost: Modeling the age of ancient ice. *Geochimica et Cosmochimica Acta*, *152*, 143–165. https://doi.org/10.1016/j.gca.2014.11.008

Ferguson, G., & Jasechko, S. (2015). The isotopic composition of the Laurentide Ice Sheet and fossil groundwater. *Geophysical Research Letters*, *42*(12), 4856–4861. https://doi.org/10.1002/2015GL064106

Fujikawa, Y., Fukui, M., Sugahara, M., Ikeda, E., & Shimada, M. (2000). Variation in Uranium Isotopic Ratios 234 U / 238 U and 235 U / total-U in Japanese Soil and Water Samples — Application to Environmental Monitoring. *IPRA 10*, *January*, P-4a-238.

Gatalski, M. A. (1954). *Groundwater and Paleozoic gases in the northern part of the Russian Platform* (Special Se).

Gerber, C., Vaikmäe, R., Aeschbach, W., Babre, A., Jiang, W., Leuenberger, M., Lu, Z. T., Mokrik, R., Müller, P., Raidla, V., Saks, T., Waber, H. N., Weissbach, T., Zappala, J. C., & Purtschert, R. (2017). Using 81Kr and noble gases to characterize and date groundwater and brines in the Baltic Artesian Basin on the one-million-year timescale. *Geochimica et Cosmochimica Acta*, *205*(October), 187–210. https://doi.org/10.1016/j.gca.2017.01.033

Gragnani R, Guglielmin M, Stenni B, Longinelli A, Smiraglia C, & Cimino, L. (1998). Origins of the ground ice in the ice-free lands of the Northern

Foothills (Northern Victoria Land, Antarctica). *Proceedings of the Seventh International Conference on Permafrost*, *55*(55), 335–340.

Gregorauskas, M., Kaušinis, K., Bujanauskas, M., Samalavičius, V., & Mokrik, R. (2017). Modelling assessment of groundwater resources and hydrochemical anomalies of Cenomanian-lower Cretaceous aquifer [in Lithuanian]. *Geologija. Geografija*, *3*(2), 73–79. https://doi.org/10.6001/geol-geogr.v3i2.3538

Gregorauskas, M., Klimas, A., & Bendoraitis, A. (2008). *Upper-middle paleozoic hydrogeological system groundwater resources [in Lithuanian]*.

Gregorauskas, M., Klimas, A., & Bendoraitis, A. (2009). *Joniškis and Biržai-Pasvalys sub-basin's groundwater resources [in Lithuanian]*.

Gregorauskas, M., Klimas, A., & Bendoraitis, A. (2012). *Cenozoic-Mesozoic hydrogeological system groundwater resources [in Lithuanian]*.

Gregorauskas, M., Mokrik, R., & Savitski, L. (1988). Formation of available groundwater resources on the northern Baltic coast [in Russian]. *Sov.Geology*, *11*, 80–88.

Grigoriev, A., Zhamoida, V., Spiridonov, M., Sharapova, A., Sivkov, V., & Ryabchuk, D. (2011). Late-glacial and Holocene palaeoenvironments in the Baltic sea based on a sedimentary record from the Gdansk Basin. *Climate Research*, *48*(1), 13–21. https://doi.org/10.3354/cr00944

Grootes, P. M., & Stuiver, M. (1997). Oxygen 18/16 variability in Greenland snow and ice with 10- 3- to 105-yeatri mer esolution. *Journal of Geophysical Research*, *102*(C12), 26,455-26,470.

Herut, B., Starinsky, A., Katz, A., & Bein, A. (1990). The role of seawater freezing in the formation of subsurface brines. *Geochimica et Cosmochimica Acta*, *54*(1), 13–21. https://doi.org/10.1016/0016-7037(90)90190-V

Hindshaw, R. S., Aciego, S. M., & Tipper, E. T. (2018). Li and U Isotopes as a Potential Tool for Monitoring Active Layer Deepening in Permafrost Dominated Catchments. *Frontiers in Earth Science*, *6*(July), 1–17. https://doi.org/10.3389/feart.2018.00102

IAEA. (2013). *Isotope Methods For Dating Old Groundwater*. IAEA. https://www-pub.iaea.org/MTCD/Publications/PDF/Pub1587_web.pdf

IAEA/WMO. (2019). Global Network of Isotopes in Precipitation. In *GNIP Maps and Animations, International Atomic Energy Agency*. http://isohis.iaea.org

Jaagus, J., Briede, A., Rimkus, E., & Remm, K. (2010). Precipitation pattern in the Baltic countries under the influence of large-scale atmospheric circulation and local landscape factors. *International Journal of Climatology*, *30*(5), 705–720. https://doi.org/10.1002/joc.1929

Jähne, B., Heinz, G., & Dietrich, W. (1987). Measurement of the diffusion coefficients of sparingly soluble gases in water. *Journal of Geophysical Research: Oceans*, *92*(C10), 10767–10776. https://doi.org/10.1029/JC092iC10p10767

Jefanova, O., Mažeika, J., Petrošius, R., Skuratovič, Ž., Paškauskas, R., Martma, T., Liblik, T., & Ezhova, E. (2020). Baltic Sea water tritium and stable isotopes in 2016–2017*. *Isotopes in Environmental and Health Studies*, *56*(2), 193–204. https://doi.org/10.1080/10256016.2020.1715969

Jessen, S., Holmslykke, H. D., Rasmussen, K., Richardt, N., & Holm, P. E. (2014). Hydrology and pore water chemistry in a permafrost wetland, ilulissat, Greenland. *Water Resources Research*, *50*(6), 4760–4774. https://doi.org/10.1002/2013WR014376

Johnsen, S. J., Dansgaard, W., & White, J. W. C. (1989). The origin of Arctic precipitation under present and glacial conditions. *Tellus B*, *41 B*(4), 452–468.

Jouzel, J., Alley, R. B., Cuffey, K. M., Dansgaard, W., Grootes, P., Hoffmann, G., Johnsen, S. J., Koster, R. D., Peel, D., Shuman, C. A., Stievenard, M., Stuiver, M., & White, J. (1997). Validity of the temperature reconstruction from water isotopes in ice cores. *Journal of Geophysical Research: Oceans*, *102*(C12), 26471–26487. https://doi.org/10.1029/97JC01283

Jouzel, J., Koster, R. D., Suozzo, R. J., & Russell, G. L. (1994). Stable water isotope behavior during the last glacial maximum: A general circulation model analysis. *Journal of Geophysical Research*, *99*, 25791–25801. https://doi.org/10.1029/94JD01819

Juodkazis, V. (1980a). *Formation and consumption of the groundwater resources of Baltic States [in Russian]* (A. Zuzevičius, A. Grigelis, V. Juodkazis, V. Kadūnas, P. Suveizdis, & J. Vaitiekūnas, Eds.). Academy of Lithuania.

Juodkazis, V. (1980b). *Hydrogeological Map of the Pre-quaternary Deposits of the Soviet Baltic Republics*. Ministry of Geology of the USSR.

Juodkazis, V. (1989). *Regional hydrogeology of the Baltic region* (In russian). Mokslas.

Juodkazis, V. (1994). Groundwater Quality and Its Monitoring in the Baltic States. *GeoJournal*, *33*(1), 63–70. http://www.jstor.org/stable/41146199

Juodkazis, V. (2003). *Regional hydrogeology foundations [in Lithuanian]*. Vilnius University Publishing House.

Juodkazis, V., & Mikalauskas, V. (1994). Groundwater. In A. Grigelis & V. Kadūnas (Eds.), *Geology of Lithuania [in Lithuanian]* (pp. 334–398). Science and encyclopedia publishing house.

Juodkazis, V., & Mokrik, R. (1981). Hydrogeology of submarine part of the Baltic Artesian Basin. In *Sediments in the Baltic Sea [in Russian]* (p. 248). Mokslas.

Juodkazis, V., Suveizdis, P., & Rastenienė, V. (1997). Geothermal and mineral water resources of Lithuania. *Mineral and Thermal Groundwater Resources*, 281–316. https://doi.org/10.1007/978-94-011-5846-6_11

Juodkazis, V., & Tibar, K. (1989). Helium in groundwater on the northern flank of the Baltic Artesian Basin. *International Geology Review, 31*(7), 736–743.

Karro, E., Marandi, A., & Vaikmäe, R. (2004). The origin of increased salinity in the Cambrian-Vendian aquifer system on the Kopli Peninsula, northern Estonia. *Hydrogeology Journal*, *12*, 424–435. https://doi.org/10.1007/s10040-004-0339-z

Karro, E., Marandi, A., Vaikmäe, R., & Uppin, M. (2009). Chemical peculiarities of the Silurian–Ordovician and Cambrian–Vendian aquifer systems in Estonia: an overview of hydrochemical studies. *Estonian Journal of Earth Sciences*, *58*(4), 342. https://doi.org/10.3176/earth.2009.4.12

Kirs, J., Puura, V., Soesoo, A., Klein, V., Konsa, M., Koppelmaa, H., Niin, M., & Urtson, K. (2009). Eesti kristalne aluskord: Paleoproterosoilised Orosiri ja Statheri ning mesoproterosoilised Calymmi ajastu kivimkompleksid ja regionaalne korrelatsioon. *Estonian Journal of Earth Sciences*, *58*(4), 219–228. https://doi.org/10.3176/earth.2009.4.01

Kirsimae, K., & Jorgensen, P. E. R. (2000). *Mineralogical and Rb-Sr isotope studies of low temperature diagenesis of lower Cambrian clays of the Balic paleobasin of north Estonia*. *48*(1), 95–105.

Klimas, A., & Plankis, M. (2007). Water budget and quality in Vilnius wellfields studied by isotope methods. *Geologija*, *59*(3), 65–71. http://mokslozurnalai.lmaleidykla.lt/publ/1392-110X/2007/3/Geol_065_071.pdf

Koch, J. C., Ewing, S. A., Striegl, R., & McKnight, D. M. (2013). Rapid runoff via shallow throughflow and deeper preferential flow in a boreal catchment underlain by frozen silt (Alaska, USA). *Hydrogeology Journal*, *21*(1), 93–106. https://doi.org/10.1007/s10040-012-0934-3

Kondratas, A., Mikalauskas, V., Grigelis, A., & et. al. (1969). *Hydrogeology USSR. Lithuania. Volume 32. [in Russian]*. Nedra.

Kononova, R. (1979). A cryogenic factor of groundwater chemistry formation and zonality features of permafrost territories. *Problems of Theoretical and Regional Hydrogeochemistry [in Russian]*, 119–123.

Kriaučiūnienė, J., Meilutyte-Barauskiene, D., Reihan, A., Koltsova, T., Lizuma, L., & Sarauskiene, D. (2012). Variability in temperature, precipitation and river discharge in the Baltic States. *Boreal Environment Research*, *17*(2), 150–162. https://helda.helsinki.fi/bitstream/handle/10138/229865/ber17-2-150.pdf

Krynicki, K., Green, C. D., & Sawyer, D. W. (1978). Pressure and temperature dependence of self-diffusion in water. *Faraday Discussions of the Chemical Society*, *66*(0), 199–208. https://doi.org/10.1039/DC9786600199

Kurylyk, B. L., MacQuarrie, K. T. B., & McKenzie, J. M. (2014). Climate change impacts on groundwater and soil temperatures in cold and temperate regions: Implications, mathematical theory, and emerging simulation tools. *Earth-Science Reviews*, *138*, 313–334. https://doi.org/10.1016/j.earscirev.2014.06.006

Kuzinas, A., Jurkonis, A., Šonta, Z., & Zuzevičius, A. (1981). *Hydrogeological research of centralized groundwater distribution in Panevėžys [in Russian]*.

Kuzinas, A., Jurkonis, A., Šonta, Z., & Zuzevičius, A. (1982). *Hydrogeological research of centralized groundwater distribution in Utena [in Russian]*.

Lacelle, D., Lauriol, B., & Clark, I. D. (2006). Effect of chemical composition of water on the oxygen-18 and carbon-13 signature preserved in cryogenic carbonates, Arctic Canada: Implications in paleoclimatic studies. *Chemical Geology*, *234*(1–2), 1–16. https://doi.org/10.1016/j.chemgeo.2006.04.001

Lauriol, B., Lacelle, D., St-Jean, M., Clark, I. D., & Zazula, G. D. (2010). Late quaternary paleoenvironments and growth of intrusive ice in eastern Beringia (Eagle River valley, northern Yukon, Canada). *Canadian Journal of Earth Sciences*, *47*, 941–955. https://doi.org/10.1139/E10-012

Lehmann, M., & Siegenthaler, U. (1991). Equilibrium oxygen- and hydrogen-isotope fractionation between ice and water. *Journal of Glaciology*, *37*(125), 23–26. https://doi.org/10.3189/S0022143000042751

Levina, L. E., Demanov, V. V., Stadnik, V. E., Galaskokov, V.V. Ermakov, N.N. Gartayenov., Yu. A., & Yanitskii, I. N. (1975). A measuring device for helium analysis in geological investigations. *EI. VEAMS Series*, *10*, 1–22.

Levins, I. (1990). *Hydrogeological map of Latvia scale 1:500000, Explanatory note*. State Geological Survey.

Levins, I., Levina, N., & Gavena, I. (1998). *Latvian groundwater resources*.

Lhomme, N. (2005). *Modelling water isotopes in polar ice sheets*.

Lipp, G., Körber, Ch., Englich, S., Hartmann, U., & Rau, G. (1987). Investigation of the behavior of dissolved gases during freezing. *Cryobiology, 24*(6), 489–503. https://doi.org/10.1016/0011-2240(87)90053-8

Loose, B., McGillis, W. R., Schlosser, P., Perovich, D., & Takahashi, T. (2009). Effects of freezing, growth, and ice cover on gas transport processes in laboratory seawater experiments. *Geophysical Research Letters*, *36*(5), 1–5. https://doi.org/10.1029/2008GL036318

Lu, Z. T., Schlosser, P., Smethie, W. M., Sturchio, N. C., Fischer, T. P., Kennedy, B. M., Purtschert, R., Severinghaus, J. P., Solomon, D. K., Tanhua, T., & Yokochi, R. (2014). Tracer applications of noble gas radionuclides in the geosciences. *Earth-Science Reviews*, *138*, 196–214. https://doi.org/10.1016/j.earscirev.2013.09.002

Malov, A. I. (2017). Evolution of Uranium Isotopic Compositions of the Groundwater and Rock in a Sandy-Clayey Aquifer. In *Water* (Vol. 9, Issue 12). https://doi.org/10.3390/w9120910

Malov, A. I., & Tokarev, I. v. (2019). Using stable isotopes to characterize the conditions of groundwater formation on the eastern slope of the Baltic Shield (NW Russia). *Journal of Hydrology, 578*, 124130. https://doi.org/10.1016/j.jhydrol.2019.124130

Matsumoto, T., Solomon, D. K., Araguás-Araguás, L., & Aggarwal, P. (2017). The IAEA’s Coordinated Research Project on “Estimation of Groundwater Recharge and Discharge by Using the Tritium, Helium-3 Dating Technique”: In Lieu of a Preface. *GEOCHEMICAL JOURNAL*, *51*(5), 385–390. https://doi.org/10.2343/geochemj.2.0500

Mažeika, J. (1999). *Regularities of Radionuclide Migration and Transformation in Lithuanian Geological Environment*.

Mažeika, J. (2007). *Evaluation of tritium volumetric activity in water samples*. Institute of Geology and Geography.

Mažeika, J., Martma, T., Petrošius, R., Jakimavičiūtė-Maselienė, V., & Skuratovič, Ž. (2013). Radiocarbon and other environmental isotopes in the groundwater of the sites for a planned new nuclear power plant in Lithuania. *Radiocarbon, 55*(2–3), 951–962.

McCaffrey, M. A., Lazar, B., & Holland, H. D. (1987). The evaporation path of seawater and the coprecipitation of Br - and K + with halite. *Journal of Sedimentary Petrology, 57*(5), 928–937. https://doi.org/10.1306/212f8cab-2b24-11d7-8648000102c1865d

McEwen, T., & Marsily, G. (1991). *The potencial significance of permafrost to the behaviour of a deep radioactive waste repository*.

Mejean, P., Pinti, D. L., Ghaleb, B., & Larocque, M. (2017). Fracturing-induced release of radiogenic 4He and 234U into groundwater during the last deglaciation: An alternative source to crustal helium fluxes in periglacial aquifers. *Journal of the American Water Resources Association*, *53*(7), 5677–5689. https://doi.org/10.1002/2016WR020014

Michel, F. A. (1986). Isotope geochemistry of frost-blister ice, North Fork Pass, Yukon, Canada. *Canadian Journal of Earth Sciences*, *23*, 543–549. https://doi.org/10.1139/e86-054

Mix, A. C., & Ruddiman, W. F. (1984). Oxygen-isotope analyses and Pleistocene ice volumes. *Quaternary Research*, *21*(1), 1–20. https://doi.org/10.1016/0033-5894(84)90085-1

Mokrik, R. (1978). *Peculiarities and assessment features of the groundwater resources in the northern part of Baltic region*.

Mokrik, R. (1996). Pecularities of the formation of the isotopic composition of underground waters on the southern slope of the Baltic shield. *Geologija*, *19*, 16–25.

Mokrik, R. (1997). *The Palaeohydrogeology of the Baltic Basin. Vendian and Cambrian*. Tartu University Press.

Mokrik, R. (2003). *The paleohydrogeology of the Baltic basin*. Vilnius University Publishing House.

Mokrik, R., Juodkazis, V., Štuopis, A., & Mažeika, J. (2014). Isotope geochemistry and modelling of the multi-aquifer system in the eastern part of Lithuania. *Hydrogeology Journal*, *22*(4), 925–941. https://doi.org/10.1007/s10040-014-1120-6

Mokrik, R., & Mažeika, J. (2006). *Hydrogeochemistry*. Vilnius University Publishing House.

Mokrik, R., Mažeika, J., Baublyte, A., & Martma, T. (2009). The groundwater age in the Middle-Upper Devonian aquifer system, Lithuania. *Hydrogeology Journal*, *17*(4), 871–889. https://doi.org/10.1007/s10040-008-0403-1

Mokrik, R., Monkevicius, A., Floden, T., Puura, V., & Zuzevicius, A. (2000). The Pleistocene icings evidences and their influence on the formation of the groundwater discharge areas in the Baltic Basin. Geophysics in the Baltic Region: Problems and Prospects for the New Millennium.

Geophysics in the Baltic Region: Problems and Prospects for the New Millennium, 45–46.

Mokrik, R., Petkevičius, R., & Kirsimae, K. (2000). The Palaeohydrogeology of the Cambrian-Vendian Aquiferous System in the Baltic Basin. *Geologija*, *31*, 79–92.

Mokrik, R., Petkevičius, R., Zuzevičius, A., Klimas, A., Diliūnas, J., & Rastenienė, V. (2004). Evolution of underground hydrospere and groundwater resources. In D. Griniūtė (Ed.), *Evolution of Earth Crust and Its Recources in Lithuania* (p. 699). Petro Ofsetas.

Mokrik, R., Puura, V., Floden, T., & Petkevičius, R. (2002). Peculiarities of helium distribution in the Baltic Basin. *Litosfera, 6*, 121–123.

Mokrik, R., & Samalavičius, V. (2022). Interpretation of the anomalous groundwater chemistry and 234U/238U activity ratio disequilibrium in the northern part of the Baltic region (accepted for publishing). *Lithuanian Journal of Physics*, *62*(1). https://doi.org/10.3952/physics.v62i1.4645

Mokrik, R., Samalavičius, V., Bujanauskas, M., & Gregorauskas, M. (2021). Environmental isotopes and noble gas ages of the deep groundwater with coupled flow modelling in the Baltic artesian basin. *Lithuanian Journal of Physics, 61*(1), 53–65. https://doi.org/10.3952/physics.v61i1.4407

Mokrik, R., Samalavičius, V., Gregorauskas, M., Jakimavičiūtė-Maselienė, V., & Arustienė, J. (2022). "Integrated studies of crustal permeability based on environmental isotopes, noble gas data, and shallow-deep groundwater flow and mass transport modeling in the surrounding area of Ignalina Nuclear Power Plant (NPP)"// Chapter in "Use of Isotope Hydrology to Characterize Groundwater Systems in the Vicinity of Nuclear Power Plants. Results of a Coordinated Research Project F33022, 2016-2020, Institute for Safety Problems of Nuclear Power Plants, National Academy of Sciences of Ukraine - Chornobyl (Kiev region) and International Atomic Energy Agency - Vienna (Austria): 200 p. (Accepted for publishing)

Mokrik, R., Savitskaja, L., & Savitski, L. (2005). Aqueous geochemistry of the Cambrian–Vendian aquifer system in the Tallinn intake, northern Estonia. *Geologija, 51*(3), 50–56. http://mokslozurnalai.lmaleidykla.lt/geologija/2005/3/2867

Mokrik, R., & Vaikmäe, R. (1988). Paleohydrogeological aspects of Cm-V groundwater isotope content formation in Baltic region. *Isotope Geochemistry Research in Baltic and Belarus [in Russian]*, 133–143.

Murozumi, M., Chow, T. J., & Patterson, C. (1969). Chemical concentrations of pollutant lead aerosols, terrestrial dusts and sea salts in Greenland and Antarctic snow strata. *Geochimica et Cosmochimica Acta*, *33*(10), 1247–1294.

Oelkers, E. H., & Helgeson, H. C. (1988). Calculation of the thermodynamic and transport properties of aqueous species at high pressures and temperatures: dissociation constants for supercritical alkali metal halides at temperatures from 400 to 800.degree.C and pressures from 500 to 4000 bar. *The Journal of Physical Chemistry*, *92*(6), 1631–1639. https://doi.org/10.1021/j100317a049

O'Neil, J. R. (1968). Hydrogen and oxygen isotope fractionation between ice and water. In *Journal of Physical Chemistry* (pp. 3683–3684). https://doi.org/10.1021/j100856a060

Ozima, M., & Podosek, F. A. (2002). Noble Gas Geochemistry. In *Noble Gas Geochemistry*. https://doi.org/10.1017/cbo9780511545986

Pärn, J. (2018). *Origin and Geochemical Evolution of Palaeogroundwater in the Northern Part of the Baltic Artesian Basin*. Doctoral Thesis.

Pärn, J., Affolter, S., Ivask, J., Johnson, S., Kirsimäe, K., Leuenberger, M., Martma, T., Raidla, V., Schloemer, S., Sepp, H., Vaikmäe, R., & Walraevens, K. (2018). Redox zonation and organic matter oxidation in palaeogroundwater of glacial origin from the Baltic Artesian Basin. *Chemical Geology*, *488*, 149–161. https://doi.org/10.1016/j.chemgeo.2018.04.027

Pärn, J., Raidla, V., Vaikmäe, R., Martma, T., Ivask, J., Mokrik, R., & Erg, K. (2016). The recharge of glacial meltwater and its influence on the geochemical evolution of groundwater in the Ordovician-Cambrian aquifer system, northern part of the Baltic Artesian Basin. *Applied Geochemistry*, *72*, 125–135. https://doi.org/10.1016/j.apgeochem.2016.07.007

Pärn, J., Walraevens, K., van Camp, M., Raidla, V., Aeschbach, W., Friedrich, R., Ivask, J., Kaup, E., Martma, T., Mažeika, J., Mokrik, R., Weissbach, T., & Vaikmäe, R. (2019). Dating of glacial palaeogroundwater in the Ordovician-Cambrian aquifer system, northern Baltic Artesian Basin. *Applied Geochemistry*, *102*, 64–76. https://doi.org/10.1016/j.apgeochem.2019.01.004

Paškevičius, J. (1994). *Geology of Baltic States*. Vilnius University Publishing House.

Paukštys, B., Cooper, A. H., & Arustiene, J. (1999). Planning for gypsum geohazards in Lithuania and England. *Engineering Geology*, *52*(1–2), 93–103. https://doi.org/10.1016/S0013-7952(98)00061-1

Paukštys, B., & Narbutas, V. (1996). Gypsum karst of the Baltic Republics. *International Journal of Speleology*, *25*(3/4), 279–284. https://doi.org/10.5038/1827-806x.25.3.21

PerkinElmer. (2008). *Optima 7x00 Series, ICP-OES Sytems*. PerkinElmer.

Petrošius, R. (1990). *Tritium study methods in Baltic Highland Quaternary groundwater*.

Porcelli, D., & Turekian, K. K. (2014). *6.16 - The History of Planetary Degassing as Recorded by Noble Gases* (H. D. Holland & K. K. B. T.-T. on G. (Second E. Turekian, Eds.; pp. 353–382). Elsevier.

Potter, R. W., & Clynne, M. A. (1978). The solubility of the noble gases He, Ne, Ar, Kr, and Xe in water up to the critical point. *Journal of Solution Chemistry*, *7*(11), 837–844. https://doi.org/10.1007/BF00650811

Priestley, S. C., Kleinig, T., Love, A. J., Post, V. E. A., Shand, P., Stute, M., Wallis, I., & Wohling, D. L. (2017). Palaeohydrogeology and transport parameters derived from 4he and cl profiles in aquitard pore waters in a large multilayer aquifer system, central Australia. *Geofluids*, *2017*. https://doi.org/10.1155/2017/9839861

Punning, J.-M., Toots, M., & Vaikmae, R. (2008). Oxygen-18 in Estonian Natural Waters. *Isotopes in Environmental and Health Studies - ISOT ENVIRON HEALTH STUD*, *23*, 232–234. https://doi.org/10.1080/10256018708623797

Punning, J.-M., Toots, M., & Vaikmäe, R. (1987). Oxygen-18 in Estonian natural waters. In G. Strauch (Ed.), *Proceedings of the Fourth Working Meeting Isotopes in Nature* (p. 688).

Purtschert, R., Yokochi, R., Jiang, W., Lu, Z. T., Mueller, P., Zappala, J., van Heerden, E., Cason, E., Lau, M., Kieft, T. L., Gerber, C., Brennwald, M. S., & Onstott, T. C. (2021). Underground production of 81Kr detected in subsurface fluids. *Geochimica et Cosmochimica Acta*, *295*, 65–79. https://doi.org/10.1016/j.gca.2020.11.024

Puura, V., Klein, V., Koppelmaa, H., & Niin, M. (1997). Precambrian basement. In A. Raukas & A. Teedumae (Eds.), *Geology and Mineral Resources of Estonia* (pp. 27–34). Estonian Academy Publishers.

Raidla, V. (2010). *Chemical and isotope evolution of groundwater in the Cambrian-Vendian aquifer system in Estonia*.

Raidla, V., Kern, Z., Pärn, J., Babre, A., Erg, K., Ivask, J., Kalvāns, A., Kohán, B., Lelgus, M., Martma, T., Mokrik, R., Popovs, K., & Vaikmäe, R. (2016). A δ^{18}O isoscape for the shallow groundwater in the Baltic Artesian Basin. *Journal of Hydrology*, *542*, 254–267. https://doi.org/10.1016/j.jhydrol.2016.09.004

Raidla, V., Kirsimäe, K., Vaikmäe, R., Jõeleht, A., Karro, E., Marandi, A., & Savitskaja, L. (2009). Geochemical evolution of groundwater in the Cambrian-Vendian aquifer system of the Baltic Basin. *Chemical Geology, 258*(3–4), 219–231. https://doi.org/10.1016/j.chemgeo.2008.10.007

Raidla, V., Kirsimäe, K., Vaikmäe, R., Kaup, E., & Martma, T. (2012). Carbon isotope systematics of the Cambrian-Vendian aquifer system in the northern Baltic Basin: Implications to the age and evolution of groundwater. *Applied Geochemistry, 27*(10), 2042–2052. https://doi.org/10.1016/j.apgeochem.2012.06.005

Raidla, V., Pärn, J., Aeschbach, W., Czuppon, G., Ivask, J., Kiisk, M., Mokrik, R., Samalavičius, V., Suursoo, S., Tarros, S., & Weissbach, T. (2019). Intrusion of Saline Water into a Coastal Aquifer Containing Palaeogroundwater in the Viimsi Peninsula in Estonia. *Geosciences, 47*(9). https://doi.org/10.3390/geosciences9010047

Raidla, V., Pärn, J., Schloemer, S., Aeschbach, W., Czuppon, G., Ivask, J., Marandi, A., Sepp, H., Vaikmäe, R., & Kirsimäe, K. (2019). Origin and formation of methane in groundwater of glacial origin from the Cambrian-Vendian aquifer system in Estonia. *Geochimica et Cosmochimica Acta, 251*, 247–264. https://doi.org/10.1016/j.gca.2019.02.029

Raudsep, R. (1997). Mineral occurrence. In A. Raukas & A. Teedumäe (Eds.), *Geology and Mineral Resources of Estonia* (p. 436). Estonian Academy Publishers. https://geoloogia.info/geology/

Rozanski, K., & Zuber, A. (2000). Glacial infiltration in Europe – myth or reality. *Przegląd Geologiczny*, *48*, 796–803.

Rudzianskaitė, A. (2017). Investigation of Water Quality in the Agricultural Area of Lithuanian Karst Region. *Cave Investigation*, *August*. https://doi.org/10.5772/intechopen.68536

Rumbaugh, D. B., & Rumbaugh, J. O. (2011). *Groundwater Vistas [Guide to Using]*.

Samalavičius, V. (2015). *Pecularities of Fresh Groundwater Isotope-Geochemistry Anomalies in the Baltic Artesian Basin*. Thesis.

Samalavičius, V., & Mokrik, R. (2016). Tritium activity trend formation in groundwater of Quaternary aquifer system, south-eastern Lithuania. *Geologija. Geografija*, *2*(4), 173–181. https://doi.org/10.6001/geol-geogr.v2i4.3399

Samalavičius, V., & Mokrik, R. (2021). Noble gas characteristics of the Baltic Artesian Basin groundwater. *Bioateitis, Gamtos Ir Gyvybės Mokslų Perspektyvos*, 46.

Sano, Y., Marty, B., & Burnard, P. (2013). *Noble Gases in the Atmosphere BT - The Noble Gases as Geochemical Tracers* (P. Burnard, Ed.; pp. 17–31). Springer Berlin Heidelberg. https://doi.org/10.1007/978-3-642-28836-4_2

Savitski, L., & Belkina, V. (1985). Revealing of formation sources of the exploitation resources in the coastal part using isotope surveys. In Kolesnikova (Ed.), *Hydrosphere isotopes. Symposium abstracts* (pp. 206–207). VSEGINGEO Publishers.

Schneider, R., Schmitt, J., Köhler, P., Joos, F., & Fischer, H. (2013). A reconstruction of atmospheric carbon dioxide and its stable carbon isotopic composition from the penultimate glacial maximum to the last glacial inception. *Climate of the Past*, *9*(6), 2507–2523. https://doi.org/10.5194/cp-9-2507-2013

Skridlaite, G., & Motuza, G. (2001). Precambrian domains in Lithuania: Evidence of terrane tectonics. *Tectonophysics*, *339*, 113–133. https://doi.org/10.1016/S0040-1951(01)00035-X

Skuratovič, Z. (2013). *Aeration zone models and their applications and safety analysis of radioactive waste repository*. Doctoral Thesis.

Šliaupa, S. (2009). Lithuaniain Geothermal Resaurces (in Lithuanian). *Geologijos Akiračiai*, *3–4*, 11–19.

Šliaupa, S., Motuza, G., Korabliova, L., Ciuraite, K., & Puronas, V. (2010). *Geothermal Potential of Hot Granites of Lithuania*. *April*, 25–29.

Solubility Data Series, Argon. (1980). In H. L. Clever (Ed.), *International union of pure and applied chemistry* (Vol. 4). PERGAMON PRESS OXFORD. https://doi.org/10.1515/ci.2008.30.6.19

Solubility Data Series, Helium and Neon. (1979). In H. L. Clever (Ed.), *International union of pure and applied chemistry* (Vol. 1). Pergamon press Oxford. https://doi.org/10.1515/ci.2008.30.6.19

Solubility Data Series, Krypton, Xenon and Radon. (1979). In H. L. Clever (Ed.), I*nternational union of pure and applied chemistry*. Pergamon press Oxford. https://doi.org/10.1016/0378-3812(80)80030-6

Souchez, R., Tison, J. ‐ L, & Jouzel, J. (1987). Freezing rate determination by the isotopic composition of the ice. *Geophysical Research Letters*, *14*(6), 599–602. https://doi.org/10.1029/GL014i006p00599

Starinsky, A., & Katz, A. (2003). The formation of natural cryogenic brines. *Geochimica et Cosmochimica Acta*, *67*(8), 1475–1484.

https://doi.org/10.1016/S0016-7037(02)01295-4
Steiger, R. H., & Jager, E. (1977). Subcommission on geochronology : convention on the use of decay constants in geo- and cosmochronology compded by On August 24, 1976 the lUGS Subcommlsslon on Geochronology met in Sydney, Australia, during the 25th International Geological Congress. *Earth and Planetary Science Letters, 36*, 1977.
Sterckx, A., Lemieux, J. M., & Vaikmäe, R. (2017). Representing glaciations and subglacial processes in hydrogeological models: A numerical investigation. *Geofluids, 2017*. https://doi.org/10.1155/2017/4598902
Sterckx, A., Lemieux, J.-M., & Vaikmäe, R. (2018). Assessment of paleo-recharge under the Fennoscandian Ice Sheet and its impact on regional groundwater flow in the northern Baltic Artesian Basin using a numerical model. *Hydrogeology Journal, 26*(8), 2793–2810. https://doi.org/10.1007/s10040-018-1838-7
Stotler, R. L., Frape, S. K., Ruskeeniemi, T., Pitkänen, P., & Blowes, D. W. (2012). The interglacial-glacial cycle and geochemical evolution of Canadian and Fennoscandian Shield groundwaters. *Geochimica et Cosmochimica Acta*, *76*, 45–67. https://doi.org/10.1016/j.gca.2011.10.006
Stravinskas, V., Bendoraitis, A., & Saulis, K. (1984). *Hydrogeological research of centralized groundwater distribution in Kėdainiai [in Russian]*.
Štuopis, A., Juodkazis, V., & Mokrik, R. (2012). The quaternary aquifer system flow model by chemical and tritium isotope data: Case of south-east Lithuania. *Baltica*, *25*(2), 91–98. https://doi.org/10.5200/baltica.2012.25.09
Stute, M., & Schlosser, P. (1993). *Principles and Applications of the Noble Gas Paleothermometer*. 89–100. https://doi.org/10.1029/gm078p0089
Suckow, A., Gröning, M., Jaklitsch, M., Han, L.-H., & Aggarwal, P. (2007). The noble gas facility for isotope hydrology at IAEA, Vienna: goals, technical principles and first results. *Noble Gases in the Hydrosphere and Natural Gas Reservoirs*, 115. https://doi.org/10.2312/GFZ.mga.050
Suursoo, S., Hill, L., Raidla, V., Kiisk, M., Jantsikene, A., Nilb, N., Czuppon, G., Putk, K., Munter, R., Koch, R., & Isakar, K. (2017). Temporal changes in radiological and chemical composition of Cambrian-Vendian groundwater in conditions of intensive water consumption. *Science of the Total Environment*, *601–602*, 679–690. https://doi.org/10.1016/j.scitotenv.2017.05.136
Suveizdis, P. (1994). Tectonics. In A. Grigelis & V. Kadūnas (Eds.), *Geology of Lithuania [in Lithuanian]* (pp. 213–227).

Suveizdis, P. (2000). Geothermal potential of Lithuania and outlook for its utilization. *Proceedings World Geothermal Congress 2000, Kyushu - Tohoku, Japan*, 461–468. http://www.geothermal-energy.org/pdf/IGAstandard/WGC/2000/R0653.PDF

Suveizdis, P. (2003). *Lithuania tectonical structure (in Lithuanian)*.

Suzuoki, T., & Kimura, T. (1973). D/H and 18O/16O Fractionation in Ice-Water System. *Journal of the Mass Spectrometry Society of Japan*, *21*, 229–233. https://doi.org/10.5702/massspec1953.21.229

Taminskas, J., & Marcinkevicius, V. (2002). Karst geoindicators of environmental change: The case of Lithuania. *Environmental Geology*, *42*(7), 757–766. https://doi.org/10.1007/s00254-002-0553-8

Tokarev, I., Zubkov, A. A., Rumynin, V. G., Polyakov, V. A., Kuznetsov, V. Yu., & Maksimov, F. E. (2006). *Origin of high 234U/238U ratio in post-permafrost aquifers BT - Uranium in the Environment: Mining Impact and Consequences* (B. J. Merkel & A. Hasche-Berger, Eds.; pp. 847–856). Springer Berlin Heidelberg. https://doi.org/10.1007/3-540-28367-6_88

Torgersen, T., & Stute, M. (2013). Helium (and other noble gases) as a tool for the understanding long time-scale groundwater transport. In *Isotope methods for dating old groundwater* (p. 376). International Atomic Energy Agency. https://www-pub.iaea.org/MTCD/Publications/PDF/Pub1587_web.pdf

Tsironi, I., Schlesinger, D., Späh, A., Eriksson, L., Segad, M., & Perakis, F. (2020). Brine rejection and hydrate formation upon freezing of NaCl aqueous solutions. *Physical Chemistry Chemical Physics*, *22*(14), 7625–7632. https://doi.org/10.1039/c9cp05436g

UOV. (2019). Instructions for Use of the Inductively Coupled Plasma (ICP) Optical Emission Spectrometer (OES). http://www.uvm.edu/~gpetrucc/courses/Chem219/Resources from 201-S17/Lab %235 (ICP)/chem219_ICP_instr_quick_startup.pdf

Utting, N., Lauriol, B., Lacelle, D., & Clark, I. (2016). Using noble gas ratios to determine the origin of ground ice. *Quaternary Research (United States)*, *85*(1), 177–184. https://doi.org/10.1016/j.yqres.2015.12.003

Vaikmäe, R., Martma, T., Ivask, J., Kaup, E., Raidla, V., Rajamäe, R., Vallner, L., Mokrik, R., Samalavičius, V., Kalvāns, A., Babre, A., Marandi, A., Hints, O., & Pärn, J. (2020). *Baltic groundwater isotope-geochemistry database* (Department of Geology, Tallinn University of Technology). ent of Geology, Tallinn University of Technology. https://doi.org/10.15152/GEO.488

Vaikmäe, R., Vallner, L., Loosli, H. H., Blaser, P. C., & Juillard-Tardent, M. (2001). Palaeogroundwater of glacial origin in the Cambrian-Vendian aquifer of northern Estonia. *Geological Society, London, Special Publications*, *189*, 17–27. https://doi.org/10.1144/GSL.SP.2001.189.01.03

Vasil'chuk, Yu. K. (2007). Chemical Properties of Glacial and Ground Ice. In *Types and properties of water* (Vol. 2, Issue September).

Virbulis, J., Bethers, U., Saks, T., Sennikovs, J., & Timuhins, A. (2013). Hydrogeological model of the Baltic Artesian Basin. *Hydrogeology Journal*, *21*(4), 845–862. https://doi.org/10.1007/s10040-013-0970-7

Walvoord, M. A., & Kurylyk, B. L. (2016). Hydrologic Impacts of Thawing Permafrost-A Review. *Vadose Zone Journal*, *15*(6), vzj2016.01.0010. https://doi.org/10.2136/vzj2016.01.0010

Weiss, R. F. (1970). The solubility of nitrogen, oxygen and argon in water and seawater. *Deep Sea Research and Oceanographic Abstracts*, *17*(4), 721–735. https://doi.org/10.1016/0011-7471(70)90037-9

Weiss, R. F. (1971). Solubility of helium and neon in water and seawater. *Journal of Chemical & Engineering Data*, *16*(2), 235–241. https://doi.org/10.1021/je60049a019

Weißbach, T. (2014). Noble gases in palaeogroundwater of glacial origin in the Cambrian-Vendian aquifer system, Estonia. Thesis.

Wise, D. L., & Houghton, G. (1966). The diffusion coefficients of ten slightly soluble gases in water at 10–60°C. *Chemical Engineering Science*, *21*(11), 999–1010. https://doi.org/10.1016/0009-2509(66)85096-0

Wiszniewska, J., & Krzemińska, E. (2005). Precambrian crystalline basement of northeastern Poland – new approach. *Mineralogical Society of Poland – Special Papers*, *26*, 97–104.

Yde, J. C., Knudsen, N. T., Hasholt, B., & Mikkelsen, A. B. (2014). Meltwater chemistry and solute export from a Greenland Ice Sheet catchment, Watson River, West Greenland. *Journal of Hydrology*, *519*(PB), 2165–2179. https://doi.org/10.1016/j.jhydrol.2014.10.018

Yezhova, M., Polyakov, V., Tkachenko, A., Savitski, L., & Belkina, V. (1996). Paleowaters of North Estonia and their influence on changes of resources and quality of fresh groundwaters of large coastal water supplies. *Geology*, *19*, 37–40.

Zhang, M., & Frape, S. K. (2003). Permafrost: evolution of shield groundwater compositions during freezing. Report No: 06819-REP-01200-10098-R00.

Zhao, X., Fritzel, T. L. B., Quinodoz, H. A. M., Bethke, C. M., & Torgersen, T. (1998). Controls on the distribution and isotopic composition of helium in deep ground-water flows. *Geology*, *26*(4), 291–294. https://doi.org/10.1130/0091-7613(1998)026<0291:COTDAI>2.3.CO;2

Zuzevičius, A. (2010). The groundwater dynamics in the southern part of the Baltic artesian Basinduring the Late Pleistocene. *Baltica*, *23*(1), 1–12.

Zuzevičius, A., Mažeika, J., & Baltrūnas, V. (2007). A model of Brakish groundwater formation in the Nemunas River Valley. *Geologija*, *60*, 63–75.

SANTRAUKA

ĮVADAS

Žinios apie Baltijos artezinio baseino (BAB) požeminio vandens formavimąsi vaidina svarbų vaidmenį hidrogeologijoje. BAB požeminio vandens sudėties tyrimai apima daugybę temų: regioniniai tyrimai, klasifikacijos, paleohidrogeologija, datavimas, kilmė ir formavimosi scenarijai. Požeminio vandens izotopiniai ir cheminiai parametrai yra naudojami vertinant išteklius, taršą, gėlo, mineralizuoto ir sūraus požeminio vandens susidarymą BAB. Tačiau izotopinė ar cheminė sudėtis ar kiti parametrai ne visada yra lengvai paaiškinami esama geologine ir hidrogeologine aplinka ar kitais veiksniais. Toks vanduo traktuojamas kaip anomalija. Anomalaus požeminio vandens apibrėžimai gali būti įvairūs: 1. nukrypimas nuo aplinkinių vietovių požeminio vandens cheminės ar izotopinės sudėties charakteristikų; 2. unikalios geologinės-hidrogeologinės sąlygos litologiniai ypatumai arba fiziniai veiksniai, lemiantys požeminio vandens pokyčius; 3. ribinių sąlygų įvairovės įtaka požeminio vandens srautams.

Šio tyrimo tikslas buvo ištirti Baltijos artezinio baseino požeminio vandens izotopinės ir geocheminės sudėties fonines reikšmes, anomalijų kilmę ir jų susidarymo scenarijus.

Šio tyrimo objektas buvo seklaus, vidutinio gylio ir gilaus požeminio vandens srautai ir jų sąveika, sukelianti izotopines ir chemines anomalijas BAB.

Pagrindiniai šio tyrimo uždaviniai:

1. Naudojant izotopinius ir cheminius duomenis apibūdinti anomalines seklaus (< 300 m), vidutinio gylio (300–1000 m) ir gilaus (> 1000 m) požeminio vandens vietas ir atskleisti pagrindinius veiksnius, turinčius įtakos jo susidarymui: geologinės ir hidrogeologinės sąlygos, paleoklimato aspektai pleistoceno ir holoceno laikotarpiu.

2. Nustatyti skirtumus tarp foninės ir anomalijų požeminio vandens sudėties lokalių, vidutinio gylio ir giliųjų srautų sistemų sąveikos kontekste.

3. Panaudoti kombinuotą radioizotopų ir vandens tėkmės modeliavimą su dalelių sekimo schemomis vandens amžiui nustatyti, siekiant nustatyti požeminio vandens tekėjimo kelius ir amžių.

Mokslinis naujumas:

• Požeminio vandens anomalijų erdvinio pasiskirstymo struktūra yra grindžiama jo izotopine ir chemine sudėtimi, kilme ir migracija.

• Pasiūlyta nauja Estijos monoklinos Cm-V ir O-Cm vandeningųjų sluoksnių požeminio vandens izotopinių ir geocheminių anomalijų formavimo koncepcija. Izotopiškai frakcionuotas požeminis vanduo susidaro dėl kriogeninių procesų ir talikų sistemos tinklo įtakos.

• Pirmą kartą atliktas BAB vidutinio gylio ir gilaus požeminio vandens ^{81}Kr ir ^{4}He datavimo rezultatų palyginimas su tėkmės dalelių sekimo trukmės modeliavimu.

Ginami teiginiai:

1. Remiantis izotopinės ir cheminės sudėties tyrimais ir termodinaminiais skaičiavimais nustatyta, jog didesnė dalis šiaurinio BAB Cm-V ir O-Cm vandeningųjų sluoksnių požeminio vandens susiformavo periglacialinėje aplinkoje prieš paskutinio apledėjimo maksimumą. Nuskurdintos $\delta^{18}O$ vertės ir inertinių dujų ekscesas Estijos O-Cm-V-B hidrogeologiniame vienete atsirado dėl vandens užšalimo *in situ*.

2. Seklaus ir vidutinio gylio požeminio vandens srautų sąveika pietinėje BAB vyksta šalia tektoninių linijų, upių slėnių bei žemumų, kur anomalijos pasireiškia izotopinės ir cheminės sudėties pokyčiais lokaliose ir plotinėse iškrovų vietose. Pietinio regiono link $\delta^{18}O$ praturtinimo tendencija vyrauja vidutinio gylio požeminio vandens iškrovos tektoninių lūžių vietose.

3. Gilūs ir vidutinio gylio požeminio vandens srautai yra atskirti regioninėmis vandensparomis. Tai įrodo stacionarios filtracijos 3D MODPATH modeliuotos trajektorijos ir laikai, palyginti su radioizotopinio datavimo rezultatais. Skirtumai tarp radiokriptono bei helio amžių ir modeliuoto amžiaus yra reikšmingi. Jei skaitmeniniame modelyje nėra lūžių zonų pralaidumo charakteristikų, jos gali būti surandamos atlikus išsamesnius sluoksnių hidraulinių parametrų lauko tyrimus. Norint gauti patikslintus vandens amžiaus duomenis, masės transporto modeliavimas turėtų būti taikomas kartu su tėkmės dalelių sekimo trukmės modeliavimu.

Tyrimo rezultatų aprobavimas. Disertacijos rezultatai publikuoti keturiuose moksliniuose straipsniuose, iš kurių du „Clarivate Analytics Web of Science“ (CA WoS su IF) duomenų bazėje; keturi pranešimai tarptautinėse konferencijose.

1. BALTIJOS ARTEZINIS BASEINAS

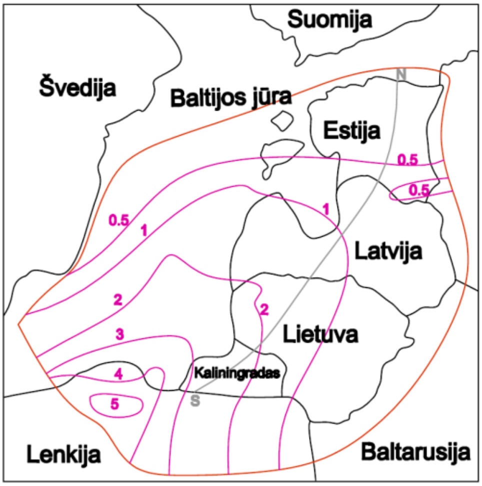

a)

b)

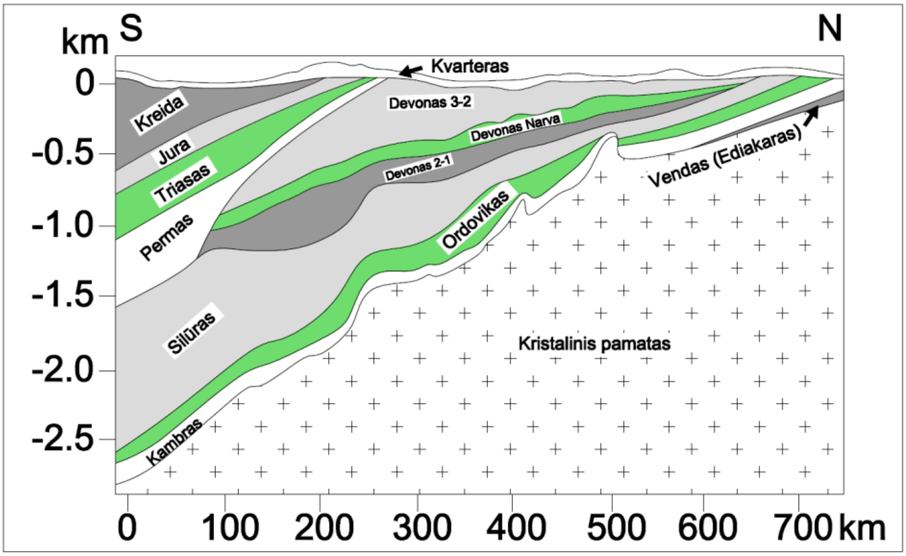

c)

1 pav. a) Baltijos artezinis baseinas. N–S pjūvio linija. Ruda linija – BAB riba, purpurinės linijos ir skaičiai – kristalinio pamato gylis, km, žemiau jūros lygio. b) Pagrindiniai BAB struktūriniai elementai O-Cm vandeningojo sluoksnio mineralizacija (Mokrik, 2003). c) BAB išilginis skerspjūvis Š–P. Modifikuota (Juodkazis, 1980a, b; Pärn ir kt., 2016; Virbulis ir kt., 2013; Mokrik ir kt., 2021).

Baltijos artezinis baseinas yra nuosėdinis baseinas šiaurės Europoje, slūgsantis ant Rytų Europos kratono kristalinių uolienų. Bendras Baltijos artezinio baseino plotas yra apie 426 tūkst. kvadratinių kilometrų (Kondratas ir kt., 1969; Juodkazis, 1980a; Juodkazis ir Mokrik, 1981; Juodkazis, 1989; Cheban, 1966; Delina ir kt., 2012). Baseinas apima visą Lietuvos, Latvijos, Estijos ir Kaliningrado (Rusija) teritoriją bei Lenkijos dalį iki Teiserio-Tornkvisto zonos (1 pav.). Nemaža dalis BAB yra po Baltijos jūra (Juodkazis ir Mokrik, 1981). Visi pagrindiniai sistemos sluoksniai randami BAB skerspjūvyje nuo ediakaro (vendo) iki kvartero (1 pav.) (Kondratas ir kt., 1969; Juodkazis, 1980a, 1989, 2003). Būtina pažymėti, kad viršutinė kristalinių uolienų pamato dalis veikia kaip papildomas vandeningasis sluoksnis, regioniniu mastu reikšmingai keičiantis supratimą apie požeminio vandens tėkmę, masės transportavimą, kilmę, sudėtį ir kitus ypatumus. Estijos monoklinoje kristalinio pamato vandenyje yra aptinkama anomalijų, analogiškų Cm-V sluoksniui. Tai įrodo, jog ši dalis yra neatsiejama nuo aukščiau slūgsančių nuosėdinių vandeningųjų sluoksnių. Regioniniu mastu BAB skirstomas į tris pagrindines zonas: seklus gėlas vanduo (aktyvios apykaitos zona, gylis < 360 m), sūrokas arba sūrus požeminis vanduo (sulėtėjusios apykaitos zona, gylis 360–1850 m) ir sūrymai (lėtos apykaitos zona, gylis > 1850 m) (Mokrik, 2003). BAB požeminio vandens klasifikacija pagrįsta keliais parametrais ir išvestiniais rodikliais: hidrocheminiu tipu, mineralizacija, vandening ojo sluoksnio gyliu ir pagrindinių jonų santykiais (Mokrik, 1996, 1997, 2003).

Aktyvios apykaitos zonos požeminio vandens mityba vyksta žemyninėje dalyje, aukštumose vykstant kritulių infiltracijai. Iškrova vyksta upių slėniuose ir žemumose, į Baltijos jūrą (Kondratas ir kt., 1969; Juodkazis, 1980a, 1989; Mokrik, 2003). Požeminio vandens $\delta^{18}O$ Lietuvoje, Latvijoje, Kaliningrado srityje svyruoja nuo –7,7 iki –13,9 ‰ (Mokrik, 2003; Rozanski ir Zuber, 2000). Estijoje požeminis vanduo yra stipriai izotopiškai nuskurdintas – jo $\delta^{18}O$ nuo –14 iki –22,5 ‰. Visiškai kitaip yra Gotlando saloje, kur tame pačiame gylyje randamas turtingas izotopų druskingas požeminis vanduo, kurio $\delta^{18}O$ reikšmės yra nuo –5,7 iki –6,1 ‰ (Mokrik, 1997).

Aktyvios apykaitos zonos požeminis vanduo daugiausia yra Ca-Mg-HCO_3 tipo su išimtimis kai dominuoja Na katijonas. Šis tipas susiformuoja dėl dabartinės meteorinio vandens mitybos. Požeminio vandens mineralizacija retai viršija 1 g/l, toks vanduo slūgso iki 360 m gylio (Mokrik, 2003; Juodkazis ir Mikalauskas, 1994). Na-HCO_3 ir (Ca-Na)-(Cl-HCO_3) tipai yra susiję su Šiaurės Estijos O-Cm ir Cm-V sluoksnių anomalijomis

(Vaikmäe ir kt., 2001; Cheban, 1966; Mokrik, 1996, 1997, 2003; Mokrik ir Vaikmäe, 1988).

Sulėtėjusios apykaitos zonoje mineralizacijos reikšmės svyruoja nuo 5 iki ~100 g/L. Dėl hidrostatinio ir litostatinio slėgio vidutinio gylio ir giliuose vandeninguosiuose sluoksniuose vanduo teka iš baseino centro į periferiją (Mokrik, 2003). Stabiliųjų izotopų $\delta^{18}O$ reikšmės yra nuo –13 iki –6 ‰. Pagal izotopinę ir cheminę sudėtį ši zona yra tarpinė tarp giluminių sūrymų ir seklaus gėlo vandens – toks vanduo dažniausiai susidarė maišantis *in situ* požeminiam vandeniui (Mokrik, 2003). Sulėtėjusios apykaitos zonoje esančio natrio chlorido tipas yra aptinkamas visose Baltijos šalyse. Remiantis stabiliųjų izotopų duomenimis, jo kilmė gali būti skirtinga. Atskiras Na-Cl požeminio vandens atvejis yra Pietų Lietuvos anomalija, kai sūrus požeminis vanduo patenka į seklius vandeninguosius gėlo vandens sluoksnius, todėl jame dominuoja natris ir chloridas (mineralizacija nuo 2 iki 50 g/L) (Juodkazis, 1989; Juodkazis ir Mikalauskas, 1994; Juodkazis ir kt., 1997; Zuzevičius, 2010; Zuzevičius ir kt., 2007).

Lėtos apykaitos zonoje esantys sūrymai slūgso BAB vandeninguosiuose sluoksniuose > 1,5 km gylyje. Dėl padidėjusio temperatūros gradiento ir slėgio šiame gylyje mineralizacija gali siekti 140–400 g/L. Šie sūrymai yra labiausiai praturtinti $\delta^{18}O$ – nuo –6 iki –3 ‰ (Mokrik, 2003; Mokrik ir kt., 2021).

Natrio-kalcio-chlorido (kraštutiniais atvejais kalcio-natrio-chlorido) tipo sūrymai susidaro dėl ilgai stovinčio požeminio vandens katijonų mainų su mineralais > 1 km gylyje. Metamorfizacijos laipsnis ($(rNa+rCl)/rHCO_3$) yra naudojamas klasifikuoti požeminį vandenį BAB iki 1800 m gylio. Giliau ima vyrauti kalcio jonai; todėl rCa/rNa santykis (ekv/L) yra tinkamesnis (Mokrik, 1996, 1997, 2003). Šis santykis atskleidžia Ca-Cl tipo požeminio vandens anomaliją O-Cm vandeningojo sluoksnio sūrymų lėtos apykaitos zonoje, kuri yra Lietuvos–Kaliningrado pakrantėje ir jūrinėje dalyje (plotas apie 5 tūkst. km^2). Šios anomalijos atsiradimą nulėmė vietinis geoterminis režimas (Mokrik, 2003). Dėl geoterminio gradiento heterogeniškumo visame BAB temperatūra O-Cm vandeningajame sluoksnyje Vakarų Lietuvoje ir Rygoje, Latvijoje, atitinkamai svyruoja nuo 98 °C iki 21 °C (Mokrik, 2003; Mokrik ir kt., 2021a). Aukštesnė temperatūra katalizuoja požeminio vandens izotopinės geocheminės sudėties pokyčius, pavyzdžiui, jonų mainus, ultrafiltraciją, izotopų frakcionavimą, dujų tirpimą ir ištirpusių medžiagų difuziją per sluoksnius.

2. METODAI

Dauguma šiame tyrime naudotų duomenų buvo paimti iš anksčiau paskelbtos medžiagos ir duomenų bazių. Šio tyrimo autorius kartu su Vilniaus universiteto Hidrogeologijos ir inžinerinės geologijos katedros (HEG) bei Lietuvos geologijos tarnybos darbuotojais 2017 m. dalyvavo lauko darbuose, kurių metu buvo imami požeminio vandens mėginiai Lietuvoje. Paimta 15 požeminio vandens mėginių, aštuoni iš seklių kvartero vandeningųjų sluoksnių ir septyni iš vidutinio gylio ir gilių vandeningųjų sluoksnių. Mėginių ėmimas ir analizė buvo atlikti visuose taškuose analogiškai, išskyrus tritį, kuris buvo išmatuotas tik kvartero vandeningojo komplekso požeminio vandens mėginiuose.

2017 metų lauko darbų mėginių paėmimas. Bendrai cheminei analizei požeminio vandens mėginiai buvo paimti į 0,5 l plastikinius butelius. Mikroelementų analizei mėginiai parūgštinti azoto rūgštimi ir paimti į plastikinį indą (50 ml). Vandens mėginiai stabiliųjų izotopų (deuterio ir deguonies-18) analizei buvo paimti į 50 ml plastikinius butelius. Tričio tūriniam aktyvumui nustatyti į plastikinius butelius buvo pilamas 1 l požeminio vandens. Helio analizei naudojant INGEM-1 prietaisą mėginiai buvo paimti į stiklinius butelius (0,33 l), o šie sandariai užkimšti guminiais kamščiais. Oro perteklius iš butelių buvo pašalintas metaline viela priveržiant kamštį. Inertinių dujų analizei Tarptautinės atominės energijos agentūros (TATENA) Izotopų hidrologijos laboratorijoje mėginiai buvo paimti į varinius vamzdelius. Per varinį vamzdelį paleidus pastovų požeminio vandens srautą, užspausti abu vamzdelio galai nesustabdant vandens srovės. Toks paėmimas užtikrina, kad požeminis vanduo nebūtų užterštas atmosferos oru.

2017 metų lauko darbų mėginių analizė. Lietuvos geologijos tarnybos laboratorija atliko pagrindinių jonų sudėties analizę spektrofotometru „Genesys 20“ ir „Jemway PFP7“. Šios analizės paklaida ± 10 %. Būtini parametrai pH; Eh (redokso potencialas), mV, ir temperatūra buvo matuojami mėginių ėmimo metu nešiojamaisiais prietaisais „Multi-Line F/Set 3“ arba VWR MU6100H. Mikroelementų analizė atlikta Hidrogeologijos ir inžinerinės geologijos katedros Hidrochemijos laboratorijoje naudojant induktyviai susietos plazmos optinės emisijos spektrometrą (ICP-OEC) „Perkin Elmer Optima 7000 DV“. Šios analizės paklaida ± 6 %. Talino technologijos universiteto Geologijos katedros laboratorijoje stabilieji izotopai deuteris ir deguonis-18 buvo nustatyti naudojant masės spektrometrą „Picaro“. Tipinė šios analizės paklaida yra $\delta^{18}O$ ± 0,1 ‰ ir δD ± 1 ‰. Tritis buvo išmatuotas Gamtos tyrimų centro laboratorijoje, naudojant „Quantulus Tri-Carb 3170 Tr/Sl“. Elektrolitiniu būdu koncentruotų mėginių paklaidos yra ± 0,2 TU, o tiesioginio matavimo – ± 2,4 TU. Inertinės dujos (He^3/He^4, He, Ne, Ar, Kr ir Xe) buvo išmatuotos TATENA Izotopų hidrologijos laboratorijoje. Inertinių dujų kiekiui požeminio vandens mėginiuose nustatyti buvo naudojama mėginių ištraukimo sistema, masės spektrometras MM5400 ir du kvadrupoliniai masės spektrometrai (QMS). Apskaičiuotos paklaidos He^3/He^4 ±5 %, He ± 5 %, Ne ± 4 %, Ar ± 1 %, Kr ± 6 % ir Xe ± 10 %.

Duomenys. Šiame tyrime buvo naudojami duomenys iš dviejų pagrindinių duomenų bazių.

Duomenų bazė **A,** sudaryta Estijos mokslininkų, bendradarbiaujant su Latvijos ir Lietuvos tyrėjais, paskelbta kaip vienas dokumentas (Vaikmäe ir kt., 2020) – šiame tyrime vadinama duomenų rinkiniu A. Į šią duomenų bazę įtraukti 2017 m. laukų darbų metu paimtų mėginių duomenys. Šioje duomenų bazėje trūksta giliųjų ir vidutinio gylio izotopinės ir cheminės sudėties duomenų iš Lietuvos.

Duomenų bazė **B**. Duomenis rinkti pradėta 1976–2000 m. Lietuvos geologijos institute, vėliau pastaruosius 40 metų tęsiama Vilniaus universiteto Hidrogeologijos ir inžinerinės geologijos katedroje. Šioje duomenų bazėje yra būtini Lietuvos giliojo ir vidutinio gylio požeminio vandens izotopiniai ir cheminiai duomenys. Į šią duomenų bazę yra įtraukta Vilniaus universiteto, Estijos geologijos tarnybos, Geologijos instituto ir Talino technikos universiteto mokslininkų paskelbta medžiaga, taip pat dalis nepublikuotų duomenų. Duomenų bazė B papildyta prisotinimo mineralais rodiklių (SI) reikšmėmis, modeliuotomis programos kodu „Phreeqc“, naudojantis „wateq4“ duomenų baze.

Dėl didelio duomenų įrašų skaičiaus A ir B duomenų bazėse buvo būtina atlikti duomenų filtravimą, siekiant surinkti tinkamą informaciją ir sukurti reprezentatyvius pavyzdžius, neprarandant jokios svarbios informacijos. Iš duomenų bazių A ir B buvo gauti iš viso penki duomenų rinkiniai. Toliau paaiškinami duomenų filtravimo principai.

1. Inertinių dujų duomenų rinkinys (sudaro 48 įrašai).

2. Izotopinės ir cheminės sudėties duomenų rinkinys buvo sudarytas iš A ir B duomenų bazių. Iš viso šiame duomenų rinkinyje yra 215 įrašų. Duomenų rinkinį sudaro Lietuvos, Estijos, Latvijos ir Kaliningrado srities sekliojo (< 300 m), tarpinio (300–1000 m) ir gilaus (> 1000 m) vandeningojo sluoksnio požeminis vanduo.

3. Kreigo diagramoms sukurti išskirtas duomenų rinkinys (174 įrašai).

4. Vidutinio gylio ir gilaus požeminio vandens duomenų rinkinys, kuriame buvo apskaičiuotas vandens amžius kriptono-81 ir helio-4 metodais ir MODPATH modeliavimu.

5. Duomenų rinkinys kriogeninių anomalijų tyrimui Estijoje buvo sudarytas iš A ir B duomenų bazių (102 įrašai).

Talikų aplinkos įtakos Estijos monoklinos požeminiame vandenyje analizei buvo naudoti papildomi duomenys. Estijos požeminio vandens ^{14}C ir ^{4}He duomenys buvo surinkti 1974–1975 m. Lietuvos geologijos instituto kampanijos metu (14 mėginių) ir Estijos geologijos tarnybos 1981–1982 m. Taline ir Pernu (15 gręžinių). Mėginiai ištirti Hidrogeologijos ir inžinerinės geologijos instituto Izotopų laboratorijoje (Maskvoje) ir Lietuvos geologijos institute (Mokrik ir Samalavičius, 2022).

Požeminio vandens amžiaus skaičiavimai. Vilniaus universiteto Hidrogeologijos ir inžinerinės geologijos katedroje buvo sukurtas regioninis 3D matematinis BAB nuosėdinio baseino požeminio vandens tėkmės modelis (BABHEGM), kuris buvo kalibruotas ir verifikuotas (2016–2019 m.). Skaitiniai modeliai sukurti naudojant „Groundwater VISTAS 6 Pro“ vartotojo sąsają ir kodą su gruntinio vandens modeliavimo programa. BAB srauto modelis buvo kalibruotas naudojant faktinius požeminio vandens lygius (MODFLOW). Modeliuojamas plotas yra apie 500 000 km^2, apimantis BAB ir jo ribas su kitais reikšmingais baseinais. Bendras langelių skaičius yra 614 823, tinklelio dydis 5 x 5 km. Hidrostratigrafinis padalijimas apima 31 atskirtą sluoksnį (vandensparas ir vandeninguosius sluoksnius) nuo kristalinio pamatinio vandeningojo sluoksnio iki kvartero vandeningųjų sluoksnių sistemos (Mokrik ir kt., 2021). Modeliuojamas požeminio vandens amžius buvo gautas naudojant MODPATH.

Apskaičiuojant helio-4 amžių (tHe), būtini parametrai yra urano ir torio kiekis žemyninėje plutoje (kristaliniame pagrinde) ir vandeningojo sluoksnio matricoje, helio koncentracija požeminiame vandenyje, vandeningojo sluoksnio poringumas ir tankis bei atidavimo faktorius $\Lambda_{He}1$. Helio gamybos greitis J' buvo apskaičiuotas pagal (Torgersen ir Stute, 2013), naudojant vidutines torio (1500 ppm) ir urano (440 ppm) vertes iš Estijos kristalinio rūsio uolienų (Raudsep, 1997; Mokrik ir kt., 2021). Uolienų tankis, vandeningųjų sluoksnių matricos poringumas ir išsiskyrimo faktorius $\Lambda_{He}1$ naudoti koreguotam helio akumuliacijos greičiui J apskaičiuoti.

Kriptono-81 datavimo rezultatai šiame tyrime nebuvo skaičiuojami, bet paimti iš publikacijų (Vaikmäe ir kt., 2020; Gerber ir kt., 2017). Radiokriptono mėginių ėmimo kampanija vyko 2013–2017 m. (Gerber ir kt., 2017).

3. REZULTŲ APTARIMAS

3.1. Bendra BAB požeminio vandens anomalijų charakteristika

Ankstesniuose tyrimuose buvo aptikta daug anomalijų, o tai padeda jas identifikuoti. Tokiais atvejais analizė gali būti tęsiama toliau – atsižvelgiant į surinktus duomenis ir žinomus parametrus paaiškinama anomalijos kilmė, formavimasis ar raida. Kitais atvejais analizės metu sudaromas naujas anomalijų formavimosi modelis. Ne visada anomalijų susiformavimo scenarijus yra neabejotinai aiškus, tokiais atvejais pateikiamos kelios versijos. Duomenų bazėse pasitaikantys netikslumai ir klaidos taip pat gali būti klaidingai apibūdinti kaip anomalija. Kilus abejonių, šiame darbe buvo paminėta, kur tokie įtarimai kyla autoriui ar aprašomi kitose publikacijose.

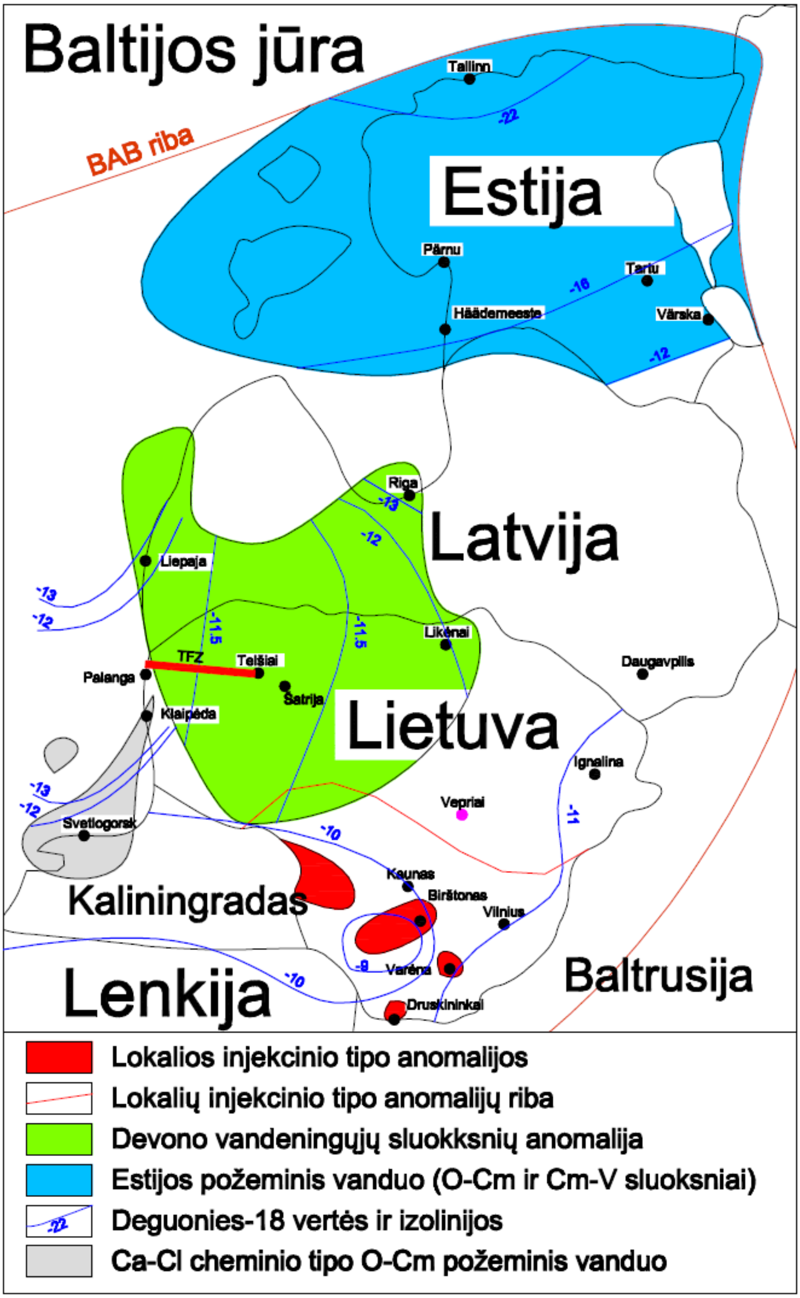

2 pav. Hidrogeologinių anomalijų BAB schema. Lokalios injekcinio tipo anomalijos ir ribos pagal (Juodkazis ir kt., 1997). Evaporitų tirpimo paveiktas požeminis vanduo, Ca-Cl tipo anomalijos, deguonies-18 duomenys Lietuvoje ir Latvijoje pagal (Mokrik, 2003)., Estijos anomalija pagal talikų tinklo schemą (Mokrik ir Samalavičius, 2022).

Hidrogeodinamika lemia požeminio vandens pasiskirstymą ir zoniškumą. Hidraulinis gradientas yra vandens srauto varomoji jėga, jis yra suskirstytas į **regioninius ir lokalius** seklaus, vidutinio gylio ir gilaus intervalus. Erdviškai šie intervalai pasiskirsto gėlo, sūroko, sūraus, vandens ir sūrymų zonose.

Struktūrinė BAB požeminio vandens savybių ir anomalijų analizė atskleidė tokias schemas:

1. Seklaus ir vidutinio gylio regioninio srauto O-Cm ir Cm-V požeminio vandens anomalija Estijos monoklinoje (2 pav.).

2. Gilaus ir vidutinio gylio regioninių srautų sąveika sukėlė helio pasiskirstymo ir migracijos anomalijas centrinėje ir pietinėje BAB dalyse, dėl to susidaro požeminio vandens amžiaus skirtumai.

3. Lokalios seklaus ir vidutinio gylio vandens srautų sąveikos sukurtos anomalijų grupės: Pietų Lietuvos injekcinio tipo anomalijos (2 pav.), plotinės anomalijos centrinio BAB devono sluoksniuose.

Regioniniai požeminio vandens srautai paprastai išskiriami pagal aukštumose esančias mitybos sritis. Seklaus ir vidutinio gylio požeminio vandens srautai išsikrauna į upių slėnius, pakrantės žemumas ir povandeninių sluoksnių atodangas (Mokrik, 1997, 2003). Priešingai, giluminis požeminio vandens srautas yra orientuotas iš centrinės baseino dalies į periferiją ir aukštumų šlaitus. Monoklinų, anteklizių ar kitų teigiamų struktūrų šlaituose susidaro seklaus ir vidutinio gylio požeminio vandens srautų hidrocheminiai ir hidrodinaminiai barjerai. Dėl to susiformuoja tarpinės mineralizacijos (sūrokas, 1–10 g/l) vanduo (Mokrik, 1997, 2003).

Prie šių barjerų gali atsirasti specifinių požeminio vandens anomalijų. Baseino kraštinėse dalyse arba ant šlaitų (tarp aukštumų ir žemumų) susidaro **sūroko mineralinio vandens tipai – anomalijos**. Panašus perėjimas yra prie šiaurinės Lenkijos–Lietuvos duburio dalies, kur susijungia vidutinio gylio ir giluminis požeminis vanduo. Šis reiškinys pasireiškia giliausiose BAB vietose, kur vyksta požeminio vandens mineralizacijos didėjimas (Mokrik, 1997, 2003). Kelių kilometrų juostose apie lūžius atsiranda sūraus vandens, kurio metamorfizacijos koeficientas yra 12–100, anomalijos (Mokrik, 2003). Šios juostos tęsiasi baseino pakraščiuose ir geostruktūrų šlaituose.

Anomalijų klasifikavimui gali būti naudojami hidrocheminiai, hidrodinaminiai ir erdvinio pasiskirstymo aspektai bei parametrai. Tačiau paskirai naudojami šie aspektai turi didelių trūkumų, todėl juos būtina derinti. Šiame darbe anomalijų klasifikacija gali būti atliekama tokia tvarka: 1. nustatyti izotopinės ir cheminės sudėties ypatumus; 2. klasifikuoti filtruotus duomenis pagal anomalijų atsiradimą plotiniuose, profiliniuose pjūviuose, pasiskirstymą susiejant su struktūriniais BAB elementais. Tokiu būdu išskirtos penkios anomalijų grupės.

Pietų Estijos plotinių anomalijų grupė. Plotinis pasiskirstymas apima pietinę ir dalį rytinės Estijos Cm-V ir O-Cm požeminius vandenis. Estijos monoklinos vandeningi sluoksniai dengia kristalinį pamatą 400–600 m gylyje. Pagrindinės lūžių zonos, turinčios įtakos srauto sąlygoms, yra Pärnu-Tapa ir Vidurio Estijos. Požeminio vandens mineralizacija yra 1–4 g/l (Värska 18 g/l), deguonies-18 vertės svyruoja nuo –19 iki –12 ‰.

Centrinės BAB srities plotinių anomalijų grupė. Devono vandeninguosiuose sluoksniuose 400–800 m gylyje yra anomalaus sūroko požeminio vandens. Prie šios anomalijos susidarymo gali būti priskirtos pagrindinės lūžių zonos: Latvijoje Liepoja–Ryga–Pskovas, Šiaurės Lietuvoje Telšių ir Baltijos lūžių zonos. Požeminio vandens cheminiam tipui įtakos turi evaporito mineralų (gipso, karbonato mineralų) tirpimas. Dėl gilaus vandens iškrovos šalia tektoninių linijų padidėja natrio ir chlorido kiekis. Deguonies-18 kiekis nuo –13 iki –11 ‰, mineralizacija 1–11 glL.

Pietų Lietuvos lokalių anomalijų grupė. Šių anomalijų yra aptinkama prie tektoninių lūžių ir didelių upių slėnių triaso, kreidos periodo vandeninguose sluoksniuose 300–400 m gylyje. Kai kuriose jų vertikali iškrova pasiekia žemės paviršių, kur susidaro mineralinis vanduo. Požeminis vanduo yra praturtintas Na ir Cl, deguonimi-18 (kinta nuo –11 iki –7 ‰), mineralizacija yra 1–15 g/l, bet gali būti didesnė, jei vieta yra arti giluminės iškrovos vietos. Šiose vietose taip pat aptinkama helio anomalijų, kurios rodo hidrogeologiškai aktyvius lūžius.

Vakarų Lietuvos ir Kaliningrado priekrantės ir jūrinės dalies anomalijų grupė. Šioje BAB dalyje požeminio vandens anomalijų pasitaiko Kaliningrado juros ir Lietuvos dalyje devono vandeninguose sluoksniuose. Šią sritį kerta keli dideli lūžiai (Telšiai, Pregolis, Nemunas), todėl sūrymų poveikis vidutinio ir gilaus gylio sąveikos lygyje yra didesnis. Vidutinio gylio požeminio vandens TDS yra iki 20–30 g/l, deguonies-18 nuo –10 iki –7 ‰. Helio kiekis, deguonis-18 ir chloridai (TDS) yra pagrindiniai parametrai, rodantys anomaliją. Kitas svarbus veiksnys, išskiriantis šią regioninę anomaliją iš kitų, yra padidėjęs geoterminis srautas.

Rytų Lietuvos anomalijų grupė. Ši anomalijų grupė yra Mozūrijos ir Baltarusijos anteklizės šlaite. Pietų Lietuvos ir Ašmenos lūžiai turi įtakos gilaus ir vidutinio gylio požeminio vandens sąveikos anomalijoms. Kambro, ordoviko ir vidurinio–žemutinio devono vandeninguosiuose sluoksniuose yra sūroko arba sūraus požeminio vandens, kurio TDS 1–10 (30) g/l. Požeminis vanduo gėlėja pietryčių kryptimi, kylant Mozūrijos–Baltarusijos anteklizės šlaitu. Deguonies-18 kiekis kinta nuo –12 iki –10 ‰; Ignalinos vietovėje vertė –7,2 ‰. Sūroko požeminio vandens plotas (1–10 g/l) yra siauras, formuojantis juostą BAB pietrytinės dalies periferijoje.

3.2. Estijos monoklinos požeminio vandens anomalija

Egzistuoja dvi pagrindinės hipotezės apie Estijos požeminio vandens izotopinės ir cheminės anomalijos susidarymą. Pirma hipotezė teigia, kad anomalija susidarė dėl ledynų tirpsmo vandens, šiuolaikinių kritulių infiltracinio ir mineralizuoto požeminio vandens maišymosi (Pärn ir kt., 2018; Raidla ir kt., 2009; Vaikmäe ir kt., 2001). Antra hipotezė tvirtina, jog požeminis vanduo buvo paveiktas daugiamečio įšalo sukeltos kriogenezės pleistoceno laikotarpiu (Mokrik, 1996, 1997, 2003; Mokrik ir Vaikmäe, 1988). Šiame tyrime buvo atlikta analizė, siekiant identifikuoti izotopinio nuskurdinimo kilmę.

Šiaurinėje BAB dalyje, remiantis dabartinėmis jūros dugno ir sausumos įdubomis, rekonstruota konceptuali talikų schema. Pleistocene buvusi talikų sistema galėjo veikti kaip mitybos kritulių ir paviršiniu vandeniu lokalios teritorijos daugiamečio įšalo apimtose zonose periglacialinėmis sąlygomis (3 pav.). Toks mechanizmas paveikė O-Cm ir Cm-V požeminio vandens izotopinę ir cheminę sudėtį ir vandens tipų įvairovę (Mokrik ir Samalavičius, 2022).

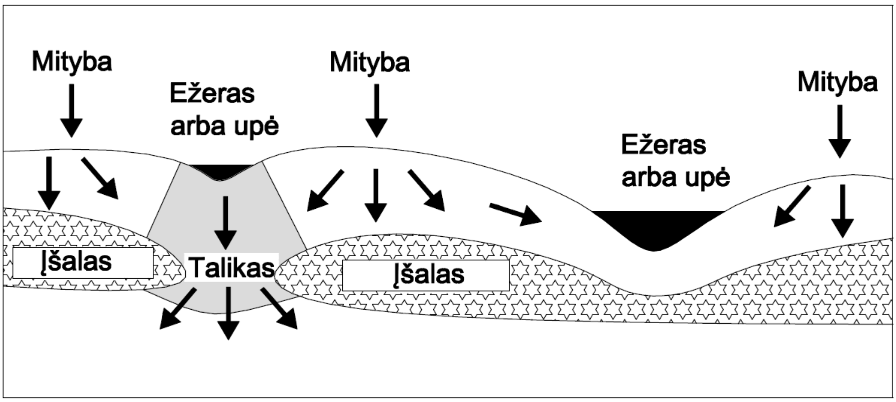

3 pav. Taliko zonos pjūvio schema, pagal (Walvoord ir Kurylyk, 2016; Kurylyk ir kt., 2014; Mokrik ir Samalavičius, 2022).

Talikų įtaka yra pagrįsta izotopiniais ir cheminiais duomenimis. Deguonies-18 anomalija netoli Talino (Kopli ir Viimsi pusiasaliai) sutampa su padidėjusiu urano izotopų $^{234}U/^{238}U$ aktyvumų nukrypimu nuo pusiausvyros (Mokrik, 1997; Yezhova ir kt., 1996). Dėl užsitęsusio daugiamečio įšalo poveikio požeminiam vandeniui Cm-V vandeningajame sluoksnyje ir kristaliniame pamate gerokai padidėjo ^{234}U kiekis (Yezhova ir kt., 1996). Uždarosiose sistemose $^{234}U/^{238}U$ santykis yra > 1, o atvirose ~1 (Fujikawa ir kt., 2000). Daugiametis įšalas fiksuoja urano izotopus (nėra mobilios fazės, skysto vandens); todėl ^{234}U negali pasišalinti. Atitirpus įšalui padidėja ^{234}U išplovimas (Tokarev ir kt., 2006). Urano-234 ir helio-4 produkcijos didėjimas gali būti susijęs su uolienų suskeldėjimu dėl slėgio sumažėjimo atsitraukus ledynui (Mejean ir kt., 2017). Helio atveju ši produkcija gali padidėti iki 30 000 kartų (Mejean ir kt., 2017). Tokia situacija galėjo padidinti urano izotopų santykį ir gerokai pailginti apskaičiuotą helio amžių Cm-V vandeningojo sluoksnio požeminiame vandenyje.

Talino teritorijoje Cm-V vandeningojo sluoksnio požeminiame vandenyje urano izotopų santykis svyruoja nuo 3,6 iki 26. Tikėtina, kad holocene Eh Cm-V šiame požeminiame vandenyje buvo –150 – –250 mV (redukcinės sąlygos). Šių sąlygų inversija į oksiduojančią aplinką daugiausia atsiranda dėl kritulių ir paviršinio vandens mitybos šalia palaidotų slėnių ir talikų (Mokrik ir Samalavičius, 2022). Dėl urano valentingumo įtakos jo tirpumui absoliutūs urano kiekiai yra kur kas didesni, atitinkamai veikiantys ir izotopinio santykio nukrypimą nuo 1. Estijos monoklinos požeminiame vandenyje aptinkama ^{234}U anomalija sutampa su pagrindiniais talikais Šiaurės Estijos pakrantės lygumoje, Vakarų Estijos žemumoje, Alutagezės-Peipaus ežero žemumoje. Įšalusius O, Cm, V nuosėdinius sluoksnius ir kristalinio pamato viršutinę dalį galima traktuoti kaip tuo laikotarpiu buvusį hidrauliškai susijusį vieną hidrostratigrafinį vienetą.

Šiuolaikinio infiltracinės kilmės požeminio vandens iškrova slėniuose sumažina urano izotopų santykį (artėja prie pusiausvirinio 1). Panašų efektą turi jūrinio vandens intruzija.

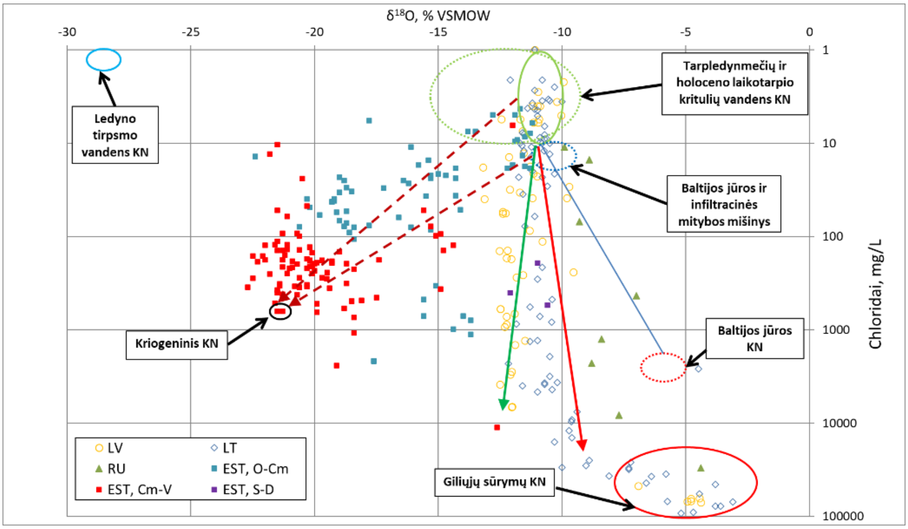

4 pav. Chloridų ir deguonies-18 diagrama. BAB požeminis vanduo: LT – Lietuvoje, LV – Latvijoje, EST – Estijoje (S-D, Cm-V ir O-Cm vandeninguosiuose sluoksniuose), RU –Kaliningrado sritis. Kraštiniai nariai – KN. Mėlyna linija – jūros vandens skiedimo trendas. Rudos brūkšninės rodyklės – kriogeninis trendas, raudonos ir žalios rodyklės – seklaus ir vidutinio gylio požeminio vandens sąveika atitinkamai Lietuvoje ir Latvijoje.

Vandens užšalimo (įšalo formavimosi) metu pagrindiniai procesai, veikiantys izotopinės ir cheminės sudėties kitimą, yra druskos (sūrymo) atmetimas (Starinsky ir Katz, 2003; Tsironi ir kt., 2020) ir izotopinis Reilio (Rayleigh) distiliavimas (Gragnani ir kt., 1998; Lehmann ir Siegenthaler, 1991; Souchez ir kt., 1987). Dėl didėjančio pagrindinių jonų kiekio požeminiame vandenyje atsiranda mineralų persotinimas, dėl to gali įvykti jų iškritimas (Jessen ir kt., 2014; Kononova, 1979; Mcewen ir Marsily, 1991). Vykstant šiems procesams likutinis vanduo yra praturtinamas cheminiais elementais ir vyksta deguonies-18 ir deuterio izotopų frakcionavimas link nuskurdinimo (labiau neigiamų reikšmių). Stipriai izotopiškai nuskurdinto ir padidėjusios mineralizacijos vandens genezė negali būti paaiškinta prieš tai atliktų tyrimų metu išvestais kraštiniais nariais. Papildomas – kriogeninis kraštinis narys paaiškina šios anomalijos kilmę, remiantis Reilio distiliavimo ir druskų atmetimo procesais užšalimo metu (4 pav.).

Na/Cl ir Br/Cl santykių diagrama atskleidė užšalimo įtaką Estijos požeminio vandens cheminei sudėčiai (5 pav.). Diagrama papildyta požeminio vandens duomenimis iš Äspö ir Palmottu vietovių Skandinavijoje. Yra įrodyta, kad šis vanduo buvo suformuotas kriogenezės (Zhang ir Frape, 2003). Palyginimui pateikti du trendai, jūros vandens sudėties kitimas garavimo ir užšalimo procesų metu (5 pav.). Estijos anomalaus požeminio vandens pradinė (ikikriogeninė) sudėtis nebūtinai buvo artima jūros vandeniui, todėl trendai gali skirtis. Sūrymo atmetimas turi daugialypį poveikį požeminio vandens cheminei sudėčiai: didėja ištirpusių medžiagų kiekis (selektyviai skirtingiems jonams), persotinimas ištirpusiais jonais gali sukelti mineralų iškritimą. Šie procesai turi įtakos Na/Cl ir Br/Cl santykiams, pasireiškiantiems specifiniu požeminio vandens pasiskirstymu (tai matyti diagramoje (5 pav.)).

Tirtų Cm-V ir O-Cm vandeningųjų sluoksnių požeminio vandens raidos tendencijos yra visiškai skirtingos, o tai rodo skirtingus formavimosi scenarijus ir aplinkas bei pirminio vandens sudėtį. O-Cm požeminio vandens pirminė kompozicija buvo su dominuojančiu Ca katijonu, kuris iškrito tirpale, jį persotinus. Todėl vanduo tapo gėlas, Na-HCO_3-Cl tipo ir padidėjo jo pH (Mokrik ir Samalavičius, 2022). Kriogeninę jo kilmę galima netiesiogiai paremti Äspö ir Palmottu analogais. Pradinis vanduo Cm-V sluoksnyje buvo mišinys jūrinio, kritulių infiltracinio ir buvusio *in situ* sluoksnyje, kuriame dominavo Na katijonas. Tokio vandens užšalimo trendas yra artimas jūrinio vandens (Mokrik ir Samalavičius, 2022).

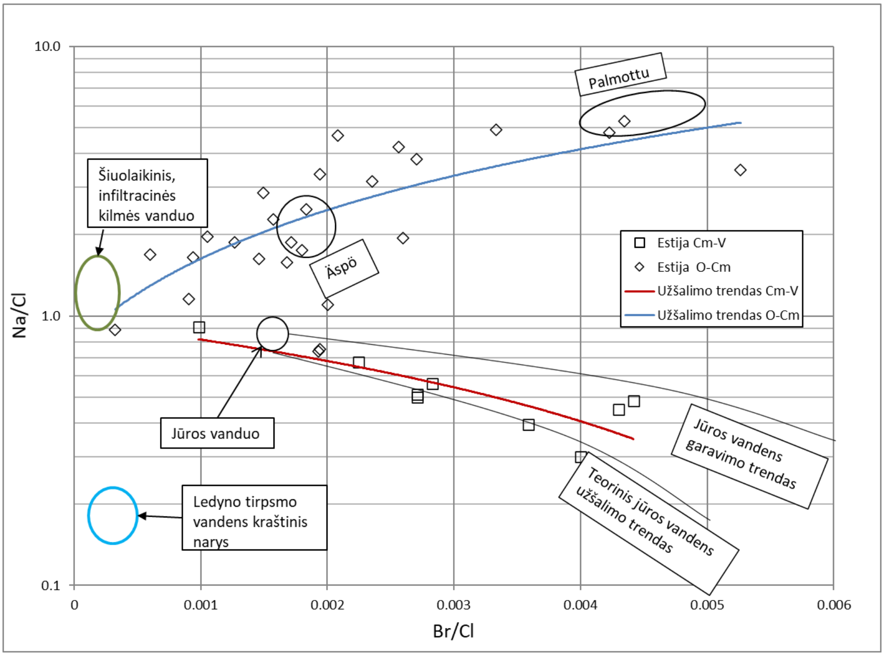

5 pav. BAB požeminio vandens natrio, chlorido ir bromido santykių diagrama (Mokrik ir Samalavičius, 2022) bei teorinis jūros vandens užšalimo (Herut ir kt., 1990) ir jūros vandens garavimo (McCaffrey ir kt., 1987) trendai. Äspö ir Palmottu požeminio vandens duomenys pateikiami kaip nuoroda į kriogeninius pokyčius Fenoskandijos skyde (Zhang ir Frape, 2003).

Apskaičiuoti Estijos anomalijos vandens prisotinimo mineralais rodikliai (SI) leidžia įvertinti vandens kilmę ir formavimosi ypatumus iš termodinaminės sistemos mineralas–vanduo perspektyvos. Apskaičiuotos kalcito SI buvo išlygintos taikant slankiųjų vidurkių metodą pagal $\delta^{18}O$ verčių eiliškumą. Slankieji vidurkiai apskaičiuoti iš visos duomenų sekos naudojant du intervalų kriterijus, siekiant nustatyti apibendrintą ir tikslesnę tendencijas. Gauti rezultatai atskleidė, jog kalcito SI padidėjimas koreliuoja su $\delta^{18}O$ išeikvojimu nuo –22 iki –19 ‰. Didėjant prisotinimui kalcitumaksimumas pasiekiamas, kai $\delta^{18}O$ vertės yra labiausiai nuskurdintos.

Lyginant požeminio vandens mineralizaciją ir prisotinimą halitu BAB kontekste, Estijos anomalijos vanduo ryškiai išsiskiria. Esant vienodoms mineralizacijos vertėms Estijos anomalijos vanduo yra labiau prisotintas (1 vienetas SI) halito nei Lietuvos ir Latvijos požeminis vanduo. Tai paaiškinama kriogenezės sukeltu sūrymo atmetimu dėl kurio išauga Na^{+} ir Cl^{-} koncentracijos požeminiame vandenyje. Halito tirpumas yra kur kas didesnis nei karbonatinių mineralų ar gipso, atitinkamai natris ir chloridai, skirtingai nei kalcis ar magnis, neiškrinta tirpale. Dėl to anomalus Estijos vanduo gali turėti didesnes prisotinimo halitu vertes. Prisotinimas mineralais yra nulemtas sūrymo atmetimo proceso, tiek kalcito, tiek halito atvejais.

Inertinių dujų Ar, Kr, Xe kiekiai ir jų santykiai gali būti naudojami kriogeninio vandens kilmei identifikuoti atskiriant ledyno tirpsmo ir *in situ* užšalimą (Utting ir kt., 2016). Inertinių dujų ekscesas buvo pastebėtas ankstesniuose tyrimuose ir aiškinamas atmosferos oro, pagauto ledyno formavimosi metu, sukeltu papildomu ištirpimu. Toks tirpsmo vanduo maitino vandeninguosius sluoksnius, kur yra anomalija (Weißbach, 2014). Tačiau Kanados tyrėjai nustatė, kad toks vanduo turėtų turėti inertinių dujų reikšmes ir ekscesą, artimą atmosferinei sudėčiai (Utting ir kt., 2016). Priešingai, užšalusio požeminio vandens inertinių dujų kiekis turi būti artimesnis vandeniui pusiausvyroje su atmosferos oru, esant standartinėms termodinaminėms sąlygoms (Utting ir kt., 2016). Siekiant nustatyti Estijos požeminio vandens anomalijos kilmę, iš turimų inertinių dujų duomenų rinkinio apskaičiuoti santykiai δ(Ar/Xe) ir δ(Kr/Xe). Remiantis gautais rezultatais Estijos požeminis vanduo ($\delta^{18}O$ < –15 ‰) susidarė užšalus požeminiam vandeniui; dauguma mėginių yra arčiau įšalo kraštinio nario (mėlynos rodyklės) (6 pav.) (Samalavičius ir Mokrik, 2021). Argono, kriptono ir ksenono kiekio ir eksceso nepakanka, kad jie būtų susiformavę iš ledyno, firno ar sniego tirpsmo. Tačiau inertinių dujų ekscesas egzistuoja Estijos anomalijoje ir gali būti paaiškinamas dujų atmetimu užšalimo metu. Keliose vietose (Nõva, Harju-Risti) galima ledyno tirpsmo vandens mityba, bet tai yra išimtys.

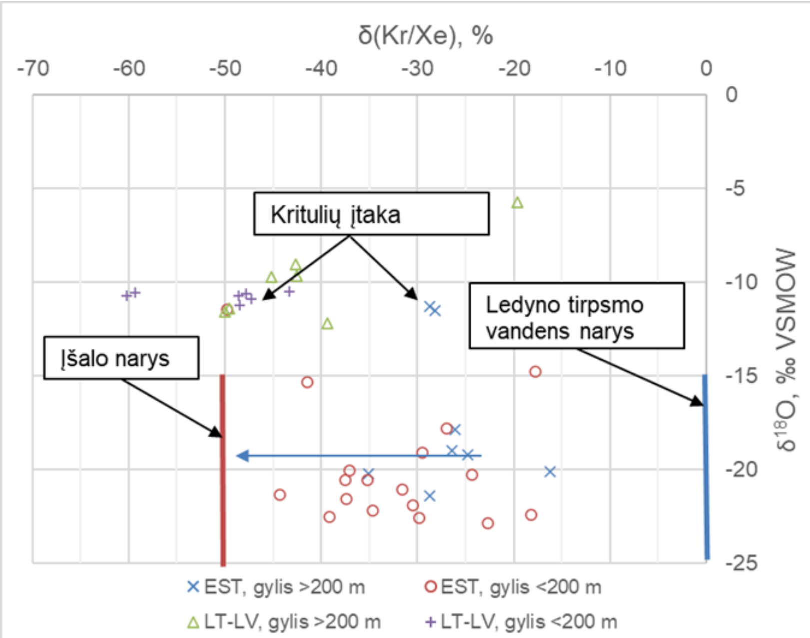

6 pav. Delta kriptono / ksenono ir deguonies-18 diagrama. Duomenys skirstomi į Lietuvos–Latvijos ir Estijos regionus didesniame ir mažesniame nei 200 m gylyje. Mėlyna linija žymi ledyno tirpsmo vandens kraštinį narį, o raudona – daugiamečio įšalo kraštinį narį.

3.3. Gilaus ir vidutinio gylio regioninių srautų sistemų sąveika

Požeminio vandens datavimo rezultatai giliame (> 1000 m) požeminiame vandenyje atskleidė reikšmingą skirtumą tarp radioizotopinio datavimo metodų ir modeliavimo (7 pav.). Kriptono-81 metodu gautas požeminio vandens amžius yra > 2 kartus senesnis nei gautas remiantis helio ir modeliavimo rezultatais. Šiose vietose (Klaipėdoje, Rygoje) vandeningieji sluoksniai yra apriboti regioninio masto regionine vandenspara arba vandensparomis. Mažas helio kiekis amžiaus skaičiavimuose lemia mažesnes vertes (jaunesnį amžių). Taip gali atsitikti dėl helio akumuliacijos po vandensparomis ir heterogeniško pasiskirstymo vandeninguose sluoksniuose (Mokrik ir kt., 2021, 2022). MODPATH modeliavimo metu gauti vandens amžiaus rezultatai yra mažesni nei kriptono-81, bet didesni nei helio-4. Skaitmeninio modelio vandeningieji sluoksniai yra tolydūs, lūžiai ir panašios geologinės struktūros, kurios ribotų lateralų vandens srautą, nėra įskaitmeninamos. Dėl to vandens amžiaus vertės yra mažesnės nei kriptono-81 (Mokrik ir kt., 2021, 2022).

Vidutinio gylio požeminiame vandenyje helio-4 ir MODPATH laikai yra skirtingi (7 pav.). Lietuvos vidutinio gylio sluoksnių izoliuotumas vandensparomis lemia padidėjusį helio kaupimąsi požeminiame vandenyje. Rytinėje Saldaus–Rygos–Pskovo lūžio zonos dalyje (Latvija) ir pietryčių Estijos aukštumose situacija yra priešinga – iš vidutinio gylio vandeningųjų sluoksnių (Häädemeeste ir Värska) helis pasišalina greičiau.

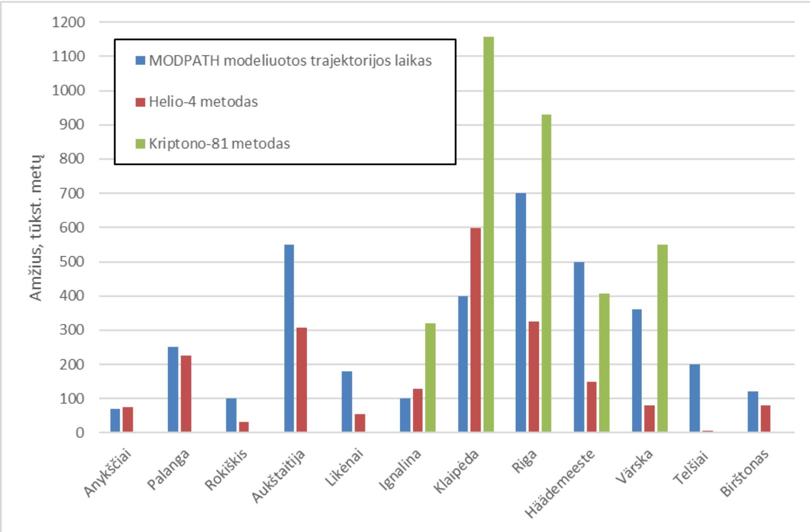

7 pav. Vidutinio gylio ir gilaus BAB požeminio vandens amžius pagal helio-4, kriptono-81 ir MODPATH simuliacjos metodus.

Helio migracija per vandens lūžius nulemia specifinį vertikalų pasiskirstymą vandeninguosiuose sluoksniuose lokaliai arba regione. Vienas iš būdų įvertinti tokį pasiskirstymą profilyje arba pjūvyje yra agreguotas helio-4 amžius – bendras viso vandeningųjų sluoksnių helio kiekis vienoje teritorijoje (Mokrik ir kt., 2021, 2022). Agreguoto helio kiekis (visų vandeningųjų sluoksnių verčių suma) turėtų būti lygi jo produkcijai kristaliniame pamate ir pačiuose sluoksniuose. Agreguoto helio kiekį perskaičiavus į amžių gaunama vertė, lygi visų sluoksnių amžių sumai. Toks metodas buvo taikytas dviejose lokacijose – Klaipėdoje ir Värska.

Agreguotas helio amžius Klaipėdos taške yra 1484 tūkst. m. Agreguota amžiaus vertė gali patikslinti giliausio vandeningojo sluoksnio vandens amžių šiuo atveju, O-Cm. Įprastu helio-4 metodu nustatytas amžius yra 662 tūkst. m. Aukščiau esančiame D_{2-1} vandeningajame sluoksnyje kriptonu-81 datuotas vanduo yra 1,2 mln. m. Agreguotas helio amžius išsprendžia gylio inversiją šioje vietoje (Mokrik ir kt., 2022). Värska atvejis taip pat atskleidžia amžiaus inversiją su gyliu (Mokrik ir kt., 2022). Giliau slūgsančiame V_2gd vandenyje helio yra 40 kartų mažiau nei dengiančiame V_2vr. Agreguoto helio amžius Värska taške yra 204 tūkst. įprasto – 2 tūkst.

m. V_2vr sluoksnio vandens įprasto helio-4 datvimo rezultatas – 86 tūkst. m. Agreguoto helio metodas ir čia gali išspręsti inversiją. Būtina pažmėti, kad agreguotas helio amžius turi trūkumų: nėra atsižvelgiama į lateralią vandens ir helio migraciją. Taigi metodas turi būti taikomas atsižvelgiant į vandensparų pralaidumą, lūžių aktualumą. Siekiant įvertinti paklaidas, helio produkcija turėtų būti lygi akumuliuoto helio kiekiui visuose sluoksniuose (Mokrik ir kt., 2022).

Helio kiekis vidutinio gylio ir giliame požeminiame vandenyje svyruoja nuo $1E^{-5}$ iki $1E^{-4}$ ccSTP/g. Helio koncentracija priklauso nuo gylio, giliau helio vertės yra didesnės. Analogiškai helio kiekis koreliuoja su chlorido kiekiu arba mineralizacija. Daugiausia helio aptinkama kambro vandeninguosiuose sluoksniuose (Likėnai, Klaipėda ir Ryga) > 1 km gylyje. Šios vietos sutampa su pagrindiniais Rapakivi masyvais, kuriuose gaminamas didžiausias helio kiekis (Juodkazis ir Tibar, 1989). Birštono taške buvo aptikta nedidelė požeminio vandens amžiaus inversija. Pagal vandens amžiaus priklausomybės nuo gylio lygtis teorinis požeminio vandens amžius turėtų būti modernus. Tai parodo, kad lygtys ir priklausomybės turi trūkumų – gylio, amžiaus arba helio kiekio anomalijos nukrypsta nuo bendros tendencijos (8 pav., geltonas apskritimas ir rodyklė).

Analizuojant ir interpretuojant požeminio vandens amžių, būtina atsižvelgti į chemines bei izotopines anomalijas ir regioninius požeminio vandens sudėties skirtumus. Pagrindinių jonų kiekis giliame požeminiame vandenyje didėja ilgėjant vidutinei buvimo požemyje trukmei dėl daugelio veiksnių: pradinės vandens sudėties, vandens ir uolienų sąveikos, garavimo, gravitacinio grimzdimo, ultrafiltracijos ir kt. Gilaus ir vidutinio gylio požeminio vandens srautai, atskirti regioninėmis vandensparomis, apriboja vandeninguosius sluoksnius; todėl svarbiausia helio migracija turėtų būti siejama su hidrauliškai aktyviais lūžiais ir jų zonomis. Vertikalios dislokacijos gali sumažinti lateralinį tėkmės greitį, dėl to gaunami dideli datavimo rezultatų skirtumai. Helio kiekio nukrypimai nuo bendros tendencijos gali būti laikomi anomalijomis, kurios nebūtinai bus aptinkamos pagal kitus parametrus.

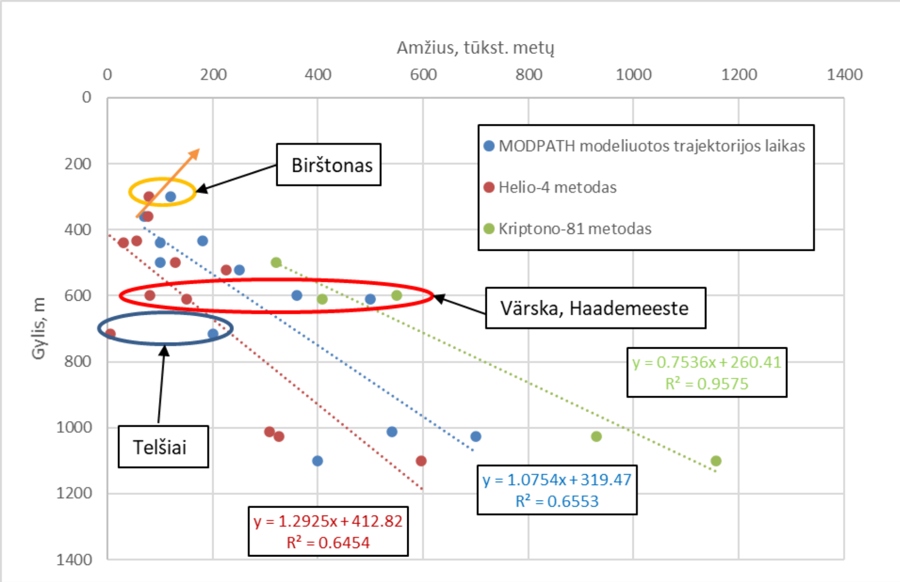

8 pav. Vidutinio gylio ir gilaus požeminio vandens amžiaus ir gylio diagrama (Mokrik ir kt., 2021). Nubraižytos tiesinės trendų linijos helio, radiokriptono ir MODPATH datavimo rezultatams. Geltonas apskritimas ir rodyklė žymi Pietų Lietuvos anomaliją (Birštono vietą). Raudonas apskritimas žymi Pietų Estijos anomalijas (Värska ir Häädemeeste vietovės). Mėlynas apskritimas žymi Telšių anomaliją.

3.4. Sekliųjų ir tarpinio gylio srautų sąveika

Sekliojo ir vidutinio gylio požeminio vandens sąveika vyksta visoje BAB per vandensparas arba tektoninius lūžius. **Pietų Lietuvos požeminio vandens lokalios injekcinio tipo anomalijos** pasireiškia vertikalia iškrova aukštyn, kur sekliuose vandeninguosiuose sluoksniuose formuojasi mineralinis vanduo. Susidaro kupolo formos hidrogeologiniai vienetai, kuriems būdinga kaiti izotopinė ir cheminė sudėtis ir helio anomalijos vienete (Juodkazis ir kt., 1997; Juodkazis, 2003; Mokrik, 2003; Mažeika, 1999).

Dėl hidrauliškai aktyvių tektoninių lūžių helis gali migruoti, taip pat kaip ir vanduo su jame ištirpusiomis medžiagomis. Chlorido ir helio kiekis kiekybiškai koreliuoja. Toks stebėjimas patvirtina gilesnio požeminio vandens sūrymo išleidimo ir maišymosi su sekliu gėlu vandeniu teoriją (Zuzevičius ir kt., 2007; Gregorauskas ir kt., 2017; Mokrik, 2003; Juodkazis ir kt., 1997; Mažeika, 1999). Galima išvesti tris pagrindines požeminio vandens chemines facijas: natrio-kalcio-chlorido (kai kuriais atvejais dominuojantis Ca katijonas), kalcio-magnio-bikarbonato gėlo vandens galutinio nario natrio-bikarbonato. Dviejų skirtingų vandenų maišymasis suformuoja tarpinius tipus tarp sūraus Na-Cl (M < 50 g/l) ir gėlo vandens Ca-Mg-HCO_3 (M < 1 glL). Pagal helio-4 metodą ir MODPATH simuliaciją nustatytas sūraus vandens amžius Birštone yra 79 ir 120 tūkst. m. Tačiau dėl aktyvių tektonių lūžių buvimo dalis helio gali pasišalinti ir iškraipyti datavimo rezultatus. Tokia problema galėtų būti metodiškai sprendžiama tiriant vandenį iš to paties sluoksnio toliau nuo identifikuotų lūžių. Taip pat kriptono-81 datavimas duotų vertingos informacijos apie tokių anomalijų vandens amžių. Tokių anomalijų tyrimus gali stipriai paveikti vandens išgavimas, nes dėl natūralių vandens lygių sumažėjimo išauga seklaus ir gėlo vandens mineralizacija (Gregorauskas ir kt., 2017).

Aiški chlorido ir helio kiekio koreliacija yra Lietuvos požeminiame vandenyje sąveikaujant sekliam ir vidutinio gylio srautams, įskaitant Pietų Lietuvos anomalijas (Gregorauskas ir kt., 2017; Zuzevičius ir kt., 2007; Mokrik, 2003; Mažeika, 1999; Juodkazis ir kt., 1997).

Anomalus helio trūkumas aptinkamas Druskininkų ir Birštono aikštelėse (9 pav., mėlynas ratas). Šios anomalijos greičiausiai atsiranda dėl kelių priežasčių. Požeminiame vandenyje, esančiame netoli lūžio, helio kiekis gali reikšmingai sumažėti, palyginti su foninėmis reikšmėmis, dėl vertikalios migracijos į viršų. Tačiau chloridas, kitaip nei helis, nereaguoja į geologinės aplinkos pokyčius ir negali pasišalinti iš tirpalo.

$\delta^{18}O$ sodrėjimo tendencija į iškrovos zonas yra priešinga Latvijos ir Estijos anomalijoms dėl izotopiškai sunkesnio požeminio vandens injekcijos į seklius vandeninguosius sluoksnius.

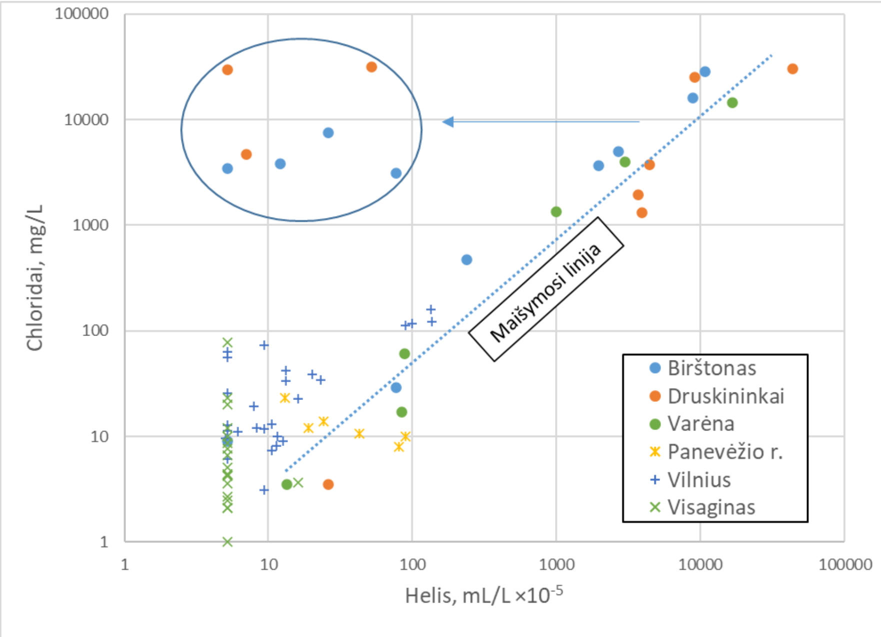

9 pav. Seklaus ir vidutinio gylio požeminio vandens Lietuvoje chlorido ir helio diagrama (Juodkazis ir kt., 1997; Mažeika, 1999; Mokrik, 2003; Zuzevičius ir kt., 2007; Gregorauskas ir kt., 2017).

Sekliame Latvijos ir Šiaurės Lietuvos požeminiame vandenyje devono sluoksniuose yra aptinkama **plotinė izotopinės ir hidrocheminės sudėties anomalija**. Ši anomalija pasireiškia chlorido kiekio padidėjimu ir $\delta^{18}O$ sumažėjimu. Nuskurdinimas $\delta^{18}O$ yra nuo –13,2 iki –11,5 ‰, Ca-Mg-SO_4 hidrocheminis tipas susijęs su karbonatinių ir sulfatinių mineralinių uolienų tirpimu devono vandeningųsiuose sluoksniuose (Mokrik, 2003). Kuržemės–Žemaitijos aukštumoje ir Vidurio Lietuvos žemumoje susidaroa anomalija, kur aptinkamos didesnės mineralizacijos reikšmės, bet $\delta^{18}O$ vertės nėra nuskurdintos (–11 iki –10 ‰). Ši anomalija ribojasi su pereinamąja zona nuo seklaus iki vidutinio gylio tėkmės aplinkos. Šių srautų sąveikai didelę įtaką daro Narvos vandenspara ir tektoniai lūžiai.

Izotopinis šios anomalijos aspektas yra galbūt susijęs su padidėjusia seklių vandens sluoksnių mityba žiemos sezono krituliais. Išskirtinė anomalija yra Telšių taške, kur 715 m gylyje aptinkamas 1,3 g/l mineralizacijos, izotopiškai nuskurdintas ($\delta^{18}O$ nuo –13,2 iki –11,6 ‰) Ca-Mg-SO_4 tipo vanduo. Ši anomalija taip pat pasireiškia mažu helio kiekiu vandenyje. Tikėtiniausias tokios anomalijos paaiškinimas yra gėlo modernaus vandens prietaka iš aukščiau slūgsančių sluoksnių. Tačiau ar ši prietaka yra natūrali, ar vyksta dėl gręžinio konstrukcijos ypatumų, nėra aišku.

IŠVADOS

Požeminio vandens anomalijas BAB yra sudėtinga klasifikuoti dėl izotopinės ir cheminės sudėties įvairovės, jų erdvinio pasiskirstymo. Moksliniu požiūriu dažnai pasitaiko, kad galimas daugiau nei vienas formavimosi scenarijus, todėl šiuo metu nėra aiškios, tvirtos išvados. Nepaisant to, kai kurie kritiniai pastebėjimai, tezės ir pasiūlymai gali būti pateikti ir įrodyti remiantis šiuo metu turimais duomenimis. Analizė patvirtino daugybę anksčiau nurodytų anomalijų formavimosi dėsningumų, taip pat jų kilmę. Kitos požeminio vandens anomalijos yra peržiūrėtos ir atnaujinamos naudojant originalų konceptualų modelį, kuriame pateikiami visiškai skirtingi paaiškinimai, hipotezės ir įrodymai. Konceptualizuotos BAB požeminio vandens anomalijų erdvinio pasiskirstymo vietos buvo pagrįstos tėkmės formavimosi modelių ir kilmės analize. Buvo įvertinti pagrindiniai veiksniai, turėję įtakos anomalijų susidarymui, pavyzdžiui, geologinė ir hidrogeologinė padėtis bei paleoklimato ypatumai holoceno ir pleistoceno laikotarpiu. Buvo atliktas lokalių, linijinių ir plotinių anomalijų sekliame, vidutinio gylio ir giliame požeminiame vandenyje foninės požeminio vandens sudėties atskyrimas.

Naujas konceptualus Estijos monoklinos Cm-V ir O-Cm vandeningųjų sluoksnių sistemų požeminio vandens modelis rodo, kad daugiamečio įšalo sąlygos ir talikų tinklas nulėmė šios anomalijos susidarymą. Įšalo formavimosi metu veikė sūrymo atmetimas (kriogeninis cheminis koncentravimas) ir Reilio (Rayleigh) distiliacija (deguonies-18 nuskurdinimas).

Estijos požeminio vandens prisotinimas kalcitu sutampa su $\delta^{18}O$ mažėjimo tendencija ir patvirtina kriogeninį koncentravimą.

Pagal Na/Cl ir Br/Cl santykius ir pleistoceno laiko vidutinius metinius temperatūros svyravimus, pradinė, ikikriogeninė požeminio vandens sudėtis turėtų būti artima paleokritulių, pirminio sluoksnio ir jūros vandens mišiniui. Urano izotopų santykis ($^{234}U/^{238}U$) ir helio kiekiai rodo, kad požeminis vanduo buvo užšalęs. Tačiau vanduo galėjo įsifiltruoti į sluoksnius taliko aplinkoje.

Argono, kriptono ir ksenono dujų kiekio santykiai Estijos sekliame anomaliniame požeminiame vandenyje rodo, kad požeminis vanduo susiformavo dėl užšalimo *in situ*, o ne dėl ledyno tirpsmo vandens prietakos. Inertinių dujų ekscesas šiuo atveju gali būti paaiškintas dujų atmetimu užšalimo metu.

BAB požeminiame vandenyje gerai koreliuoja chlorido ir helio vertės. Aukštumose esančiose mitybos zonose seklaus požeminio vandens helio kiekis yra praskiedžiamas krituliais. Helis intensyviai migruoja vidutinio gylio ir seklaus požeminio vandens riboje, todėl jo kiekis mažėja. Tai matyti vietose, esančiose šalia hidrogeologiškai aktyvių tektoninių lūžių zonų.

Gilaus ir vidutinio gylio požeminio vandens srautai yra atskirti regioninėmis vandensparomis. Tai įrodo stacionarios filtracijos 3D požeminio vandens tėkmės modelis ir radioizotopinio datavimo rezultatai. Šių srautų sąveikos zonoje helio migracija ir pasiskirstymas nebūtinai gali sutapti su požeminio vandens tėkme. Svarbiausi veiksniai, lemiantys helio kiekį požeminiame vandenyje, yra regioninės vandensparos ir hidrogeologiniai langai (tektoniniai lūžiai).

Regioninės požeminio vandens izotopinės ir cheminės sudėties ypatybės, formavimosi aplinka ir procesai yra reikšmingi helio amžiaus pagrįstumui įvertinti. Kelių datavimo metodų kombinavimas, apimantis MODPATH modeliavimą ir kriptoną-81, suteikia reikiamų duomenų apie helio pasiskirstymą.

MODPATH simuliacija parodė, kad skaitmeniniame modelyje trūksta struktūrinių BAB elementų, o tai smarkiai iškraipo datavimo rezultatus, palyginti su kriptono-81 rezultatais. Ši problema turi būti išspręsta koreguojant hidraulinius parametrus arba įtraukiant lūžių geometriją į modelį. Požeminio vandens masės transportavimo modeliavimas taip pat gali padėti iš naujo įvertinti požeminio vandens amžių.

ACKNOWLEDGEMENTS

I would like to thank my academic supervisor Prof. Habil. Dr. Robert Mokrik for help and insights while working on this project. I'd also like to express my gratitude to Dr. Žana Skuratovič and assoc. Prof. Dr. Marius Gregorauskas for reviewing the thesis and providing valuable feedback. I'm also thankful to Dissertation Defence Panel members for taking time to read this work and an opportunity to defend it, in alphabetical order on the last name: Prof. Dr. Albertas Bitinas, Assoc. Prof. Dr. Kęstutis Jokšas (chairman), Prof. Dr. Egidijus Rimkus, Dr. Tomas Saks, Dr. Žana Skuratovič. My wife's Agnė Pažusytė-Samalavičienė support and patience with my impatience made it possible to go through numerous times. For that, I am grateful and indebted.

LIST OF PUBLICATIONS

Published in journals that have impact factor in the Clarivate Analytics Web of Science databases.

- Mokrik, R. and Samalavičius, V.: *Interpretation of the anomalous groundwater chemistry and 234U/238U activity ratio disequilibrium in the northern part of the Baltic region* (accepted for publishing), 62(1), Lithuanian Journal of Physics, https://doi.org/10.3952/physics.v62i1.4645, 2022.
- Mokrik, R., Samalavičius, V., Bujanauskas, M. and Gregorauskas, M.: *Environmental isotopes and noble gas ages of the deep groundwater with coupled flow modelling in the Baltic artesian basin*, Lithuanian Journal of Physics, 61(1), 53–65, https://doi.org/10.3952/physics.v61i1.4407, 2021.
- Raidla, V., Pärn, J., Aeschbach, W., Czuppon, G., Ivask, J., Kiisk, M., Mokrik, R., Samalavičius, V., Suursoo, S., Tarros, S. and Weissbach, T.: *Intrusion of Saline Water into a Coastal Aquifer Containing Palaeogroundwater in the Viimsi Peninsula in Estonia*, Geosciences, 47(9), https://doi.org/10.3390/geosciences9010047, 2019.

  Other.
- Vaikmäe R., Martma T., Ivask J., Kaup E., Raidla V., Rajamäe R., Vallner L., Mokrik R., Samalavičius V., Kalvāns A., A. Babre, A. Marandi, O. Hints, J. Pärn, *Baltic groundwater isotope-geochemistry database*, https://doi.org/10.15152/GEO.488, 2020
- Gregorauskas, M., Kaušinis, K., Bujanauskas, M., Samalavičius, V. and Mokrik, R.: *Cenomanio-apatinės kreidos sluoksnio požeminio vandens išteklių ir hidrocheminių anomalijų modelinis įvertinimas*, Geologija. Geografija, 3(2), https://doi.org/10.6001/geol-geogr.v3i2.3538, 2017.
- Mokrik, R., Samalavičius, V., Gregorauskas, M., Maseliene-Jakimaviciute, V., Arustiene, V.: *"Integrated studies of crustal permeability based on environmental isotopes, noble gas data, and shallow-deep groundwater flow and mass transport modeling in the surrounding area of Ignalina Nuclear Power Plant (NPP)"*// Chapter in "Use of Isotope Hydrology to Characterize Groundwater Systems in the Vicinity of Nuclear Power Plants. Results of a Coordinated Research Project F33022, 2016-2020, Institute for Safety Problems of Nuclear Power Plants, National Academy of Sciences of Ukraine - Chornobyl (Kiev region) and International Atomic Energy Agency - Vienna (Austria): 2022. – 200 p. ISBN 978-966-02-9876-7. (Accepted for publishing)

CONFERENCES

- *Bioateitis: gamtos ir gyvybės mokslų perspektyvos (Biofuture: Perspectives for the Natural and Life Sciences)*, Vilnius, Lithuania. Noble Gas Characteristics of the Baltic Artesian Basin Groundwater, 25 November 2021.
- *2nd International Conference on Water Management and its Surroundings - Theoretical and Practical Aspects*, Olsztyn, Poland. The Numerical 3D Steady-State Groundwater Flow Model Verification by MODPATH Particle Tracking and Noble Gas Ages in the Baltic Artesian Basin, 20-21May 2021.
- *International Symposium on Isotope Hydrology: Advancing the Understanding of Water Cycle Processes*, Vienna, Austria, Integrated Studies of ^{4}He and ^{81}Kr Noble Gas Ages of the Deep Aquifers with Coupled Particles Track Modeling in the Baltic Artesian Basin, 20-24 May 2019.
- *International Symposium on Isotope Hydrology: Advancing the Understanding of Water Cycle Processes*, Vienna, Austria, Conventional Tritium Method Calibration with ^{3}H/^{3}He Ratio in the Eastern Lithuanian Groundwater, 20-24 May 2019.
- *61st International Conference for Students of Physics and Natural Sciences OPEN READINGS 2018*, Vilnius, Lithuania. Helium Migration in the Groundwater of Lithuania, 20 March 2018.

CURRICULUM VITAE

Full name: Vytautas Samalavičius
Date of birth: 09/06/1988
E-mail: vytautas.samalavicius@chgf.vu.lt
Education:

- Vilnius University, Institute of Geosciences, Ph.D. studies: *Geology*. 2017-2021.
- Vilnius University, Institute of Geosciences (former Faculty of Natural Sciences), Master studies: *Hydrogeology and Engineering Geology* 2013-2015.
- Vilnius University, Institute of Geosciences (former Faculty of Natural Sciences), Bachelor studies: *Environmental Hydrogeology and Geoengineering* 2009-2013.

Professional experience:

- Vilnius University, Junior researcher/Junior assistant 2016-2021.
- Vilnius University, Laboratory technician 2012-2015.

Research project:

- Participation in the Coordinated Research Project (CPR) F33022 within the International Atomic Energy Agency (IAEA) 2016-2020, intended for Lithuania: "*Integrated studies of crustal permeability based on environmental isotopes, noble gas data, and shallow-deep groundwater flow and mass transport modeling in the surrounding area of Ignalina Nuclear Power Plant (NPP)".*

NOTES

NOTES

NOTES

Vilnius University Press
Saulėtekio Ave. 9, Building III, LT-10222 Vilnius
E-mail: info@leidykla.vu.lt, www.leidykla.vu.lt
Print run 20 copies